



5-1-1995

Spontaneous Luteolysis in the Cyclic Golden Hamster: Evidence for Mediation Through Inflammation and Apoptosis

Mark W. Rodacker

[How does access to this work benefit you? Let us know!](#)

Follow this and additional works at: <https://commons.und.edu/theses>

Recommended Citation

Rodacker, Mark W., "Spontaneous Luteolysis in the Cyclic Golden Hamster: Evidence for Mediation Through Inflammation and Apoptosis" (1995). *Theses and Dissertations*. 2720.
<https://commons.und.edu/theses/2720>

This Dissertation is brought to you for free and open access by the Theses, Dissertations, and Senior Projects at UND Scholarly Commons. It has been accepted for inclusion in Theses and Dissertations by an authorized administrator of UND Scholarly Commons. For more information, please contact und.common@library.und.edu.

SPONTANEOUS LUTEOLYSIS IN THE CYCLIC GOLDEN HAMSTER:
EVIDENCE FOR MEDIATION THROUGH INFLAMMATION
AND APOPTOSIS

by

Mark W. Rodacker

Bachelor of Science, North Dakota State University, 1986

A Dissertation

Submitted to the Graduate Faculty

of the

University of North Dakota

in partial fulfillment of the requirements

for the degree of

Doctor of Philosophy


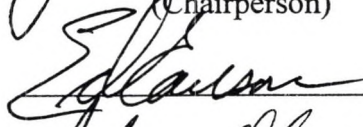
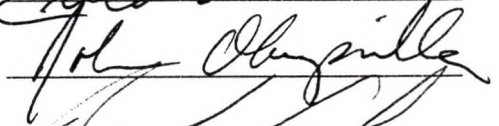
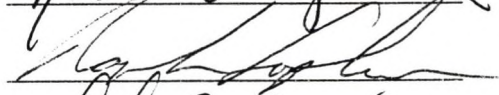
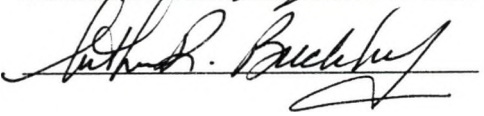
Grand Forks, North Dakota

May

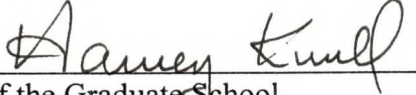
1995

T1995
R61

This dissertation, submitted by Mark W. Rodacker in partial fulfillment of the requirements of the degree of Doctor of Philosophy from the University of North Dakota, has been read by the Faculty Advisory Committee under whom the work has been done and is hereby approved.


(Chairperson)





This dissertation meets the standards for appearance, conforms to the style and format requirements of the Graduate School of the University of North Dakota, and is hereby approved.


Dean of the Graduate School
April 17, 1995

PERMISSION

Title Spontaneous Luteolysis In The Cyclic Golden Hamster: Evidence For
Mediation Through Inflammation And Apoptosis

Department Anatomy and Cell Biology

Degree Doctor of Philosophy

In presenting this dissertation in partial fulfillment of the requirements for a graduate degree from the University of North Dakota, I agree that the library of this University shall make it freely available for inspection. I further agree that permission for extensive copying for scholarly purposes may be granted by the professor who supervised my dissertation work or, in his absence, by the chairperson of the Department, or the Dean of the Graduate School. It is understood that any copying or publication or other use of this dissertation or part thereof for financial gain shall not be allowed without my written permission. It is also understood that due recognition shall be given to me and the University of North Dakota in any scholarly use which may be made of any material in my dissertation.

Signature

Mark W Rodacker

Date

4/11/95

TABLE OF CONTENTS

LIST OF PLATES AND FIGURES.....	v
ACKNOWLEDGEMENTS.....	xxi
ABSTRACT.....	xxii
CHAPTER	
I. AN INTRODUCTION TO LUTEAL STRUCTURE AND FUNCTION IN THE HAMSTER WITH A DISCUSSION OF MODES OF CELL DEATH.....	1
II. AN ASSESSMENT OF THE FINE STRUCTURE OF THE CORPUS LUTEUM DURING LUTEOLYSIS IN THE HAMSTER.....	22
III. INCREASED NONSPECIFIC ESTERASE ACTIVITY IN OVARIAN FOLLICULAR ATRESIA AND CORPUS LUTEUM REGRESSION IN THE CYCLIC GOLDEN HAMSTER.....	36
IV. WESTERN BLOT DEMONSTRATION OF MYELOPEROXIDASE AS A BIOMARKER OF ACUTE INFLAMMATION IN LUTEOLYSIS.....	45
V. A SUMMATION OF THE UNIQUE CHARACTERISTICS OF LUTEOLYSIS IN THE HAMSTER.....	57
APPENDICES.....	64
APPENDIX A. PLATES AND FIGURES.....	65
LITERATURE CITED.....	185

LIST OF PLATES AND FIGURES

PLATE I.....64

Figure

1. Light micrograph of a section through a hamster corpus luteum on D1 at 0900 hours.
2. Light micrograph of a section through a hamster corpus luteum on D1 at 0900 hours.

PLATE II.....66

Figure

3. Light micrograph of a section through a hamster corpus luteum on D2 at 0900 hours.
4. Light micrograph of a section through a hamster corpus luteum on D2 at 0900 hours.

PLATE III.....68

Figure

5. Light micrograph of a section through a hamster corpus luteum on D2 at 0900 hours.
6. Light micrograph of a section through a hamster corpus luteum on D2 at 0900 hours.

PLATE IV.....70

Figure

7. Light micrograph of a section through a hamster corpus luteum on D2 at 0900 hours.
8. Light micrograph of a section through a hamster corpus luteum on D2 at 2400 hours.

PLATE V.....72

Figure

9. Light micrograph of a section through a hamster corpus luteum on D3 at 0300 hours.
10. Light micrograph of a section through a hamster corpus luteum on D3 at 0400 hours.

PLATE VI.....74

Figure

11. Light micrograph of a section through a hamster corpus luteum on D3 at 0500 hours.
12. Light micrograph of a section through a hamster corpus luteum on D3 at 0500 hours.

PLATE VII.....76

Figure

13. Light micrograph of a section through a hamster corpus luteum on D3 at 0600 hours.

14. Light micrograph of a section through a hamster corpus luteum on D3 at 0600 hours.

PLATE VIII.....78

Figure

15. Light micrograph of a section through a hamster corpus luteum on D3 at 0600 hours.

16. Light micrograph of a section through a hamster corpus luteum on D3 at 0600 hours.

PLATE IX.....80

Figure

17. Light micrograph of a section through a hamster corpus luteum on D3 at 0600 hours.

18. Light micrograph of a section through a hamster corpus luteum on D3 at 0900 hours.

PLATE X.....82

Figure

19. Light micrograph of a section through a hamster corpus luteum on D3 at 0900 hours.

20. Light micrograph of a section through a hamster corpus luteum on D3 at 0900 hours.

PLATE XI.....84

Figure

21. Light micrograph of a section through a hamster corpus luteum on D3 at 0900 hours

22. Light micrograph of a section through a hamster corpus luteum on D3 at 0900 hours.

PLATE XII.....86

Figure

23. Light micrograph of a section through a hamster corpus luteum on D3 at 0900 hours.

24. Light micrograph of a section through a hamster corpus luteum on D3 at 0900 hours.

PLATE XIII.....88

Figure

25. Light micrograph of a section through a hamster corpus luteum on D3 at 0900 hours.

26. Light micrograph of a section through a hamster corpus luteum on D3 at 1300 hours.

PLATE XIV.....90

Figure

27. Light micrograph of a section through a hamster corpus luteum on D3 at 1300 hours.

28. Light micrograph of a section through a hamster corpus luteum on D3 at 1300 hours.

PLATE XV.....92

Figure

29. Light micrograph of a section through a hamster corpus luteum on D3 at 1300 hours.

30. Light micrograph of a section through a hamster corpus luteum on D3 at 1300 hours.

PLATE XVI.....94

Figure

31. Light micrograph of a section through a hamster corpus luteum on D3 at 1300 hours.

32. Light micrograph of a section through a hamster corpus luteum on D3 at 1300 hours.

PLATE XVII.....96

Figure

33. Light micrograph of a section through a hamster corpus luteum on D3 at 1530 hours.

34. Light micrograph of a section through a hamster corpus luteum on D3 at 1530 hours.

PLATE XVIII.....98

Figure

35. Light micrograph of a section through a hamster corpus luteum on D3 at 1530 hours.

36. Light micrograph of a section through a hamster corpus luteum on D3 at 1530 hours.

PLATE XIX.....100

Figure

37. Light micrograph of a section through a hamster corpus luteum on D4 at 0900 hours.

38. Light micrograph of a section through a hamster corpus luteum on D4 at 0900 hours.

PLATE XX.....102

Figure

39. Light micrograph of a section through a hamster corpus luteum on D4 at 0900 hours.

40. Light micrograph of a section through a hamster corpus luteum on D4 at 0900 hours.

PLATE XXI.....104

Figure

41. Light micrograph of a section through a hamster corpus luteum on D4 at 0900 hours.

42. Light micrograph of a section through a hamster corpus luteum on D4 at 0900 hours.

PLATE XXII.....106

Figure

43. Light micrograph of a section through a hamster corpus luteum on D4 at 0900 hours.

44. Light micrograph of a section through a hamster corpus luteum on D4 at 0900 hours.

PLATE XXIII.....108

Figure

45. Transmission electron micrograph of a section through hamster luteal cells on D1 at 0900 hours.

PLATE XXIV.....110

Figure

46. Transmission electron micrograph of a section through hamster luteal tissue on D2 at 0900 hours.

PLATE XXV.....112

Figure

47. Transmission electron micrograph of a section through hamster luteal tissue on D2 at 2400 hours.

PLATE XXVI.....114

Figure

48. Transmission electron micrograph of a section through hamster luteal tissue on D3 at 0300 hours.

PLATE XXVII.....116

Figure

49. Transmission electron micrograph of a section through hamster luteal tissue on D3 at 0300 hours.

PLATE XXVIII.....118

Figure

50. Transmission electron micrograph of a section through hamster luteal tissue on D3 at 0300 hours.

PLATE XXIX.....120

Figure

51. Transmission electron micrograph of a section through hamster luteal cells on D3 at 0600 hours.

PLATE XXX.....122

Figure

52. Transmission electron micrograph of a section through hamster luteal tissue on D3 at 0600 hours.

PLATE XXXI.....124

Figure

53. Transmission electron micrograph of a section through hamster luteal tissue on D3 at 0600 hours.

PLATE XXXII.....126

Figure

54. Transmission electron micrograph of a section through hamster luteal tissue on D3 at 0900 hours.

PLATE XXXIII.....128

Figure

55. Transmission electron micrograph of a section through hamster luteal tissue on D3 at 0900 hours.

PLATE XXXIV.....130

Figure

56. Transmission electron micrograph of a section through hamster luteal tissue on D3 at 0900 hours.

PLATE XXXV.....132

Figure

57. Transmission electron micrograph of a section through hamster luteal tissue on D3 at 0900 hours.

PLATE XXXVI.....134

Figure

58. Transmission electron micrograph of a section through hamster luteal cells on D3 at 1300 hours.

PLATE XXXVII.....136

Figure

59. Transmission electron micrograph of a section through hamster luteal cells on D3 at 1300 hours.

PLATE XXXVIII.....138

Figure

60. Transmission electron micrograph of a section through hamster luteal tissue on D3 at 1200 hours.

PLATE XXXIX.....140

Figure

61. Transmission electron micrograph of a section through hamster luteal tissue on D3 at 1200 hours.

PLATE XL.....142

Figure

62. Transmission electron micrograph of a section through hamster luteal tissue on D3 at 1300 hours.

PLATE XLI.....144

Figure

63. Transmission electron micrograph of a section through hamster luteal tissue on D3 at 1300 hours.

PLATE XLII.....146

Figure

64. Transmission electron micrograph of a section through hamster luteal tissue on D3 at 1300 hours.

PLATE XLIII.....148

Figure

65. Transmission electron micrograph of a section through hamster luteal tissue on D3 at 1300 hours.

PLATE XLIV.....150

Figure

66. Transmission electron micrograph of a section through hamster luteal tissue on D3 at 1530 hours.

PLATE XLV.....152

Figure

67. Transmission electron micrograph of a section through hamster luteal cells on D4 at at 0900 hours.

PLATE XLVI.....154

Figure

68. Transmission electron micrograph of a section through hamster luteal cells on D4 at 0900 hours.

PLATE XLVII.....156

Figure

69. Transmission electron micrograph of a section through hamster luteal cells on D4 at 0900 hours.

PLATE XLVIII.....158

Figure

70. Transmission electron micrograph of a section through hamster luteal tissue on D4 at 0900 hours.

PLATE XLIX.....160

Figure

71. Transmission electron micrograph of a section through hamster luteal tissue on D4 at 0900 hours.

PLATE L.....162

Figure

72. Transmission electron micrograph of a section through hamster luteal tissue on D4 at 0900 hours.

PLATE LI.....164

Figure

73. Light micrograph of a section through hamster spleen histochemically stained for α -naphthyl acetate esterase.
74. Light micrograph of a section through hamster oviduct histochemically stained for α -naphthyl acetate esterase.

PLATE LII.....166

Figure

- 75. Light micrograph of a section through hamster ovary on D4 histochemically stained for α -naphthyl acetate esterase.
- 76. Light micrograph of a section through several hamster ovarian follicles histochemically stained for α -naphthyl acetate esterase.

PLATE LIII.....168

Figure

- 77. Light micrograph of a section through hamster ovarian follicles histochemically stained for α -naphthyl acetate esterase.
- 78. Light micrograph of a section through an atretic hamster ovarian follicle histochemically stained for α -naphthyl acetate esterase.

PLATE LIV.....170

Figure

- 79. Light micrograph of a section through an atretic hamster ovarian follicle histochemically stained for α -naphthyl acetate esterase.
- 80. Light micrograph of a section through hamster granulosa cells in an atretic ovarian follicle histochemically stained for α -naphthyl acetate esterase.

PLATE LV.....172

Figure

- 81. Light micrograph of a section through a hamster corpus luteum on D1
histochemically stained for α -naphthyl acetate esterase.
- 82. Light micrograph of a section through a hamster corpus luteum on D2
histochemically stained for α -naphthyl acetate esterase.

PLATE LVI.....174

Figure

- 83. Light micrograph of a section through a hamster corpus luteum on D3
histochemically stained for α -naphthyl acetate esterase.
- 84. Light micrograph of a section through a hamster corpus luteum on D3
histochemically stained for α -naphthyl acetate esterase.

PLATE LVII.....176

Figure

- 85. Light micrograph of a section through a hamster corpus luteum on D4
histochemically stained for α -naphthyl acetate esterase.
- 86. Light micrograph of a section through a hamster luteal cells and neutrophils on
D4 histochemically stained for α -naphthyl acetate esterase.

PLATE LVIII.....178

Figure

- 87. Light micrograph of a section through a hamster corpus luteum on D4 histochemically stained for α -naphthyl acetate esterase.
- 88. Light micrograph of a section through the regressed remnants of a hamster corpus luteum from the previous cycle (on D1) histochemically stained for α -naphthyl acetate esterase.

PLATE LIX.....180

Figure

- 89. Immunoblot of hamster luteal and nonluteal tissue samples probed for myeloperoxidase enzyme presence.

ACKNOWLEDGEMENTS

I wish to thank the members who served on my faculty advisory committee, Drs. John McCormack, Ed Carlson, John Oberpriller, Roger Sopher and Arthur Buckley. I appreciated the guidance and criticisms you provided in conducting the research and in preparing the dissertation. A very special thanks is due to Mac and Carolyn for their warm friendship, support and great times which I shall always cherish.

I would like to thank Dr. Don Matthias, Dr. Ken Ruit, Dr. Mark Olson, Joe Provost, Jan Audette, Kim Young, Julie Horn, and Faye Aker who also provided valuable knowledge and assistance in accomplishing my work in the department of Anatomy and Cell Biology. Thanks also to my fellow graduate students, especially Matt Friederichs, who stood by as my good friend in the trenches when the going was tough.

I would also like to especially thank my wife, Lori Ann, who, more than anyone else, deserves a special award for her incredible patience and tolerance in support of my career. Finally, I wish to thank my parents Gary and Sandy, to whom I dedicate this dissertation. Throughout my whole life you two have been there to hold me up and to shine a guiding light of hope and inspiration. I can never thank you enough but only hope you are as proud of me as I am of you.

ABSTRACT

Mammalian corpora lutea (CL) are transient ovarian glands which function to support pregnancy by secretion of progesterone (P). Sustained P secretion during pregnancy in the hamster requires gonadotrophic support, i.e., follicle stimulating hormone (FSH) and prolactin (Prl). Infertile cycles require CL regression. In luteolysis, CL first regress functionally (FL) and then structurally (SL). FL permits the next estrous. Estrous occurs every fourth day in the hamster such that CL form, function briefly, and then regress rapidly and completely. With only one generation of CL present in each ovary at any one time, the hamster is an ideal model for studying luteolysis. FL begins on day three as P secretion plummets, and is followed immediately by SL as neutrophils --cellular markers of inflammation-- invade the CL. SL proceeds via apoptosis and is not reversible with exogenous FSH-Prl.

Apoptosis is synonymous with physiological cell death, and, as a rule, evokes no inflammation. In fact, it may have evolved to prevent inflammation and the excessive tissue damage which often accompanies pathologic cell death. Since apoptosis and inflammation coexist in luteolysis, experiments are designed in the present study to help explain this paradox.

Light and transmission electron microscopic observations of ovarian sections chronicled cyclic luteal morphology. Enzyme histochemistry was conducted on ovarian sections for lysosomal nonspecific esterase activity. Luteal and nonluteal ovarian samples were probed for neutrophilic myeloperoxidase by immunoblot.

Microscopic observations revealed that some luteal cell organelles atrophy in FL prior to the apoptosis seen in SL. Nonspecific esterase staining showed a dramatic increase in autolytic lysosomal activity during SL and follicular atresia. Immunoblots showed that myeloperoxidase is present at the onset of SL.

The findings indicate that luteolysis is a dynamic process which may require a tightly regulated acute inflammatory response for rapid completion. Neutrophils may play a role in the abrupt onset of cell death required for SL. It is possible that in hamster luteolysis the damaging sequelae of chronic inflammation is prevented by apoptosis in which viable luteal cells are transformed into phagocytes that clear the gland of apoptotic cellular debris.

**CHAPTER I: AN INTRODUCTION TO LUTEAL STRUCTURE AND FUNCTION
IN THE HAMSTER WITH A DISCUSSION OF MODES OF CELL
DEATH**

The mammalian corpus luteum (CL) is a transient ovarian endocrine gland necessary for reproduction. Its vital role is to produce progesterone (P). This steroid hormone acts on female reproductive organs such as the vagina, oviduct, uterus and mammary gland to prepare them to receive the conceptus and nurture the embryo throughout gestation and postnatal life. The CL is also capable of producing peptide hormones such as relaxin and oxytocin (Krause et al., 1992). The role of these luteal products is not as well understood in the cycling female as it is for those of term pregnancy.

Like most endocrine tissues, the CL is dependent upon trophic support. The most crucial requirements are the pituitary gonadotrophins prolactin (Prl), luteinizing hormone (LH), and in a few cases, follicle stimulating hormone (FSH). For most species LH is the most important gonadotrophin. However, this is species-specific. Particular gonadotrophin requirements are also luteal phase dependent. For example, the rising phase of P production may be highly Prl dependent while the plateau phase may be more LH sensitive. In the case of the hamster it is well established that the "luteotrophic-complex" is a Prl-FSH combination which rescues the CL from early demise

(Greenwald, 1967; Grady and Greenwald, 1968; Greenwald, 1973; Tamura and Greenwald, 1987). Without a mating stimulus the pituitary does not release ample quantities of gonadotrophins to establish pseudopregnancy. The lack of a sufficient luteotrophic complex thus curtails luteal lifespan and allows rapid progression to the next estrus.

Regression of the CL, in a functional sense, refers to the marked drop in serum P levels and cessation of its production while structural demise refers to the actual physical collapse and disintegration of the gland. Together these processes are termed luteolysis. Because functional demise (cessation of P secretion) precedes structural regression (actual physical dissolution), the two processes can be separated as functional luteolysis (FL) and structural luteolysis (SL) (Juengel et al., 1993). These processes are required for proper hormonal and architectural balance in ovarian function. The most universal luteolytic factor responsible for the onset of luteolysis is prostaglandin F2 alpha (PGF2 α). This can be produced either by the endometrium or within the CL itself (Niswender et al., 1994; Rothchild, 1981). Its mechanism of action appears to be mediated at multiple metabolically strategic points in luteal cell function and is somewhat species-specific (Niswender and Nett, 1988; Niswender et al, 1994; Michael et al., 1994).

The hamster exhibits consistent four day estrous cycles as confirmed by vaginal discharge (Greenwald and Rothchild, 1968). Maturation and ovulation of follicles are regulated by gonadotrophins. Ovulation typically occurs between 2400 on proestrous (day four) and 0100 of estrus (day one) with the mean number of oocytes ovulated being

ten (Kent, 1968). Psychic estrus occurs around eight hours prior to ovulation resulting in the female being receptive to males. Ovulation is dependent upon a rapid rise in estrogen (E) production by antral follicles, triggering a preovulatory surge of LH on the afternoon of proestrous, (Baranczuk and Greenwald, 1973). If mating occurs, a physiologic state of pseudopregnancy results. This is due to a stimulation of the cervix activating an afferent neuronal neurohumoral arc acting through the hypothalamo-hypophyseal axis with reflex stimulation of the pituitary on estrous, after which the CL of the cycle develop and become fully functional for several days, (Kent, 1968). The physiological, behavioral and histological changes occurring at this time resemble those of early pregnancy. The effects include interrupted estrous cycles by delaying complete maturation of the next cohort of follicles, progesterational modifications of the reproductive tract owing to prolonged elevation of P levels, attempted implantation of the ova, areolar development in the mammary gland, increases in body weight and elevated levels of Prl, (Kent, 1968). The typical duration of hamster pseudopregnancy is 9-10 days. The CL of pseudopregnancy are larger than cyclic CL with more proliferative vascularization and larger luteal cells but they are smaller than the CL of pregnancy. Signs of regression appear by the end of day seven in infertile matings. The state of pseudopregnancy is thus required following mating to allow time for implantation (day five or six of gestation) and uterine preparation by delaying another estrus onset.

After ovulation, CL organize rapidly from the ruptured follicles. The walls collapse and the membrana granulosa is squeezed into folds. The follicular cavity

contains liquor folliculi, blood clots and leukocytes. The hemorrhagic mass becomes infiltrated with loose connective tissue (Kent, 1968). The granulosa lutein cells undergo hypertrophy and hyperplasia with vacuolation of their cytoplasm. Gradually granulosa cells arrange into radial cords separated by developing blood vessels which migrate centrally from the former follicular theca interna. New vessel development appears to be stimulated by the action of a fibroblastic growth factor-like angiogenic growth factor (AGF), (Stern and Coulam, 1992). The theca also contributes patchy foci of cells along the peripheral margin of the CL just beneath the connective tissue capsule. These cells are smaller with more vacuolated cytoplasm and are called theca lutein or paralutein cells (Kent, 1968). These are characteristic luteal events involved on estrus in the hamster ovary. Autoradiographic data show light to moderate binding of human chorionic gonadotrophin (hCG) and Prl, with heavy FSH binding (Oxberry and Greenwald, 1982). This process is termed luteinization.

Day two (D2) involves maximal P secretion (Ridley and Greenwald, 1975; Leavitt et al., 1973). Luteal cells are hypertrophied and approximate one another with many interdigitations of their cell surfaces. There are large mitochondria with tubular cristae, extensive profiles of SER and well developed golgi formations. Autoradiography demonstrates much reduced FSH binding but heavy hCG and Prl binding (Oxberry and Greenwald, 1982).

During the late evening of D2 and early morning of D3 in the unmated animal, a remarkable process occurs known as the "luteal-follicular shift" (L-Fs) (Terranova and

Greenwald, 1978). This marks the transition in the estrous cycle from the P-secretion-dominated luteal phase to the E-secretion-dominated follicular phase. The switch is not thought to be due to any significant changes in gonadotrophin levels. Instead, failure of the cyclic CL to secrete enough P to inhibit development of E-secreting antral follicles from developing is thought to account for the short cycles of only four days.

D3 of the cycle is dominated by the process of luteolysis. Traditionally this continuous process is separated into two phases, (FL and SL), as described above. In most mammals, with the most notable exception of primates, this is brought about by endometrial production and transfer to the ovary of the luteolytic factor $\text{PGF2}\alpha$ (Michael et al. 1994; Niswender et al., 1994; and Rothchild, 1981). The anatomical relationship of the uterine veins (UV) to the ovarian artery (OA) are such that they are juxtaposed with the tortuous UV spiralling about the OA (Niswender and Nett, 1988). This intimate contact allows $\text{PGF2}\alpha$ leaving the UV to diffuse through the common adventitia of the two vessels into the OA en route to the CL. Because $\text{PGF2}\alpha$ is rapidly metabolized in the circulation it would not remain luteolytic even for one pass through the system (McCracken et al., 1970). Thus hysterectomy prolongs the luteal phase in most mammals. This is true of pseudopregnant rodents such as mice, rats and hamsters but is not true for cyclic rodents (Niswender and Nett, 1988; Lau et al., 1975).

Pharmacologically, PG production can be blocked by cyclooxygenase inhibitors such as indomethacin to prolong luteal life span (Lau et al., 1973; Dennefors, et al, 1983). Blocking the lipooxygenase pathway of arachidonic acid metabolism with substances

such as nordihydroguaiaretic acid by uterine luminal infusion can also delay luteolysis in heifers (Milvae et al., 1986). However, hysterectomy does not prevent luteolysis in the cyclic hamster (Duby et al., 1969) indicating that any potential luteolytic signal is not uterine in origin.

Luteal cells are themselves capable of producing PGs (Rothchild, 1981), as are most mammalian cell types (Devlin, 1986). Interestingly, an action of P is to set up conditions for an eventual high production rate of PG (autocatalytic). Concominantly, P suppresses actual production of PGs and also increases their inactivation. Eventually, during the regression phase of P production, its suppressing effect on PG production can no longer be overcome. Thus as P production wanes, PG synthesis takes over and inhibits further P production (Rothchild, 1981). E may potentiate the luteolytic effect of PGs in some species by upregulating the expression of PG receptors on luteal cells (Rothchild, 1981; Niswender et al., 1994).

Without pituitary release of the luteotropic complex of FSH-Prl in the hamster, P secretion wanes at the onset of the L-Fs (around 2000 hours) on D2 and plummets to a nadir at 0400 hours on D3 (Terranova and Greenwald, 1978). CL can be rescued and made to become fully functional as late as 54 hours after ovulation by the luteotropic complex as required for pseudopregnancy (Greenwald and Rothchild, 1968). Decreasing P concentration may thus allow for an increased intraluteal PG formation to induce spontaneous luteolysis (Rothchild, 1981). Therefore, the period of the L-Fs is in essence, the brief interval of FL in the hamster. However, it should be recalled that if hamsters are

hypophysectomized on D1 of the estrous cycle, the histology and growth of the CL on subsequent days is the same as intact animals. According to dogma, the growth and regression of the CL are independent of the pituitary. However, gonadotrophins can enhance function. Therefore luteolysis is due to the lack of a forthcoming luteotropic complex rather than a pituitary luteolytic hormone(s) as is the case in some animals (Greenwald and Rothchild, 1968). Results in chapter II of this work indicate the uncertainty of this contention. There are differences between species but the underlying mechanisms of luteolysis (usually brought about by $\text{PGF}_2\alpha$) include changes in ovarian blood flow, reduction in the number of luteal cell LH receptors, inhibition or uncoupling of LH-stimulated cAMP formation, protein kinase C activation, and/or direct cytotoxicity (Orlicky et al., 1992; Niswender et al., 1994). As FL concludes, SL ensues between 0500 and 0600 hours of D3, heralded by a massive wave of emigrating neutrophilic polymorphonuclear leukocytes (PMNL).

During luteolysis, luteal cell size and SER content are reduced while lipid accumulates intracellularly. A dramatic rise in lysosomal content is also seen. Hydrolytic enzymes such as alkaline phosphatase and acid phosphatase (Chatterjee and Greenwald, 1976; Niswender et al., 1994) and nonspecific esterase (see chapter III below) are seen to increase markedly in luteolysis. Protein and RNA content of the CL also decrease in luteolysis (Chatterjee and Greenwald, 1976). Autoradiography of D3 CL show no FSH binding and markedly reduced hCG and Prl binding (Oxberry and Greenwald, 1982). Cell death is recognizable by the presence of numerous pyknotic

nuclei. By midafternoon the vasculature is nonfunctional (Forsman and McCormack, 1992).

Day four (D4) of the cycle is a period of advanced luteolysis in the CL. No steroids are produced and no gonadotrophin binding can be demonstrated by autoradiography (Oxberry and Greenwald, 1982). The CL are pale and ischemic. Microscopically, many of the remaining cells have an abundance of lysosomes, myelin figures and translucent vacuoles (Leavitt et al., 1973) indicating lipid accumulation which is supported by histological demonstration of triglyceride and cholesterol storage (Guyara and Greenwald, 1965). The rate at which lysosomal elements and leukocytes appear is evidence that autolytic and heterolytic events proceed more quickly in the hamster. This is supported by the fact that the previous generation of CL are difficult to observe in ovaries collected on the day of the subsequent estrus (Oxberry and Greenwald, 1982). It is noteworthy that apoptosis is the form of cell death seen in luteolysis. This can be demonstrated by a variety of techniques including gel electrophoresis (Zeleznik et al., 1989; Juengel et al., 1993; McCormack and Greenwald, submitted), *in situ* end labelling of fragmented DNA (Friederichs and McCormack, submitted) and light and transmission electron microscopy (O'Shea et al., 1977; Azmi and O'Shea, 1984; chapter II below).

There are now two major recognized distinct forms of cell death, namely necrosis and apoptosis (Kerr et al., 1972; Buja et al., 1993). Necrosis is an accidental or nonphysiological process precipitated by events such as exposure to thermal extremes, profound ischemia, various poisons or toxins, pathogenic organisms or acute graft

rejection. On the other hand, apoptosis is frequently a programmed process and is physiological in nature. It occurs in diverse settings throughout development such as metamorphosis, organogenesis and morphogenesis in which precise genetic regulation is required. Apoptosis also occurs in hematopoiesis, lymphocyte ontogeny, atrophy of trophic deprived tissues, some targets of cell mediated immunity and a variety of pathological scenarios as well. Because of its many settings, the study of cell death is important to basic scientists and clinicians alike. As cell death is a fundamental component of luteolysis which until recently has been misinterpreted, I will more fully characterize the two processes mentioned above.

Necrotic cell death is the final outcome of a lethal "hit(s)" to a cell in which irreversible injury has been sustained. Insulting stimuli range from the extremes of gross physical trauma (crushing blow) to subtle but deadly single gene defects (sickle cell anemia). Several broad categories of stresses have been suggested to lead to irreversible injury including hypoxia, chemicals/drugs, physical agents, immunological reactions, genetic defects, nutritional imbalances and aging (Kumar et al., 1992). Cells which are challenged by sublethal forces may be able to respond in an adaptive fashion as do cardiac myocytes in the face of chronic hypertension by hypertrophy. Adaptive responses are limited however. Mortal insults such as complete coronary occlusion produce necrosis in the center of the infarcted region owing to profound hypoxia and only the peripheral areas of ischemia may adapt or recover from sublethal hypoxia. In a given tissue the pattern of necrosis that develops is dependent upon the nature of the offending

entity. If we consider further the example of severe hypoxia we can begin to understand the basic biochemical and morphological alterations which are the most typical of necrosis.

A final common pathway in cell injury is that produced by O₂-mediated damage. A lack of O₂ is obviously deadly but the production of partially reduced O₂ species such as superoxide anion, hydrogen peroxide and hydroxyl radical known as free radicals can be hazardous at sites of tissue damage (Aten et al., 1992; Wu et al., 1993). These electron-rich (extremely unstable and reactive) molecules attack tissue elements such as the plasma membrane to initiate self-propagating reactions which promote lesions such as lipid peroxidation (Sawada and Carlson, 1991; Pepperell et al., 1992). In light-moderate injury, free radical scavengers such as superoxide dismutase, glutathione reductase, catalase and vitamin E may be able to neutralize these destructive toxic "bullets". Hypoxia initially overwhelms the cells aerobic metabolism so that mitochondria fail to make enough ATP resulting in insufficient energy to run the cell membrane sodium-potassium pump which regulates osmotic balance. The cell begins depleting glycogen stores rapidly in an attempt to maintain function. Increased cAMP drives glycolysis yielding lactic acid. Hydrolysis of phosphate esters produces inorganic phosphates. The buildup of acidic metabolic byproducts lowers the intracellular pH and the cell swells. Next, ribosomes detach from RER and polysomes dissociate into monosomes. Mitochondria swell and myelin figures may appear both intra- and extracellularly. Eventually, mitochondrial cristae become severely vacuolated, the plasma membrane is

destroyed and lysosomes swell. In cases of reperfusion, the mitochondria accumulate calcium deposits in their matrices. Membranes become hyperpermeable with loss of proteins, coenzymes, RNA and other vital metabolites to the extracellular space. Low pH damages and labilizes lysosomal membranes resulting in enzyme spillage into the cytoplasm where activation of acid hydrolases produces digestion of cytoplasmic and nuclear constituents. Whatever the form(s) of lethal stimulus(i), the mechanism of demise is usually a domino effect characterized by cascading metabolic derangement. Cellular swelling is the most common morphological indicator of necrosis. Increased eosinophilia is also typical. One of three distinctive designs are followed in irreversible nonphysiologic cell death. The mass of involved cells undergoes coagulative necrosis, liquifactive necrosis or caseous necrosis or rarely, fibrinoid necrosis. Briefly, coagulative necrosis (usual pattern of hypoxic necrosis and the most common pattern) includes preservation of the basic cellular outline for several days as intracellular acidosis leads to denaturation of proteases thus prolonging complete cellular dissolution until immigrant leukocytes engulf the debris. Liquifactive necrosis is seen typically in abscesses in which a bacterial infection attracts many leukocytes. Release of leukocyte granular contents causes a dissolution of the tissue leaving a purulent debris-laden defect at the site of inflammation. Caseous necrosis is a form of coagulative necrosis seen classically at foci of tuberculous infection. These are well demarcated areas (characterized by amorphous "cheesy" looking necrotic debris) which are known as granulomata.

The key point is that necrosis customarily provokes an acute inflammatory reaction (Barr and Tomei, 1994). If not readily resolved, it may proceed to chronic inflammation and possibly scarring (Haslett, 1992). The phenomena of inflammation involve the reactions of living tissue to local injury (Cotran et al., 1989). The classic signs of inflammation described in ancient times by Celcius include rubor (redness-hyperemia) caused by initial vasodilation, tumor (swelling) due to chemical mediator-induced increased capillary permeability and plasma leakage, calor (heat) and dolor (pain) caused by tension on nerve endings from tissue swelling and damage (Gallin, 1993). Leukocyte infiltration of the inflammatory site is also seen to accompany the vascular alterations. PMNL arrive first and are followed by mononuclear cells. Leukocytes are necessary to neutralize the insulting stimuli, but discharge of their arsenal of proteolytic enzymes, and antimicrobial factors and O₂ radical production may overwhelm serum and tissue deactivating mechanisms thereby harming host tissue. This is especially troublesome in tissues with limited capacity for regeneration.

Cellular responses during physiological cell death, on the other hand, are very different. The term apoptosis derives from the ancient greek words apo (apart) and ptosis (fallen), (Kerr et al., 1972). This metaphor likens the dropout of dying cells to leaves being shed from a tree in autumn. The term was coined by University of Edinburgh biologists to describe the morphology as an entirely different process than necrosis, (Kerr et al., 1972). Interest was modest early on but of late it has gained widespread attention. Apoptosis has been described as cellular suicide reflecting the active nature of the process

whereby properly induced cells participate in their own death. This is most commonly accomplished by new RNA and protein synthesis and by efficient usage of energy stores (Waring et al., 1991). Apoptosis has been termed programmed cell death reflecting the tightly regulated genetic program operating in metamorphosis and embryonic development (Eastman, 1993; Fesus et al., 1991; Bowen, 1993). The words physiological cell death are applied to ordinary tissue turnover such as seen in gut crypt epithelium, skin cell differentiation and cyclic uterine epithelium. These phrases are commonly used interchangeably to the regret of some because they can be misinterpreted in certain contexts (Darzynkiewicz et al., 1991; Cohen, 1993). Put another way, there are multiple pathways leading to apoptosis which is a term used to define the set of morphological alterations seen in all forms of physiological cell death (Evans, 1993). Apoptosis has been further classified as the antithesis of mitosis implying that it is a counterbalance for mitosis in the regulation of tissue kinetics (Kerr et al., 1972; Schulte-Hermann et al., 1992; Bowen, 1993).

The unique morphology of apoptosis occurs with great fidelity in most tissues in which it appears (Wyllie, 1993), although variants do exist (Bowen, 1993). The morphology of classical apoptosis consists of a series of nuclear and cytoplasmic changes leading to the orderly destruction and removal of the dead cells from the tissue. The morphological alterations which have been traditionally appreciated are finding more and more underlying biochemical explanations as time passes.

The first observable change is a condensation of chromatin adjacent to the nuclear membrane appearing as peripheral caps or crescents. There are no nuclear pores in the nuclear envelope at these regions (Wyllie, 1993). Later, the nucleus implodes (further condenses) into a pyknotic "heap". The nucleolus also disintegrates in this process to leave a shower of osmiophilic particles near the center (Wyllie, 1993). Nuclear condensation is due to the effects of a $\text{Ca}^{++}/\text{Mg}^{++}$ dependent endogenous endonuclease on genomic DNA. When activated, this enzyme cleaves the genomic DNA helix at internucleosomal spacer regions (Fesus et al., 1991; Wyllie, 1993). Cleavage produces oligonucleosomal fragments which are integer multiples of the 180-200 base pair monosomes. Electrophoretic separation on agarose gels produces the classic "ladder" pattern in which the rungs of the ladder correspond to the various sized nucleosomes (Arends et al., 1991). Inhibition of Ca^{++} mobilization can block endonuclease activity and thereby prevent apoptosis (Waring et al., 1991). This internucleosomal lysis is not without exceptions in apoptotic cell death but it is seen in the vast majority of cases and when present cannot be confused with necrotic cell death in which random DNA cleavage occurs (Cohen, 1993). In random DNA cleavage, electrophoresis does not result in a distinct ladder pattern.

At the same time as nuclear alterations are occurring there is marked loss of cytoplasmic volume resulting in protein condensation and organelle compaction as the cell shrinks. Originally the term shrinkage necrosis was applied to apoptosis to depict cellular volume loss (Kerr et al., 1972). Apoptotic cells thus show increased buoyant

density in accord with their volume. This loss is possibly due to an inhibition of the Na^+ - K^+ - Cl^- cotransporter system as ions and H_2O are lost to the extracellular space and intracellular Ca^{++} elevation is sustained (Wyllie, 1993). Shrinking cells pull apart from their neighbors and lose membrane specializations such as microvilli and cell-cell junctions (Wyllie, 1993). In contrast to the impressive nuclear and cytoplasmic changes, many organelles of apoptotic cells appear relatively healthy and functional (Kerr et al., 1972). For example, mitochondria maintain their transmembrane potential (Darzynkiewicz et al., 1992). Later in apoptosis some organelle changes do appear as the ER and golgi membranes dilate and fuse with the plasma membrane. Plasmalemmae also ruffle with protuberances or "blebs" where local changes in Ca^{++} concentration are noted (Bowen, 1993). Cytoskeletal alterations cause loss of cell anchorage. Cinematographic studies demonstrate the explosion of the cell into a series of multiple oval or spherical membrane bound bodies containing cellular contents (Wyllie, 1993). The apoptotic bodies contain either condensed chromatin or tightly packed cytoplasm and organelles. The number of bodies visible by light microscopy is only a fraction of those seen by transmission electron microscopy (Kerr et al., 1972). The bodies resist leakage due to the stabilizing presence of transglutaminase enzyme activity (Fesus et al., 1991). Transglutaminases are utilized during apoptosis, allowing for strategic cross-linking of structural proteins into a tough shell, resistant to dissolution by detergents or chaotropic agents like urea (Fesus et al., 1991). Transglutaminases are Ca^{++} -dependent enzymes found in serum, differentiating epidermal cells and other cells primed for apoptosis. Transglutaminases

also bring about changes in surface glycoprotein makeup which enhance phagocytosis. For example, aged erythrocyte membranes are readily recognized by splenic macrophages promoting deletion (Fesus et al., 1991). Likewise, apoptotic thymocytes are readily engulfed by thymic macrophages (Duvall et al., 1985) as are senescent neutrophils (Savill, 1992). Transglutaminase and other effector proteins may require de novo synthesis in some primed cells. Blocking synthesis with compounds such as cyclohexamide or actinomycin D may prevent apoptosis in these cell lines (Fesus et al., 1991).

In the end stage of apoptosis, apoptotic bodies are rapidly recognized by resident histiocytes or viable neighboring cells. These phagocytes bind to altered membranes of the apoptotic cells/bodies in a receptor-ligand fashion. The apoptotic bodies are subsequently degraded in phagolysosomes. Cells with phagolysosomes markedly increase their content of acid hydrolases (Kerr et al., 1972). The rapid phagocytosis of dead cell remnants is believed to be one reason why inflammation is not induced in apoptosis (Kerr et al., 1972; Eastman, 1993). We now have a working idea of the major alterations in cell morphology and biochemistry in apoptosis; but what are the initiating mechanisms?

Cells may be activation-induced by receptor-mediated stimuli to begin apoptosis (Eastman, 1993). Polypeptides such as tumor necrosis factor (TNF) or Müllerian-inhibiting factor (a TGF- β -like molecule) may bind to cells with the proper surface receptors for these ligands (Fesus et al., 1991; Schulte-Hermann et al., 1993).

Polypeptide-receptor activation works through a host of second messengers such as inositol triphosphate (IP₃) or cAMP, etc. These second messengers frequently operate to cause a sustained rise in intracellular calcium, [Ca⁺⁺]_i, which is required for activation of effector proteins such as transglutaminase or endonuclease. Another mechanism of activation-induced apoptosis is through steroids. These lipophilic hormones like thyroxin, glucocorticoids or retinoids can bind to cytoplasmic receptors, translocate to the nucleus where they activate gene expression, and lead to subsequent death in sensitive cell populations.

In contrast, inactivation-induced apoptosis exists such that lack of, or removal of growth or survival factors can result in dependent cell death (Eastman, 1993). Loss of trophic stimuli such as erythropoietin, adrenocorticotrophic hormone, E, testosterone, nerve growth factor, interleukins, gonadotrophins, or colony stimulating factors which block the expression of a cell death program (and thus allow survival), results in apoptosis in erythroblasts, adrenal cortical cells, uterine epithelium, prostatic epithelium, neurons, leukocytes, follicular and luteal cells and myeloid cells respectively. A plethora of nonphysiologic and pathologic stimuli can also induce apoptosis, such as radiation, toxic substances and drugs (Fesus et al., 1991; Waring et al., 1991) or viral hepatitis (Cotran et al., 1989; Alison and Sarraf).

Some cell types become susceptible to apoptosis at particular check points in the cell cycle such as the G2/M boundary in which damaged cells may be prevented from further transition (Fesus et al., 1991). Thymocytes adhere to this scheme by following a

“better dead than wrong” code in which they die rather than proceeding in ontogeny or repairing any genetic damage (Cohen, 1993).

Interest in the genetic regulation of apoptosis is becoming extensive although few systems are yet well understood. A number of regulatory genes have been identified which influence cellular susceptibility to undergo apoptosis including onco- and oncosuppressor genes like c-myc, bcl-2, ras and p53. In the case of c-myc expression in fibroblasts, availability of growth factors such as IGF-1 affect growth vs. apoptosis. For example, with c-myc “off” and no growth factors present, growth arrest occurs, while with c-myc “on” and growth factors present, population expansion occurs. However, apoptosis ensues with c-myc “on” and growth factors absent (Wyllie, 1993).

With the protooncogene bcl-2, expressive cells are rescued from apoptosis during states of high turnover, favoring population expansion in thymocytes (Moore et al., 1994) and B cells (Wyllie, 1993). Overexpression of mutated ras oncogene and growth factor abundance can have a similar rescuing affect in hematopoiesis (Wyllie, 1993).

Expression of wild type p53 has an opposite affect thus inducing apoptosis in susceptible cells such as those with irreversible DNA damage. In other cells, wild p53 holds cells in a nonproliferative state in G1 arrest, allowing time for DNA repair prior to division (Barr and Tomei, 1994). Overexpression interferes with DNA synthesis by deactivating transcription activators such as c-myc, c-jun and c-fos to initiate apoptosis (Evans, 1993). The fas gene codes for lymphocyte death by apoptosis but cells lacking the gene (or cells that have mutated forms) develop lymphoaccumulation (or autoimmune disease) because

the lymphocytes do not have receptors for the signal which initiates apoptosis (Cohen, 1993). The exact mechanisms of how these regulatory genes guide cells into or out of the apoptotic pathway is not completely resolved but at least one route is through induction or depletion of effector proteins. There are a number of pro- and anti-apoptotic genes, growth and trophic factors, cell cycle stages, etc. to contend with in the analysis of a cell's potential fates. This applies to both normal and tumor cell kinetics with the important realization that many tumor cell lines have lost their dependence on growth factors. Wyllie (1993) has suggested that it may be convenient to describe cells that are induced to synthesize proeffector proteins as "primed" to distinguish them from unprimed cells that are not readily prone to undergo apoptosis. He suggests cells be labelled as "triggered" if they are already induced by activated proeffectors such as endonuclease or transglutaminase to begin apoptosis (Wyllie, 1993). I will conclude this discussion of the regulation of apoptosis with two examples of fairly well understood systems.

In an antibody mediated immune response (humoral), naïve B cells enter the center of a lymphoid follicle where they become stimulated by cytokines and direct folliculodendritic cell contact to begin division and maturation into memory cells and immunoblasts (Kosco, 1991). Most of the rapidly dividing lymphocytes undergo apoptosis because they have high c-myc expression and receive inadequate trophic support. Fortunately, a fraction of the clones with the correct surface immunoglobulin affinity for offending epitopes receive proper cytokine support, activating bcl-2 expression, required for proliferation into memory cells and antibody-secreting plasma

cells. In cases of malignant clones (lymphomas) an ability to manipulate the cells in their high rate of turnover, which is when they are the most susceptible to the sorts of signals described in detail above, would have obvious therapeutic benefits. This is the aim of many of the primitive chemotherapy regimens presently employed in cancer treatments.

Perhaps the most tightly regulated of all processes in which apoptosis is a key element in tissue status is in metamorphosis and embryonic development. The best understood system at present is the embryogenesis of the nematode Caenorhabditis elegans. At least sixteen different genes control timing and spatial development of the 1090 cell embryo in which 131 of the cells die at exact times in development (Bowen, 1993; Eastman, 1993). Genes regulating death are abbreviated ced. Mutations in ced 3 or ced 4 may halt apoptosis. Ced 9 acts similarly to bcl-2 to prevent apoptosis. Several genes are activated to govern orderly phagocytosis of dead cells. Yet another gene codes for an endonuclease in the phagocytic cells for DNA lysis. Clinical trials are already underway but certainly much remains to be learned if we are to successfully manipulate cellular fate by apoptosis as a powerful therapeutic tool without the current undesirable side affects.

In summary, hamster CL are ephemeral ovarian endocrine glands serving to produce P necessary for the support of pregnancy. The dynamic process of SL involves endocrine and immune system interaction. In many instances the presence of immunocytes is a sign of aberrant (even autoimmune) malfunction of an organ. In the ovary, however, it seems that the immune system is uniquely involved in physiologic as

well as pathologic events (Norman and Brannstrom, 1994). Interestingly, ovarian processes involving the immune system such as follicular atresia and luteolysis proceed by physiologic cell death or apoptosis. In the vast majority of apoptotic settings inflammatory phenomena are absent. This suggests that apoptosis may have a distinct biologic advantage by allowing for the orderly depletion of unwanted or unnecessary cell damage to adjacent healthy parenchyma. However, both apoptosis and inflammation are coexistent in luteolysis, and therefore an apparent paradox exists. Moreover, apoptosis in many systems is known to be genetically highly regulated. Thus, spontaneous luteolysis in the hamster provides a unique and valuable system in which to investigate these complex mechanisms of cellular demise.

CHAPTER II: AN ASSESSMENT OF THE FINE STRUCTURE OF THE CORPUS LUTEUM DURING LUTEOLYSIS IN THE HAMSTER

Introduction

Ultrastructural studies of luteal morphology have been conducted in a number of species including rat, mouse, mink, rabbit, armadillo, pig, sheep, human (Christensen and Gillim, 1969), guinea pig (Paavola, 1977) and hamster (Leavitt et al., 1973). Leavitt et al. (1973) produced the cursory description which follows, based only on one observation taken from 1000-1200 hours on each of the four days of the cycle.

D1, termed luteinization, consisted of the formation of CL from ruptured graafian follicles and the establishment of P secretion. Granulosa lutein cells were the most numerous cell type present within the developing CL. They had many microvilli, pleomorphic mitochondria with tubular cristae, scattered golgi elements, abundant SER, numerous polyribosomes and also lysosomal-like dense bodies. A small population of theca lutein cells were also present at the CL periphery.

D2, was described as the secretory phase. Luteal cells became hypertrophic and contacted one another while they formed numerous cellular interdigitations. The SER dilated markedly and the golgi apparatus was well developed. Mitochondria appeared swollen and oval-shaped with enlarged tubular cristae. A few cytoplasmic lipid droplets and dense bodies were noted. Peripheral thecal cells appeared as on D1.

D3, was described as luteolysis. A reduction in cell size or volume and disorganization of the SER coincided with an increase in extracellular space. The RER appeared unchanged. Disorganization of the SER was associated with the formation of detached and contorted cellular membranes and extracellular debris, i.e., myelin figures. Mitochondrial alterations were noted by the presence of annular and C-shaped forms. There was an increase in cytoplasmic lipid droplets and lysosomal bodies. Neutrophils were seen amongst the luteal cells. More collagen fibrils appeared to be present than on D2.

D4, was labelled advanced luteolysis. The CL appeared pale and ischemic indicating a much reduced blood supply. Advanced autolysis was apparent by the abundance of lysosomes, myelin figures and translucent vacuoles. Many cells had been phagocytized and "dead" cells with pyknotic nuclei were abundant. Neutrophils and large, debris-laden "macrophages" were distributed throughout the CL. Clumps of viable cells adjacent to "autolyzing" cells were seen. "Autolytic" cells showed much reduced SER content. Most luteal cells had abundant large lipid droplets, frequently associated with lysosomal elements.

The above investigators (Leavitt et al., 1973), also pointed out the unique nature of luteolysis in the hamster in confirmation of a previous description (Greenwald and Rothchild, 1968); that is, SL was essentially completed within one estrous cycle. This was different from other rodents such as mice and rats in which at least three generations of CL are present within the ovary. Therefore, in the hamster only the thecae folliculae of

atretic follicles contributed P to the next preovulatory surge on the afternoon of D4 because by this time the CL were in advanced regression and incapable of P production.

The above report was published at a time when apoptosis was relatively unknown. The landmark study by Kerr et al. (1972) provided evidence of a novel form of cell death which is widespread throughout cell biology. This physiological type of cell death is marked by a distinctive morphology seen in many diverse settings such as morphogenesis, ordinary tissue turnover and lymphocyte ontogeny. Features include chromatin condensation into rounded pyknotic masses and cytoplasmic volume loss or cell shrinkage. This is followed by membrane ruffling and cellular fragmentation into many intact membrane-bound vesicular bodies containing either condensed chromatin or cytoplasmic proteins and organelles. The apoptotic bodies express new epitopes on their external membrane surfaces which promote prompt phagocytosis by resident histiocytes or viable neighboring cells. Phagocytosis of dead cells by surviving resident tissue cells may account for the lack of an inflammatory response which typifies apoptotic cell death. Apoptosis differs considerably from necrosis or nonphysiological cell death. In necrosis the cell swells and ruptures releasing lytic lysosomal enzymes to the extracellular space causing further tissue damage and inflammation (Kerr et al., 1972 ; Eastman, 1993).

Apoptosis is commonly considered to be genetically regulated. It is routinely observed in hormonally-deprived target tissues. O'Shea et al., (1977) were the first to suggest that apoptotic cell death occurs in luteolysis in the ewe. More recently, evidence of apoptosis during rat (Zeleznik et al., 1989) and bovine (Juengel et al., 1993) luteolysis

has been reported. Current reports by McCormack and Greenwald (submitted) and McCormack and Friederichs (submitted) have provided strong biochemical and *in situ* end labelling evidence for apoptosis during hamster luteolysis.

In the present study the ultrastructure of the CL in the hamster is revisited. The results are largely in accord with the work of Leavitt et al.,(1973). In addition, they provide fine structural evidence for apoptotic and inflammatory phenomena occurring during SL. The classic view of apoptosis excludes an inflammatory response. My results contradict that impression and provide evidence that a modified, possibly tightly regulated, inflammatory response occurs during apoptosis.

Materials and Methods

Mature female golden hamsters were kept on a 14:10 hour light:dark cycle with lights on at 0500 and off at 1700. Each animal was caged separately following confirmation of three consecutive estrous cycles. Ralston Purina rodent chow and water were provided ad libitum. Animals were used in this study only after displaying three consecutive estrous cycles confirmed by vaginal discharge (Ward, 1946). Three animals were killed at each of the following times: D1 0900, D2 0900, 2400, D3 0300, 0600, 0900, 1300, 1500, And D4 0900. Additionally, one D3 1200 hour animal and one D2 1200 hour animal (control) were infused via abdominal vena cava with 1 ml of india ink which circulated approximately 30 minutes before death. All animals were anesthetized by i.p. sodium pentobarbital at 100 mg/kg. A midline abdominal incision was made followed by reflecting the chestplate to allow cardiac perfusion with an 18 gauge

pediatric cannula. The perfusate was delivered using a Harvard perfusion pump and included 20 ml 0.9% saline followed by 90 ml Karnovsky's fixative. Karnovsky's (1965) fixative consisted of 1% paraformaldehyde and 1.5% glutaraldehyde in 0.12 M sodium phosphate buffer, pH 7.4. Ovaries were harvested and the whole organs were placed in fixative overnight. The next day the CL were dissected from the ovaries of D3 animals and these and the ovaries from D1, D2 and D4 were post-fixed in 1% osmium tetroxide in 0.12M sodium phosphate buffer, pH 7.4 for 90 min. Ovaries were then quartered and dehydrated in a graded series of ethanol, (30%, 50%, 70%, 80%, 95%, 100%, 100%) followed by three changes of propylene oxide (PO) for 20 min. each. Polymer infiltration began with a 2:1 solution of PO: Epon/Araldite (EA) for one hour. The EA (Tousimis Research Corp.) was prepared as follows:

1. 10 ml Araldite 502
2. 10 ml Epon 812
3. 24 ml DDSA (dodecyl succinic anhydride)
4. 0.66 ml DMP-30 (tri-dimethylamine methyl phenol)

Specimens were then placed in 1:2, PO:EA for one hour, after which tissues were infiltrated in pure EA for one hour. Finally polymerization in fresh EA occurred in block molds placed in a vacuum oven at 60°C for 48 hours. Epoxy blocks were then trimmed with razor blades under a dissecting light microscope followed by thick sectioning with a glass knife at 1-2 μm on a Porter-Blum Sorvall MT-2 ultramicrotome. These sections were placed on glass slides and stained with 0.1% toluidine blue in 1% sodium borate.

Sections were coverslipped with permount resin for light microscopic observations (LMO) and photomicrography with an Olympus BH-2 microscope equipped with an Olympus C-35A camera and AD systems exposure control unit. Fuji 100 Super HG II color film was used. Results are shown in figures 1-44.

After LMO the blocks were trimmed and sections cut for examination by TEM with a JEOL-100S microscope at 80 kV. The sections were cut using a diamond knife at 0.06-0.08 μm and floated out before placement on 200 μm mesh naked copper grids.

Thin sections were then heavy metal stained with:

1. Freshly filtered saturated uranyl acetate in 50% EtOH in the dark for 10 min., wash thoroughly with dH_2O .
2. Lead citrate 10 min., wash thoroughly with dH_2O . See figures 45-72.

Results

The LMO and TEM observations in this study agree with the limited ones reported by Leavitt et al. (1973) for equivalent reference time frames unless specifically indicated. In keeping with their reporting format, results will be chronicled as D1-luteinization, D2-secretory phase, luteal-follicular shift (from D2 2400 hours to D3 0300 hours), D3-luteolysis, and D3-advanced luteolysis (from D3 1530 hours to D4 0900 hours). The major difference between this and the previous report (Leavitt et al., 1973), is the expanded number of observations made herein at critical stages of FL and SL.

D1-luteinization. At 0900 hours the forming CL are readily discernable although they are not yet well vascularized, appearing similar to ruptured follicles on low power

(figures 1-2). The ultrastructural findings are in accord with those of Leavitt et al. (1973) and as restated in the introduction to this chapter.

D2-secretory phase. The CL are well vascularized and appear functional. The LM characteristics of the CL can be appreciated in figures 3-7. The fine structure can be seen in figure 46. The description of CL from this period matches that of Leavitt et al. (1973) and is provided in the introduction to this chapter.

Luteal-follicular shift (L-Fs). From 2000 hours on D2 until 0400 hours on D3 the CL secrete maximal cyclic levels of P followed by a rapid plunge to a nadir as follicular E secretion begins to increase. This shift in the ovarian cycle from the luteal to the follicular phase has been termed the L-Fs (Terranova and Greenwald, 1978). This represents that brief period of FL in which the present findings reveal there are ultrastructural alterations detectable only at the TEM level and are unappreciated by LMO. At 2400 hours on D2, the midpoint of the L-Fs, extracellular debris begins accumulating in the form of membranous (myelin-like) figures. These probably represent sloughed SER. Mitochondria become less opaque and rarified and thus appear more electron dense. Lipid accumulates in large droplets within the cytoplasm of some luteal cells. Luteal cells remain approximated to one another except in areas of myelin figure deposition. Figure 47 shows these fine structural modifications which are not apparent in the LMO of figure 8.

Observations at the TEM level of 0300 hours on D3 luteal tissue reveal an increase in the aforementioned subtle alterations in ultrastructure. At 0300 hours,

changes in the endothelium are apparent. Myelin figures are seen in capillary lumina and transcytotic vesicles are detected (figures 48 and 49). Lysosomal elements are more frequently seen, some of which are large (figure 50). Figures 9-12 are LMO and thus show seemingly unaltered morphology from prior to the L-Fs.

Atrophic alterations of luteal cell ultrastructure at 0600 hours on D3 (post L-Fs) are only slightly increased from D3 0300 hours. Some cells have increased lipid droplet accumulation and more extracellular myelin figures are present than noted at 0300 hours. There is also an increase in intracellular debris and lysosomal formation (figure 51). Among the most remarkable changes in luteal histology is the appearance of newly emigrated neutrophils (figures 13-15). Another notable finding is the increased formation of blebs and vesicles within the endothelium. A particularly key finding is the first appearance of frequent apoptotic figures (figures 16-17, 52-53).

D3-luteolysis. Leavitt et al. (1973) included only one time reference point from D3, at approximately 1000 hours. Observations at this time were also made in the present studies for direct comparison but were found to be comparable with 0900 hours. The findings were stated in Leavitt et al. (1973) and again in the introduction to chapter II in the current work. Figures 54-55 represent results at 0900 hours. It should be noted that the incidence of apoptotic figures (previously referred to as pyknotic by Leavitt et al., 1973) is increased from 0600 hours for both luteal cells and endothelial cells (figures 18-22). Interestingly, one may occasionally observe a mitotic figure which seems oddly out of place in an apoptotic setting as shown in figure 23. In addition to forming many

transcytotic vesicles and cytoplasmic blebs, the endothelium forms bizarre transluminal membrane fusions which appear baffle-like (figures 24, 56). Numerous large endothelial blebs are demonstrated in figure 57. Other less frequent findings at 0900 hours are apoptotic PMNL and the apparent transformation of some luteal cells into phagocytic cell types which engulfed apoptotic and atrophic debris (figure 25).

At 1200-1300 hours more pronounced structural regression is apparent than at 0900 hours. Most luteal cells show dramatically reduced SER and many exhibit significant cytoplasmic lipid and lysosomal accumulations. Mitochondria are pleomorphic and quite electron dense (figure 58). There is an overall increase in extracellular space due to luteal cell dropout and atrophy. There are fewer cell-cell junctions and more "transformed" luteal cells are observed (figures 26-27, 59). The results of india ink infusion revealed that CL continue to receive some blood flow until midafternoon of D3. The capillaries are hyperpermeable as indicated by the escape of carbon particles beyond the intravascular space (figures 60-61) as compared to the intact capillaries of D2 controls. Transcapillary endothelial baffle formation and endothelial cell death progressively occlude CL blood flow (figures 28-32, 62-64).

1530 hours on D3 and beyond into D4 represents the phase of CL regression which can be regarded as advanced luteolysis. The CL are essentially avascular and apoptosis is widespread. This phase leads to grossly visible rapid reduction in CL size. The avascular quality of the CL at this time is demonstrated by figures 33, 34 and 65.

The widespread involvement and morphologic appearance of apoptosis can be seen in figures 35, 36 and 66.

D4-advanced luteolysis. Micrographs in this work mirror those presented by Leavitt et al. (1973). However, the interpretation herein is significantly different for this period of observations. This is due to the proliferation of knowledge regarding apoptosis. The CL are much reduced in size and pale (ischemic) at 0900 hours of D4 compared to D3 observations (figure 37). Many of the remaining luteal cells accumulate considerable lipid. It appeared that theca lutein cells accumulate less lipid and are less susceptible to apoptosis when compared to granulosa lutein cells (figure 38). Numerous apoptotic bodies are seen throughout the disorganized luteal parenchyma, some of which had been engulfed (figures 39, 67-68). Many transformed luteal-phagocytic cells are identified (figures 40-43, 69 -70). These were regarded previously as macrophages by Leavitt et al. (1973). Scattered atrophic cells which had not yet undergone apoptosis, are also observed. Usually (but not always) these cells tend to accumulate large lipid droplets in their cytoplasm as well as numerous lysosomes. Surviving cells have few mitochondria and scattered patches of RER remain. Their nuclei are large and nearly completely euchromatic (figure 71). Rarely, a patent capillary is found. Most are obliterated and the vast majority of those that are recognizable are blocked with apoptotic debris such as the one demonstrated in figure 72. By the end of D4 and the onset of the next cycle, only a tiny vestige of the CL remains. A fortunate section through the ovarian cortex occasionally contains one of these remnants (figure 44).

Discussion

Exposure to FSH is responsible for the differentiation of follicular epithelial cells. The preovulatory LH surge, brought about by the rapid rise in E secretion by graafian follicles, (D4), is thought to be responsible for luteinization of follicular cells and their subsequent secretion of P by the CL. If the pituitary is removed after this time on D1 the CL will develop and thereafter regress as in intact animals (Greenwald and Rothchild, 1968). Thus, it seems the pituitary does not have a role in either sustaining luteal function or in halting it through a luteolytic hormone(s) in the cyclic hamster. In response to mating (cervical stimulation) the pituitary releases a luteotrophic complex of FSH and Prl (Greenwald, 1967; Greenwald, 1973). These hormones induce a state of pseudopregnancy which prolongs luteal function for several days before luteolysis ensues. Hysterectomy of pseudopregnant animals prevents luteolysis (Duby et al., 1969). Treatment with indomethacin (cyclooxygenase inhibitor) does the same (Lau et al., 1975) whereas treatment with PGF₂α induces luteolysis (Kimball and Porteus, 1978). Taken together, these findings indicate that uterine PGF₂α release brings about spontaneous luteolysis in the pseudopregnant hamster. However, hysterectomy does not prevent luteolysis in the cyclic hamster (Duby et al., 1969). Thus, the luteolytic signal is neither of pituitary nor uterine origin. Since no significant incidence of apoptosis was seen prior to PMNL invasion in this study it is not clear whether spontaneous luteolysis is due to the lack of pituitary support necessary for prolonged luteal function or due to some affect(s) brought about by the neutrophils. It is known that the CL can be brought to full

functional capacity as late as 54 hours after ovulation with exogenous gonadotrophic support (Greenwald and Rothchild, 1968), i.e., the time at which PMNL begin emigrating *en mass*. This information makes it tempting to favor the notion that PMNL may indeed be initiating apoptosis. However, an alternative needs to be considered. According to Rothchild's (1981) hypothesis, waning P secretion at the end of the luteal phase (period of L-Fs) sets up conditions which favor the formation of intraluteal $\text{PGF}_2\alpha$. Since atrophic ultrastructural modifications occurred in the L-Fs period, it seems possible that these changes could culminate eventually in widespread luteal apoptosis. Furthermore, the PMNL normally observed may merely respond to inflammatory mediators and their presence simply coincides with the onset of apoptotic death. It is also possible that some combination of these two mechanisms can account for the onset of luteolysis. This will be discussed in the summary of the current study (chapter V).

Several important conclusions are evident. First, the results show that while FL is occurring (L-Fs) and P production is falling off, subtle atrophic (reversible) changes in CL ultrastructure take place which are not resolveable at the light microscopic level. SL and FL thus seem concurrent in the hamster as has been suggested (Leavitt et al., 1973). SL can be thought of as existing in two phases. In the preapoptotic phase of the L-Fs which coincides with FL, atrophic changes consist mainly of myelin figure formation, mitochondrial condensation and endothelial vesicle formation. In the second phase (SL) which takes place directly after the arrival of PMNL, apoptosis increases markedly in its incidence from 0600 hours on D3 throughout D4. The progressive increase in apoptosis

is in accord with that reported in the ewe (O'Shea et al., 1977; Azmi and O'Shea, 1984), the rat (Zeleznik et al., 1989), the cow (Juengel et al., 1993) and the hamster (unpublished data in this laboratory). Subcellular changes similar to those seen in the present study have been noted in apoptosis could be initiated by some factor(s) produced by the neutrophils. From the work of McCormack and Greenwald, (submitted), it is known that the PMNL produce TNF α which has been shown to have luteolytic affects in cows (Benyo and Pate, 1992). The present series of studies (see chapter IV), shows that PMNL myeloperoxidase is present in CL at 0600 hours on D3. It is possible that both of these factors, as well as other neutrophil products, could be antigonadotrophic.

Secondly, the presence of PMNL in luteolysis is an accepted cellular marker of acute inflammation. The derangement observed in vascular permeability is further evidence of inflammatory phenomena occurring in SL. Inflammation is not customarily considered to accompany apoptotic cell death. In fact, the contrary is usually true, i.e., apoptotic settings are typically devoid of inflammatory processes (Kerr et al., 1972; Fesus, 1993). Apoptotic cell death is seen as an orderly way to regulate tissue kinetics such that rampant inflammation does not destroy more tissue than is required to achieve homeostasis. Therefore, it would appear that a paradox exists in luteolysis. However, the explanation may be straight forward. For instance, if necrosis (in which inflammation is virtually always present) were to account for the regression of the CL, a large inflammatory influx into a considerable portion of the ovarian cortex would take place after each infertile cycle. A chronic state of inflammation would set in with significant

scarring, tissue destruction, and jeopardy of adjacent cortical parenchyma. On the other hand, apoptosis alone would likely take a prolonged period to deplete the considerable mass of tissue in the CL. Clearly, apoptosis, accompanied by (if not induced by) a tempered, quickly resolving inflammatory event would be an excellent mechanism to bring about the swift and orderly CL regression necessary to accommodate the extremely rapid tissue turnover in the ovary. In keeping with traditional apoptotic processes and consistent with attenuated inflammation, remaining viable tissue cells could account for the phagocytotic function seen in luteolysis (at least in the cyclic hamster). These were previously referred to as macrophages which are the central cells involved in directing chronic inflammation. As luteolysis is essentially completed in less than two days, a chronic state of inflammation is not likely to be generated..

The present study has reviewed the findings of the chief morphological study conducted in the hamster (Leavitt et al., 1973). Results interpreted with knowledge of apoptotic phenomena have revealed two significant findings. First, SL begins with an initial, short (reversible), preapoptotic phase in which inflammation is absent. This corresponds to the time of FL or the L-Fs. Secondly, the initial atrophic phase is followed by an apoptotic phase which is accompanied by a mild inflammatory reaction which appears to provide an evolutionary advantage in rapid tissue turnover.

**CHAPTER III: INCREASED NONSPECIFIC ESTERASE ACTIVITY IN
OVARIAN FOLLICULAR ATRESIA AND CORPUS LUTEUM
REGRESSION IN THE CYCLIC GOLDEN HAMSTER**

Introduction

It has long been recognized that the extensive tissue turnover and remodeling that occurs within the cycling mammalian ovary during the processes of follicular atresia and luteolysis is accomplished with the aid of both resident and newly emigrated white blood cells (Adashi, 1990; Wang et al., 1992). Previous reports described this as necrotic cell death (Guyara and Greenwald, 1965; Rothchild and Greenwald, 1968). However, with the advent of the concept of apoptosis in Kerr et al.(1972) an increasing number of instances of physiologic cell death have been recognized to be regulated in part by this process. Apoptosis can be readily observed in epithelial turnover, embryonic development (programmed cell death), hematopoiesis, lymphocyte ontogeny, neutrophil senescence, targets of trophic factor and hormonal withdrawal (post-lactational mammary glands, etc.) and many others. Recently, the processes of ovarian follicular atresia and CL regression were observed to be governed by apoptotic cell death as well (O'Shea et al.,1977; Azmi and O'Shea, 1984; Zeleznik et al., 1989; Tilly et al., 1991; Juengel et al.,1993).

On the other hand, apoptosis is considered the functional or physiologic antithesis of mitosis and, in conjunction with it, regulates organ maintenance through the growth or involution of component tissues (Bowen, 1993). Effete, damaged, precancerous or superfluous cells can be deleted through this process. Apoptosis is distinguished by distinct biochemical and morphological features. The key morphological alterations include condensation of the cell (shrinkage), condensation of the chromatin adjacent to the nuclear membrane, cell fragmentation into apoptotic bodies and phagocytosis of these bodies by viable neighboring cells and any resident histiocytes (Kerr et al., 1972). The histologic characteristics of apoptosis are of short duration, lasting about 3-4 hours (Fesus et al., 1991; Schulte-Hermann et al., 1992). The membranes of the apoptotic bodies and their component organelles are intact and the external surface of the bodies have epitopes which enhance recognition by phagocytes, i.e., resident histiocytes or viable parenchymal cells.

It has long been recognized that the extensive tissue turnover and remodeling that occurs within the cycling mammalian ovary during the processes of follicular atresia and luteolysis is accomplished with the aid of both resident and newly emigrated white blood cells (Adashi, 1990; Wang et al., 1992). Previous reports described this as necrotic cell death (Guyara and Greenwald, 1965; Rothchild and Greenwald, 1968) and only more recently have these processes been recognized to involve apoptosis. Apoptosis is carefully regulated and requires gene transcription and translation of effector proteins in many cases. In cells destined to undergo apoptosis, activation of a $\text{Ca}^{++}/\text{Mg}^{++}$ dependent

endonuclease typically occurs such that genomic DNA is cleaved into oligonucleosomic fragments, the smallest of which are 180-200 base pairs in length. This leads to the pyknotic appearance of the nucleus and the "laddering" pattern of DNA on agarose gel electrophoresis (Zeleznik et al., 1989; Juengel et al., 1993; McCormack and Greenwald (submitted)). A host of other biochemical events may occur as well, such as transglutaminase activation (Piacentini et al., 1991) and increased lysosomal hydrolase content (Kerr et al., 1972; Sarraf and Bowen, 1986; Bowen, 1993). This latter event is the focus of the current investigation. Previous reports demonstrated an increase in acid phosphatase activity during SL in the hamster (Chatterjee and Greenwald, 1976; Saidipur and Greenwald, 1978). The present study expands this finding to include demonstration of increased activity of α -naphthyl acetate esterase (ANAE) during luteal regression and follicular atresia. Increased esterase activity was also previously noted in luteolysis and follicular atresia in the rat (Banon et al., 1964; Lobel et al., 1961). The technique employed is an enzyme histochemical method designed to show cells containing enzymes capable of hydrolyzing α -naphthyl acetate (ANA) (Ranki and Häyry, 1979; Ranki et al., 1980; Kiernan, 1990). Since specific esterases like lipase, acetyl cholinesterase and cholinesterase are capable of hydrolyzing ANA, as are the nonspecific esterases (classified as types A,B,C and pseudocholinesterase), a number of chemical inhibitors were utilized to determine the nature of the enzyme operating in this system (Pearse, 1972; Bancroft and Stevens, 1990).

Materials and Methods

Three mature female golden hamsters displaying at least 3 consecutive four day estrous cycles were killed on each day of the cycle after sodium pentobarbital anesthesia (i.p at 100 mg/kg). Ovaries, oviducts and splenic samples were harvested and immersed in Formal-calcium fixative overnight at 4°C. This fixative is prepared by adding 20 g calcium acetate (CH₃COO)₂Ca H₂O to 100 ml formalin (37-40% HCHO) and bringing the volume to 1000 ml with dH₂O. Tissues were then washed in 0.07M phosphate buffer, (pH 5.3) for 30 min. The tissue was then dehydrated in 2 changes (2X) of absolute acetone for 30-60 min. each, as EtOH inhibits ANAE activity. After clearing in toluene the tissues were infiltrated with molten paraffin (MP 56.5 +/-0.5⁰C) and embedded in blocks from which 5 µm sections were cut on a rotary microtome. The sections were floated out on warm dH₂O covered, glass slides which were coated with egg albumin affixative. Sections were allowed to dry overnight on a warming plate at 43°C. ANAE staining was carried out in Coplin staining jars according to Kiernan (1990) as follows:

1. Deparaffinize sections in xylene 2X @ 3min. each
2. Displace xylene in absolute acetone 2X @ 2 min each
3. Wash in dH₂O 3X @ 1min. each
4. Expose sections for 30-45 min. to incubation medium. prepared as follows:
 - a) 40 ml 0.07M phosphate buffer, pH 5.3
 - b) 0.5 ml enzyme substrate stock solution (200 mg ANA in 10 ml acetone kept @ 4°C between uses).

c) 2.4 ml hexazonium pararosaniline. This is a combination of 1.2 ml pararosaniline (2.0 g pararosanalin) in 2.0 M HCl which is heated to boiling, allowed to cool, filtered and kept @ 4°C) and 1.2 ml sodium nitrite (1.0 g in 25 ml dH₂O made fresh each day).

d) adjust pH to 5.8 with 1M NaOH.

5. Wash sections in dH₂O 3X @ 1 min. each.
6. Counterstain in 2% methyl green for 6 min.
7. Dip slides in dH₂O for 5 sec.
8. Dip slides in acetone 2X @ 3 sec. each.
9. Clear sections in xylene 2X @ 3 min. each.
10. Mount in Permount and coverslip before viewing.

The following enzyme inhibitors were employed: 0.2M NaF, a pseudocholinesterase blocker, 0.2 mM ME-600, a B-type nonspecific esterase blocker, 0.2 mM eserine, a cholinesterase blocker, and 100 µM phenyl mercuric chloride, an A-type nonspecific esterase blocker. Each of these compounds was added to the incubation medium separately.

Results

Spleen: An occasional lymphocyte with a reddish-brown granule or two in its rim of cytoplasm could be found. Large splenic macrophages which stained diffusely throughout their cytoplasm were plentiful (figure 73).

Oviduct: All regions of the duct showed reactivity in the lining epithelia with the isthmus reacting more intensely than either the ampulla or infundibulum. A few large random cells within the wall of the duct displayed a diffuse reaction product and were taken to be macrophages. No distinctive changes were noted in reactivity in relation to the time of the cycle for this organ. Several specimens retained the proximal region of the uterus as a matter of less complete dissection. No reaction in the epithelia were observed here. However, more observations are required to draw any conclusions. See figure 74.

Ovary: Several subcompartments of the ovary demonstrated reactivity. A large number of observations were made of sections from each day of the cycle to reduce variability in results since some sections did not react while others reacted very strongly. The following remarks therefore reflect the most often encountered results.

Healthy multilaminar primary follicles which had not yet begun accumulating liquor folliculi were unreactive (figures 75-77). The thecae internae of healthy and atretic follicles of all sizes were unreactive (figures 75-80). The granulosa of secondary and graafian follicles reacted light-moderately (figure 77). Atretic granulosa cells showed remarkably intense reactivity (figures 75-80). Cells with pyknotic nuclei, typical of apoptosis, reacted very strongly as did the cytoplasmic component of the apoptotic bodies within the antra of these follicles. Enlarged healthy-appearing (nonpyknotic), detached granulosa cells within the antra of atretic follicles also demonstrated a strong cytoplasmic reaction (figure 77, 79-80). These cells are called "transformed" cells because

they appear as though they transform into phagocytes. A few of these cells remain long after a follicle regresses into the secondary interstitium although the intensity of their cytoplasmic stain fades. These cells go on to accumulate lipofuscin and iron as seen by the Perl's (Kiernan, 1990) reaction (unpublished observation).

CL from D1 and D2 of the cycle (D1 is estrus) typically reacted light-moderate throughout (figures 81-82). A few specimens did not react, however. D3 CL consistently demonstrated foci of intense reactivity above background (figure 83). At higher magnification, these areas showed cells undergoing apoptosis (figure 84). Most of these cells were either endothelial or granulosa. Neutrophils were plentiful in the CL but unreactive to ANAE (figure 84). On D4, the CL were essentially avascular with greatly increased frequency of apoptotic foci (figures 85-87). A few small remnants of CL in advanced regression were identifiable by the onset of the next estrus by their intense ANAE reactivity (figure 88).

The results of the specimens exposed to inhibitors in the incubation medium revealed that only the pseudocholinesterase blocker, NaF, inhibited enzyme activity.

Discussion

The results of this investigation highlight several important points. First, it should be noted that just as acid phosphatase activity, or any other hydrolytic enzyme activity, is not usually associated solely with cell death, neither should ANAE activity be considered a sine quo non of apoptosis. Secondly, however, it appears that elevated autophagic and heterophagic lysosomal hydrolytic enzyme function is enhanced in many apoptotic

situations. Chatterjee and Greenwald (1976) and Saidipur and Greenwald (1978) noted a marked increase in acid phosphatase and alkaline phosphatase during luteolysis in the hamster. Banon (1964) showed nonspecific esterase activity increases in both follicular atresia and luteolysis in the rat. Likewise, Bowen (1993) documented an increase in hydrolytic enzyme activity in several other systems involving apoptotic cells. Taken together these findings indicate that a considerable amount of autolytic activity occurs in apoptosis but in a fashion fundamentally unlike that of necrosis. In necrosis the enzymes leak into the cytoplasm and extracellular space where they cause tissue damage and provoke an inflammatory reaction (Schulte-Hermann et al., 1992; Fesus et al., 1991). This is clearly undesirable as it may lead to diminished tissue function. In contrast, apoptotic cells go through a series of alterations culminating in an orderly self destruction. The dead cells are readily recognized by resident histiocytes or neighboring cells and are transformed into secondary phagocytes which engulf the fragmented apoptotic bodies thus preventing an aggressive inflammatory response (Kerr et al., 1972; Fesus et al., 1991; Cohen, 1993). I believe this is the case in luteolysis and is partially so in atresia as well. Although leukocytes are present during the above events, they do not interfere with prompt and uneventful resolution in most cases. As suggested by Kerr and coworkers (1972), apoptosis, seems to be an evolutionarily derived protective mechanism of tissue dynamics which is as vitally required as mitosis for the success of the organism. Finally, the orderly utilization of hydrolytic enzymes such as acid phosphatase and

ANAE on the part of the dying cells as well as their transformed neighbors may be a fundamental component of apoptosis in the events of follicular atresia and CL regression.

CHAPTER IV: WESTERN BLOT DEMONSTRATION OF
MYELOPEROXIDASE AS A BIOMARKER OF ACUTE
INFLAMMATION IN LUTEOLYSIS

Introduction

The accumulation of neutrophils or PMNL in tissues is a hallmark of acute inflammation (Mulder and Colditz, 1993). This class of leukocytes responds first to inflammatory stimuli and as such constitute the first line of defense against bacteria, etc. (Lasky, 1993; Rochon and Frojmovic, 1992). Other major elements of acute inflammation are increased vascular permeability and altered vessel caliber, leading to plasma leakage and edema (Pettipher et al., 1993). PMNL are essential to the regulation of these events (Wedmore and Williams, 1981). The purpose of a beneficial inflammatory response is to neutralize the offending stimulus and restore tissue integrity.

PMNL develop in the bone marrow from granulocyte-macrophage stem cells over approximately a ten day period (Wedmore and Williams, 1981). Up to the myelocyte stage of development, cell divisions are common and primary and secondary cytoplasmic granules form. The post-mitotic phase involves nuclear condensation and lobulation and is a period of transition toward functional maturation. The marrow can produce more than one hundred billion new PMNL per day when challenged! PMNL are terminally

differentiated and short-lived with a half-life in the circulation of only six hours (Weiss, 1988). In fact, to extend their lifespan beyond 24 hours within tissues, colony stimulating factors are required and these can only hold back the cell destruct program briefly (Cohen, 1993). Activation occurs in the bloodstream, presumably by chemotactic stimulation (Gallin, 1993). Cell surface receptors for chemoattractants, immunoglobulins and complement fragments are increased upon activation. In addition, PMNL become primed with increased adherence factors. Chemotaxins are concentrated at inflammatory sites and the PMNL decelerate and roll along the endothelium until they marginate in a receptor-ligand fashion and leave the circulation. Emigration is then directed by chemotaxis to compounds such as leukotriene B4 (LTB₄), complement fragment C5a, interleukin-8 (IL-8), N-formyl-methionyl-leucyl-phenylalanine (f-M-L-P), tumor necrosis factor alpha (TNF- α) and bacterial lipopolysaccharide endotoxins (LPS) for which PMNL have surface receptors (Kumar et al., 1992; Mulder and Colditz, 1993). Emigration is also accompanied by granule release and generation of toxic O₂ species known as free radicals. These include H₂O₂, superoxide and hydroxyl radicals in addition to other electron-rich reactive O₂ products. PMNL use the plasma membrane -based enzyme NADPHoxidase to generate superoxide radical and H₂O₂. I suggest the simple term "*toxygens*" when referring to toxic O₂ radical species collectively.

Upon exposure to proper activating stimuli, PMNL begin to consume O₂ at up to fifty times their resting levels in a state known as the respiratory burst. This is

accomplished by increasing glucose oxidation via the hexose monophosphate shunt which is required for *toxygen* formation and effective phagocytosis (Absolom, 1986). Primary (azurophil) granules are used principally for phagolysosomal digestion, e.g., killing and degradation of microbes. Specific (secondary) granules are more likely to be utilized extracellularly to initiate inflammation by translocation to the PMNL surface and exocytosis. This allows mediation of functions such as margination, chemotaxis and activation of microbicidal pathways (Gallin, 1993). Specific granule hydrolases also produce inflammatory mediators by their actions on complement components (C5) and kinin to form C5a and kininogen and also by invoking a monocyte chemoattractant (Gallin, 1993). The significance of granule utilization is apparent in several disorders. For example, those affected by Chediak-Higashi syndrome have numerous defects in readily initiating a successful inflammatory response due, partly, to improper fusion of phagosomes with lysosomal contents (Cotran et al., 1989). Patients with congenital specific granule deficiency syndrome (rare disorder) present with reduced inflammatory responses manifested by extreme epidermal and deep tissue bacterial infections (Gallin, 1993). Those with autosomal recessive hereditary myeloperoxidase deficiency are apt to suffer recurring Candida albicans infections (Cotran et al., 1989).

In contrast to these impotent responses are states of amplified inflammatory activity which have poor resolution. These will be illustrated by three classic examples. First, in psoriasis, a chronic inflammatory dermatosis, excessive production of skin cells

with only a normal rate of loss leads to epidermal thickening and scaling overlying salmon colored plaques. Much of the psoriatic damage can be ameliorated by factors which attenuate neutrophilic function. Secondly, in chronic inflammatory bowel diseases like Chron's disease and ulcerative colitis, long standing foci of inflammatory infiltrate may produce granulomata and ulcers which can lead to fibrosing strictures, malabsorption, vitamin B12 deficiency, steatorrhea and, most ominously, carcinoma. Finally, patients with α -1-anti-trypsin deficiency are at great risk of developing emphysema because of an inability to sufficiently neutralize PMNL proteases which break down their alveolar walls. PMNL accumulation and degranulation are critical elements in the production of ongoing lesions and suffering in these patients.

It is clinically beneficial to monitor chronic inflammatory responses periodically (Krawisz et al., 1984). Several techniques to measure inflammation have been devised, all with particular drawbacks (Trush et al., 1994). A quantitative method which is gaining favor involves the enzymatic assay of tissue or body fluid samples for leukocytic myeloperoxidase (MPO) found in primary granules (Bradley et al., 1982; Krawisz et al., 1984; Trush et al., 1994; Edelstam et al., 1994).

MPO is also known as verdoperoxidase as it imparts the greenish hue seen in pus (Weiss, 1989). The function of this crucial enzyme is to catalyze the oxidation of electron donors, halides (Cl^-), by H_2O_2 . The level of MPO present by assay correlates nearly linearly with the number of PMNL found in histological sections (Krawisz et al.,

1984). Monocytes also have MPO but at much reduced levels. Histiocytes do not contain MPO. MPO has also been shown to metabolize and inactivate a number of inflammatory mediators by oxidizing methionine (Andrews and Krinsky, 1986; Gallin, 1993). These mediators include chemotactic stimuli such as C5a and f-M-L-P as well as phagocytosis stimulators such as the Fc portion of IgG and C3b coated particles. Neutrophils thus play a central role in establishment, amplification and resolution of inflammation and their degranulation activities are pivotal in the orderly occurrence of inflammatory events.

SL has been shown to involve PMNL in the hamster (Terranova and Greenwald, 1978) and rat (Brännström et al., 1994). O₂ radical formation has been implicated as an anti-gonadotrophic signal generated by infiltrating leukocytes in luteal regression (Wu et al., 1993; Aten et al., 1992; Hesla et al., 1992 Endo et al., 1993). Unchecked O₂ radicals induce plasma membrane breakdown by lipid peroxidation leading to loss of luteal membrane fluidity and function (Sawada and Carlson, 1988). Since MPO is a generator of *toxygens* and has been shown to be a valuable barometer of inflammatory intensity when assayed, I felt its detection may provide insights to the study of luteolysis. To my knowledge, only one previous investigation has performed an MPO assay using ovarian tissue and this was in an investigation of ovulatory mechanisms and not luteolysis (Chun et al., 1993). The process of ovulation is considered to be inflammatory in nature (Espey, 1980). As such, neutrophils are drawn into the area. However, according to Chun et al. (1993), PMNL are not mandatory for ovulation to occur. In their study the luteal and

nonluteal compartments were not separated. In this case, the design was valid because the rats used were superovulated, immature animals. Thus, their ovaries contained no degenerating CL (which would also contain MPO). This design is clearly not applicable to the present system in which both atretic follicles and regressive CL contain PMNL and thus presumably MPO. Here these elements must be separated to get an accurate portrayal of purely luteolytic MPO. Therefore, in the present study CL undergoing SL on the morning of D3 of the estrous cycle were dissected. The MPO assay, (Bradley et al., 1982; Krawisz et al., 1984) was found to be insensitive to the tiny amount of tissue inherent in our system. A hamster CL weighs only approximately 0.5 mg and even using several animals with roughly ten CL each, this is far less tissue than the smallest samples (200 mg) used in the above studies. As an alternative, Western blot analysis was used on luteal tissue pooled from three hamster ovaries (per time reference point) in order to demonstrate the appearance and disappearance of luteal MPO as a biomarker of acute inflammation.

Materials and Methods

Mature female hamsters were anesthetized by ethyl ether at the following reference points in their four day cycle (D1 is ovulation): 2400 hours D2, 0300 hours D3, 0600 hours D3, and 0900 hours D3. Three animals were killed from each of the above times. The ovaries were excised and the CL dissected out under a dissecting microscope. The CL and the nonluteal ovary (NLO) specimens were then minced in 0.1%

hexadecyltrimethylammonium bromide, 50 mM sodium phosphate, pH 6.0 (HTAB homogenization buffer). For each 1mg of CL or NLO tissue, 10 μ l of HTAB was added for homogenization in a microfuge tube. Cell membranes were further broken down by sonication on ice for 10 min. followed by three freeze-thaw cycles. The specimens were fractionated by differential centrifugation @ 40,000 x g for 15 min. and the supernatant solution was retained.

The Western blot was carried out according to the following protocol:

I. SDS-PAGE was carried out according to Laemmli, (1970). Approximately 30

μ g of protein were loaded in each lane and proteins resolved by SDS-PAGE, using a 15% gel.

II. Transfer of the protein from the gel to the membrane was performed as described below:

1. One layer of filter paper (Whatman 3MM) was soaked in anode buffer No.1 and the excess buffer allowed to drain from the filter paper. A drop of this buffer was placed on the middle of the electrode surface. Soaked filter paper was then layed down, centering and smoothing it out to allow good contact because any bubbles will distort the electric field and result in a poor transfer.

2. One layer of filter paper loaded in anode buffer No.2 was placed on top of the first paper. A glass rod was rolled over the filter paper to smooth and remove any trapped air bubbles.
3. A piece of Immobilon was activated by washing with methanol and then dH₂O. Immobilon was placed on top of the two pieces of paper.
4. The SDS-PAGE was placed on top of the Immobilon making sure there were no bubbles trapped between the paper and the gel.
5. A layer of paper soaked in cathode buffer was placed on top of the gel.
6. The “sandwich” was placed on the trans-unit and the lid put on without over tightening. The power supply was set at 130 mAmps constant current for 90min.

Buffers:

Anode buffer No.1: 0.3 M Tris, 10% methanol, pH 10.4

Anode buffer No.2: 25 mM Tris, 10% methanol, pH 10.4

Cathode buffer: 25 mM Tris, 40 mM 6-aminohexanoic acid, 20% methanol, pH

9.4

III. Immunodetection was accomplished using an alkaline phosphatase secondary antibody according to Bollag and Edelstein, (1991) as described below:

1. Immobilon was covered in blotto solution for one hour @ room temperature to block non-specific binding sites on the Immobilon.

2. The Immobilon was washed three times with TTBS for 5 min.
3. Immobilon was washed with TBS one time for 5 min.
4. The primary antibody was diluted into 5 ml of TBS (1:2000 rabbit anti-human MPO from Calbiochem, La Jolla, CA) and injected into a sealable plastic bag with the Immobilon on a rocker for 90 min.
5. Steps 2 & 3 were repeated.
6. The secondary antibody was applied in a total of 10 ml of TBS buffer (1:8000 goat anti-rabbit with alkaline phosphatase linkage from Sigma Chemical, St. Louis, MO) in the plastic bag and rocked for 60 min.
7. Steps 2 & 3 were repeated and one wash added with Tris-Cl for 5 min.
8. While washing in step 7, 1 tablet of 5-bromo-4-chloro-indolyl phosphate/nitro blue tetrazolium (BCIP/NBT, Sigma) was dissolved in 10 ml dH₂O. This is a precipitating substrate for the detection of alkaline phosphatase activity.
9. Immobilon was placed in a dish with BCIP solution to develop the secondary antibody. This took from 15 seconds to several min. Once bands were readily visible, the Immobilon was rinsed thoroughly with dH₂O to stop the reaction.

Buffers:

1. TBS (Tris Buffered Saline): 1.2 g Tris base (10 mM), 9.0 g NaCl (150 mM),

- 1000 ml dH₂O, pH 8.3.
2. Nonfat dry milk (blotto) 1%, 1 g in 100ml of TBS
 3. TTBS (Tween 20 in TBS): 2 ml Tween 20, 998 ml TBS
 4. Tris-Cl: 6.06 g Tris in 1000 ml dH₂O, pH 7.6

Results

The blot image is shown in figure 89. This is a labelled computerized scan of a photo taken after the blot was run. The first four lanes are consecutive luteal samples from before, during and after PMNL arrival in the CL in the peri-luteal-follicular shift period (Terranova and Greenwald, 1978). No significant reactivity for MPO presence is readily evident except for the 0600 hour sample. In the NLO samples from the same time reference points, no MPO presence is noted in the blot. The far right lane is a Sigma sample of MPO used as a control. There is a band of cross reactive protein which can be noted ubiquitously across the lower margin of the blot occurring in all lanes of both luteal and nonluteal samples.

Discussion

PMNL are the first line of defense in an inflammatory response and their actions are crucial to the proper development, maintenance and resolution of beneficial inflammatory responses. In settings of defective PMNL function, those affected suffer severe recurring infections (Krause et al., 1993). In cases of exuberant inflammatory phenomena featuring excess tissue damage, organ and host health can be at stake (Haslett,

1992). Thus, it is imperative to decipher the processes governing inflammatory responses for clinical intervention. It is often beneficial to use diagnostic indicators such as the MPO assay when evaluating inflammatory status (Bradley et al., 1982; Krawisz et al., 1984; Edelstam et al., 1994; Trush et al., 1994).

CL regression has characteristics of inflammation which occur spontaneously at the end of an infertile cycle (see chapter II above). One such indication of an acute inflammatory response is the accumulation of PMNL, heralding SL (Terranova and Greenwald, 1978). Among the most helpful techniques used to monitor inflammatory status is the measurement of MPO. In the present study, it was shown that in very small tissue samples MPO presence could be demonstrated as a biomarker of acute inflammation. This technique may have limited clinical application because it is somewhat tedious and not highly quantitative. On the other hand, it may have excellent potential as a beneficial tool in research of inflammatory phenomena in which only a limited amount of tissue is readily available.

It is interesting to note that at 0600 hours MPO is first detectable. This coincides with the arrival of PMNL to the CL. However, at 0900 hours there are still many PMNL present, yet a detectable content of MPO is not seen. This may be explained as follows: Once the NADPHoxidase system of the respiratory burst is operating to provide MPO with H_2O_2 as its substrate, HOCl is generated. As long as H_2O_2 is supplied, this will continue. However, it appears that, at least in humans, PMNL can only generate H_2O_2 for

up to three hours after specific triggering (Nathan, 1987). At that point the oxidant attacks and autoinactivates MPO itself (Weiss, 1989). Since it appears there is little increase in the accumulation of PMNL after the initial wave of 0600 hour invaders, we assume most of those present at 0900 hours have been there for several hours and may be nearly depleted of immunodetectable MPO.

Since little apoptotic death is detectable by *in situ* methodology before PMNL arrival (Friederichs and McCormack, submitted), it seems possible that PMNL may be involved in the onset of physical regression of the CL. Their ability to release *toxygens* could be one element of their anti-gonadotrophic affects and MPO activity is a critical part of *toxygen* release. Since structural regression occurs so rapidly in the hamster, PMNL may be a required factor in this process.

In summary, the appearance of MPO was demonstrated in luteal tissue at the time corresponding to the onset of SL. The use of immunoblots can be a valuable tool in the study of inflammatory processes. It is very sensitive and allows detection of MPO from samples that are too small to be useful when other methods are employed. The hamster CL provides an intriguing system for the study of several biological phenomena. Spontaneous luteolysis is an excellent system in which to examine the events involved with an acute inflammatory response. Two important questions yet to address come to mind. First, what is the chemotactic stimulus(i) directing the 0600 hour emigration? Secondly, are PMNL critical in establishing the rapid pace seen in the spontaneous SL?

CHAPTER V: A SUMMATION OF THE UNIQUE CHARACTERISTICS OF LUTEOLYSIS IN THE HAMSTER

The CL is a transient ovarian endocrine organ which is required to sustain pregnancy. It is formed from the luteinized remnants of ovulatory follicles. Its chief function is the secretion of P which maintains the uterus for reception of the conceptus and its development until parturition. The CL has varied gonadotrophic requirements which are species-specific. The formation, function and regression of the CL in the hamster are independent of the pituitary when it is removed after the preovulatory surge of FSH and LH (Greenwald and Rothchild, 1968). However, for pregnancy to occur and to be maintained, a luteotrophic complex of FSH and Prl is requisite (Greenwald, 1967; Greenwald, 1973). At the end of an infertile cycle, the CL must regress both functionally and structurally. In order for the next cycle to take place the CL must cease P secretion (FL) so that the next LH surge can induce ovulation. Physical regression (SL), is required for proper histoarchitectural balance, i.e., to ensure room for follicular development, etc. In the hamster, the switch from the luteal phase (P secretion) to the follicular phase (E secretion) occurs rapidly from 2000 hours on D2 through 0400 hours on D3. This period is known as the L-Fs (Terranova and Greenwald, 1978).

Hysterectomy prevents luteolysis in the pseudopregnant hamster but not in the cyclic hamster. Therefore, the luteolytic signal is neither of pituitary nor of uterine origin in the cyclic hamster. If $\text{PGF}_2\alpha$ is the operative luteolytic signal it would have to be generated within the CL itself, as proposed by Rothchild (1981). This is consistent with the fact that essentially all mammalian cells are capable of PG synthesis. $\text{PGF}_2\alpha$ works by a variety of anti-gonadotrophic mechanisms in which species-specific differences exist. Its proposed mechanisms of action are incompletely understood but include changes in ovarian blood flow, reduction in CL LH receptors, inhibition or uncoupling of LH-stimulated cAMP formation and protein kinase A activation, or direct cytotoxicity (Orlicky et al., 1992). In the rat, $\text{PGF}_2\alpha$ has been shown to decrease plasma membrane fluidity (lipid peroxidation) and increase superoxide radical and H_2O_2 formation (Wu et al., 1993; Niswender et al., 1994). Superoxide radical formation in turn activates phospholipase A_2 , the rate limiting enzyme in $\text{PGF}_2\alpha$ formation (Wu et al., 1992). $\text{PGF}_2\alpha$ has antisteroidogenic actions mediated through the PKC second messenger system via the activation of phospholipase C. Phospholipase C hydrolyzes the membrane lipid phosphatidylinositol 4,5-bisphosphate (PIP_2) to inositol-1,4,5-triphosphate (IP_3) and 1,2-diacylglycerol (DAG), (Niswender et al., 1994). DAG increases the affinity of PKC for Ca^{++} and IP_3 releases Ca^{++} from intracellular stores, resulting in an increase in $[\text{Ca}^{++}]_i$ and activation of PKC. Increased intracellular Ca^{++} is also involved in translocation of cytoplasmic phospholipase A_2 to the cell membrane (Wu et al., 1992). It is important to

keep in mind that $\text{PGF}_2\alpha$ will only exert its effects on luteal cells that have reached at least the mid-luteal phase or beyond. It has no luteolytic effects on young or forming CL.

It is interesting to note that a variety of apoptotic events are mediated by an increase in $[\text{Ca}^{++}]_i$, such as endonuclease and transglutaminase activation. These events are often preventable *in vitro* using chelators and are inducible using ionophores. DNA laddering has been shown to occur by gel electrophoresis of samples of hamster CL during luteolysis, (McCormack and Greenwald, submitted). It was demonstrated herein (chapter II) that apoptotic bodies are formed in luteolysis. Thus, it is a safe assertion that endonuclease activity is taking place as well. Endonuclease and transglutaminase activities only occur in "primed" cells in response to some triggering stimulus (Arends and Wyllie, 1991). Primed cells are those in a population of cells which have begun accumulating key proteins (like endonuclease) required for apoptosis to take place. Expression of these proteins is presumably genetically regulated. Most tissues have only a small percentage of cells in the primed population while others like the thymus have many. It is important to note that apoptotic stimuli such as glucocorticoids, dioxin and radiation always initiate apoptosis in cortical thymocytes and never in the medulla. Hence, only the immature (primed) cells undergo apoptosis readily. The triggering stimuli need be less specific in nature. Various mechanisms that increase $[\text{Ca}^{++}]_i$ can thus trigger a primed subpopulation of cells to undergo apoptosis. Any form of mild cellular injury which transiently increases $[\text{Ca}^{++}]_i$ would do likewise but have no such effect on unprimed cells. Arends and Wyllie, (1991) go on to make two predictions. First, primed

cells should be vulnerable to apoptosis in response to a wide variety of minor injury stimuli and second, apoptosis of this sort should take place exclusively in those regions of tissues in which primed cells lie.

Consider the CL in the context of the above scheme. Luteal cells were once follicular epithelial cells. These begin to develop and become dependent upon FSH. Once the follicle begins developing, it will either go on to ovulate (under gonadotrophic support) or undergo apoptosis. If ovulation occurs, the CL develops and functions for a time without the need for gonadotrophins. However, by the time of the L-Fs, the CL has reached a crossroads and it must have FSH-Prl to sustain function or undergo luteolysis. If, as in the case of the pseudopregnant hamster, $\text{PGF}_2\alpha$ (the 'trigger') is forthcoming at the end of pseudopregnancy, luteolysis occurs in the CL which represents a population of "primed cells" to undergo apoptosis. Interestingly, although the entire ovary is exposed to uterine $\text{PGF}_2\alpha$ only the CL responds by undergoing apoptosis. This response can be blocked by indomethacin (Lau et al., 1975) indicating its specificity. Since it is true that $\text{PGF}_2\alpha$ ultimately increases $[\text{Ca}^{++}]_i$, (as well as its other luteolytic effects) a rise in $[\text{Ca}^{++}]_i$ is necessary to activate the endonuclease required for apoptotic DNA fragmentation. In the cyclic hamster some other stimulus, neither of uterine nor of pituitary origin, must be the triggering mechanism for spontaneous luteolysis. Intraluteal $\text{PGF}_2\alpha$ alone cannot account for luteolysis either as indicated below. In this laboratory and in that of our collaborators at Kansas University (G.S. Greenwald, personal communication), pilot studies using a variety of potent cyclooxygenase and lipoxygenase inhibitors

(norhydroguaiaretic acid) as well as anti-inflammatory agents including indomethacin, dexamethasone and pentoxifylline had no effect on PMNL emigration nor in delaying luteolysis (unpublished observations).

Thus, evidence is accumulating that the most likely luteolytic candidate is a factor(s) released by PMNL. These cells were shown to produce MPO (chapter IV) which is a potent generator of HOCl⁻. In the rat, H₂O₂ is rapidly generated by PGF₂α in the CL during luteolysis in association with transient ascorbic acid depletion and lipid peroxidation (Aten et al., 1992). H₂O₂ uncouples the gonadotrophin receptor and blocks hormone and cAMP-sensitive P synthesis (Endo et al., 1993). Another other top candidate for a potent luteolytic agent in the cyclic hamster is TNF-α (McCormack and Greenwald, submitted). It is known to induce apoptosis in endothelial cells (Robaye et al., 1991). TNF-α is also a strong proinflammatory mediator which induces endothelial expression of adhesion molecules favoring leukocyte emigration and in addition it causes procoagulant activity (Nawroth and Stern, 1986). TNF-α also activates PMNL which enhances phagocytosis, induces degranulation and stimulates generation of superoxides (Vassalli, 1992). Moreover, it has been shown to be involved in the rat, rabbit, (Brännström et al., 1994) and cow (Benyo and Pate, 1992) CL during luteolysis as well. Since apoptosis is reversible until the time of PMNL arrival by supplying exogenous gonadotrophic support (Greenwald and Rothchild, 1968), and blocking intraluteal PGF₂α formation is ineffective in preventing luteolysis, some factor(s) of PMNL is the favored choice of an agent for the induction of apoptosis in the cyclic hamster.

Luteolysis in the hamster is unique in its rapid pace, i.e., completion within the same cycle as the CL were formed. FL occurs at the time of the L-Fs. Subcellular fine structural alterations take place which are reversible with gonadotrophic (FSH-Prl) support. These early atrophic changes consist of disaggregation of SER into myelin figures, increased mitochondrial density and increased autophagic lysosomal activity. These are common alterations of luteal cellular form seen in other species as well such as the guinea pig (Paavola, 1977) and the ewe (McClellan and Niswender, 1977) in luteolysis. As FL is completed, an acute inflammatory reaction begins with the most obvious tell tale sign consisting of PMNL invasion. The nature of the chemotactic stimulus(i) which direct the PMNL invasion is unknown. It may be any of a number of inflammatory mediators. One interesting potential chemoattractant is f-M-L-P, a product of bacterial protein breakdown which is also found in degrading mitochondrial proteins (Carp, 1982). Since altered mitochondria are present in luteolysis, investigation of the release of this powerful chemoattractant is indicated.

Concurrent with the influx of PMNL is the onset of irreversible apoptotic cell death which rapidly becomes widespread and accounts for SL. There is a great increase in autophagic and transformed luteal cell heterophagic lysosomal enzyme activity. In apparent opposition to the observed luteolytic inflammatory phenomena is the fact that inflammation is typically absent in apoptotic cell death. Since both processes are noted to take place in luteolysis (and follicular atresia) regulation of cyclic ovarian function is unusual. The acute inflammatory reaction in luteolysis may serve to hasten the essential

process of structural demise and thus enable the vast tissue turnover present in the ovary to occur efficiently. On the other hand, in order to ensure that a chronic or widespread and damaging state of inflammation does not develop, it appears that apoptosis provides an advantageous mechanism for dampening proinflammatory signals by providing transformed parenchymal cells as phagocytes of the debris left behind by their dead neighboring cells. Luteolysis is thus a fascinating and unique process which, at first glance, involves seemingly paradoxical events consisting of complex interactions between the endocrine and immune systems.

APPENDICIES

APPENDIX A Plates and Figures

PLATE I

Figure 1. Photomicrograph of a section through a hamster CL from D1 at 0900 hours which is still organizing and not yet vascularized. Theca lutein cells (arrows) are located peripherally. Granulosa lutein cells are central. X 200.

Figure 2. Photomicrograph of a section through a D1 0900 hours hamster CL at higher magnification than shown in figure 1. Area of developing blood vessels is indicated by arrows. X 400.

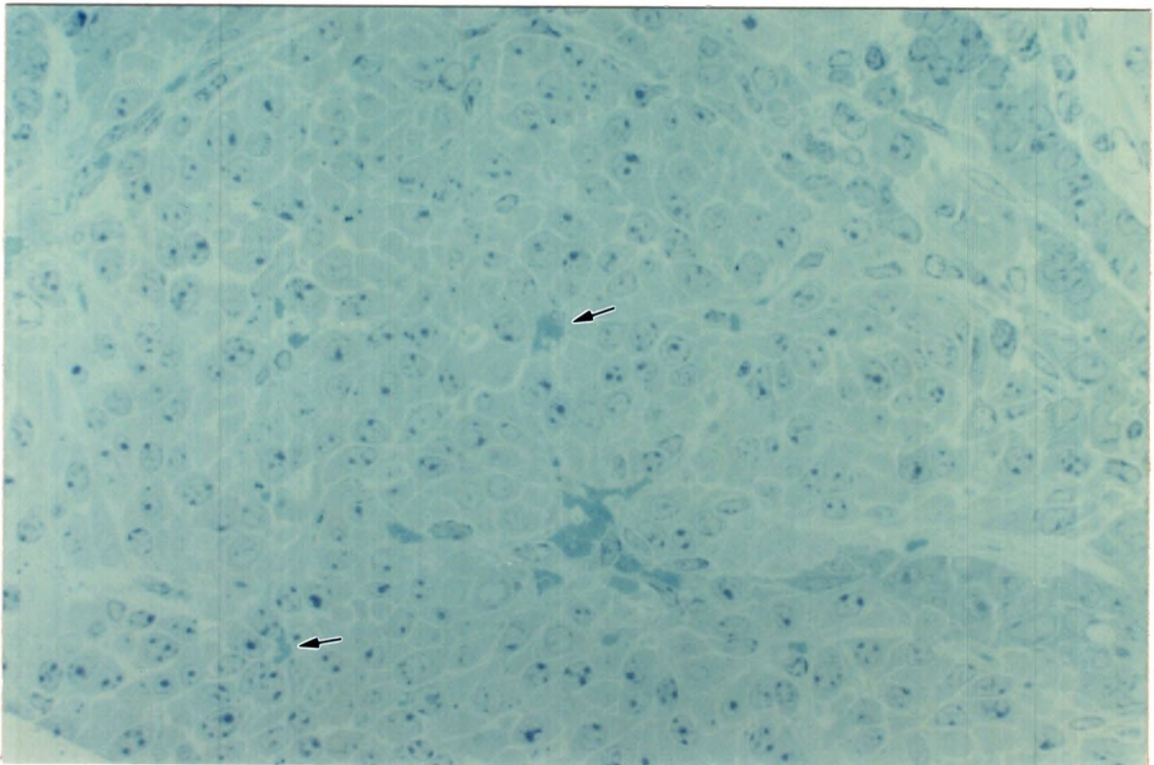
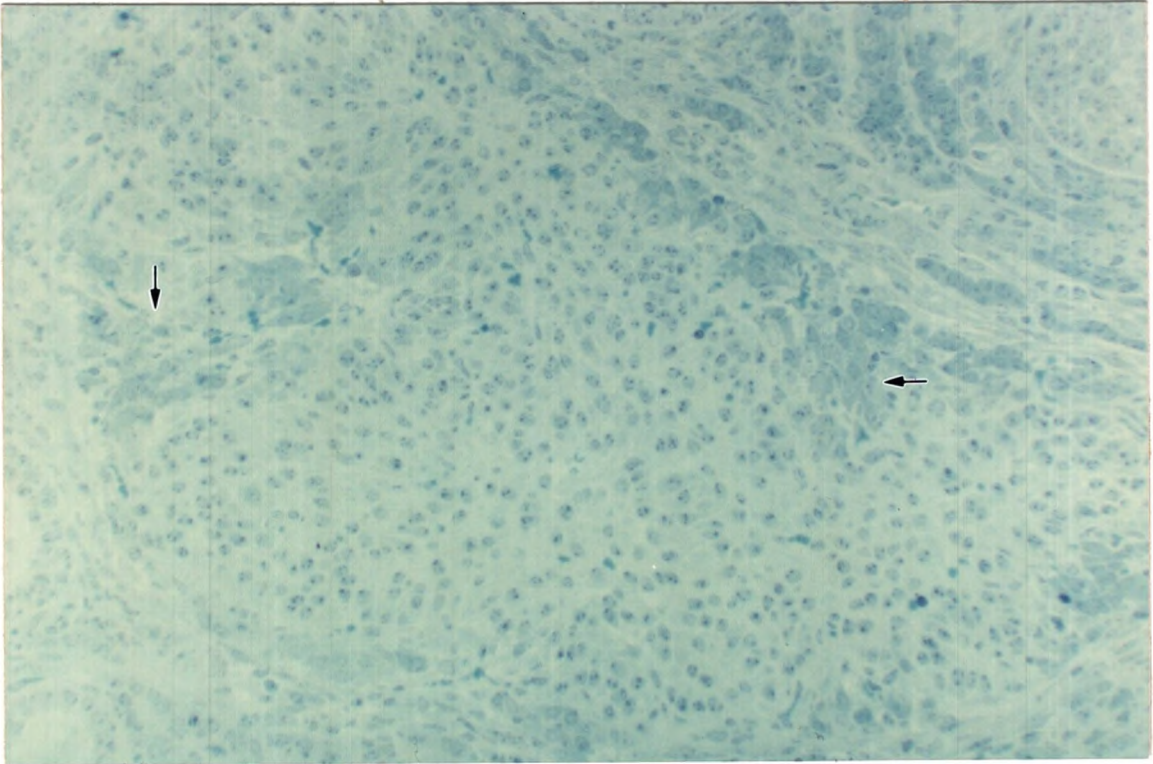


PLATE II

Figure 3. Lowpower photomicrograph of a section through a D2 hamster CL at 0900 hours. The central cavity (CC) does not fill with parenchyma. This cavity represents the antral remnant of the graafian follicle from which the CL formed. X 100.

Figure 4. Photomicrograph of a section through a hamster CL on D2 at 0900 hours. Note the highly vascular nature of this endocrine organ. X 200.

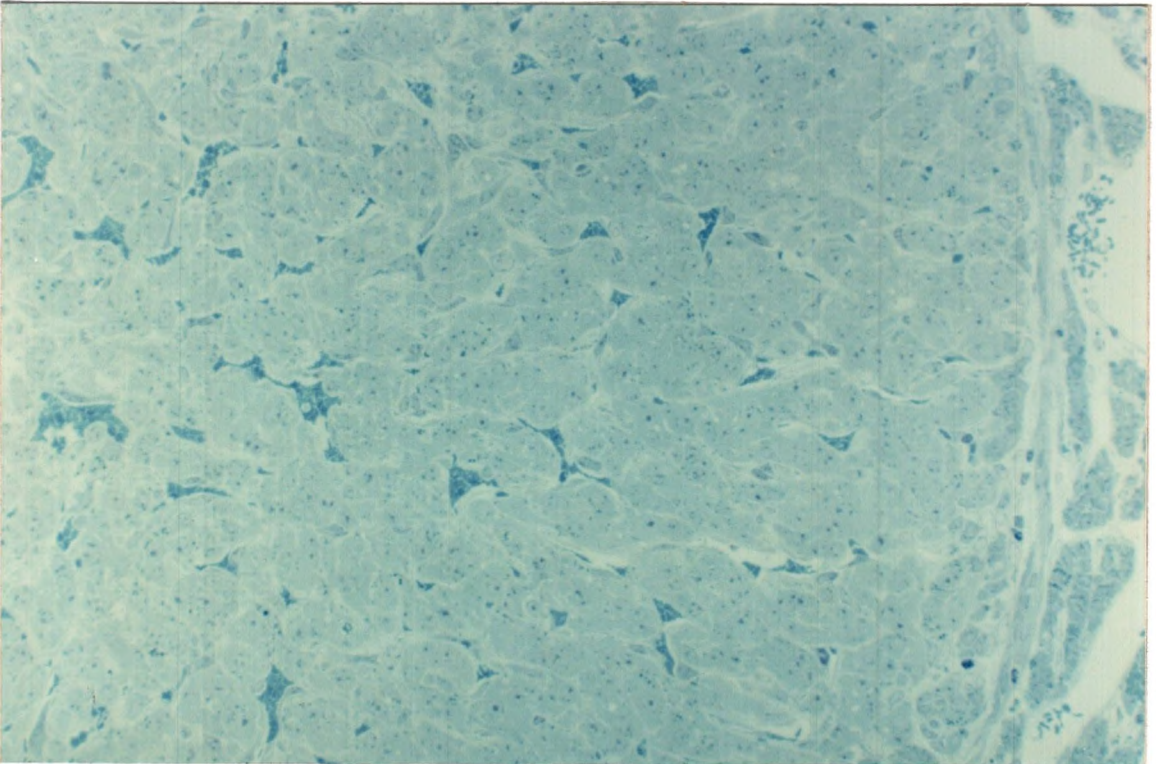
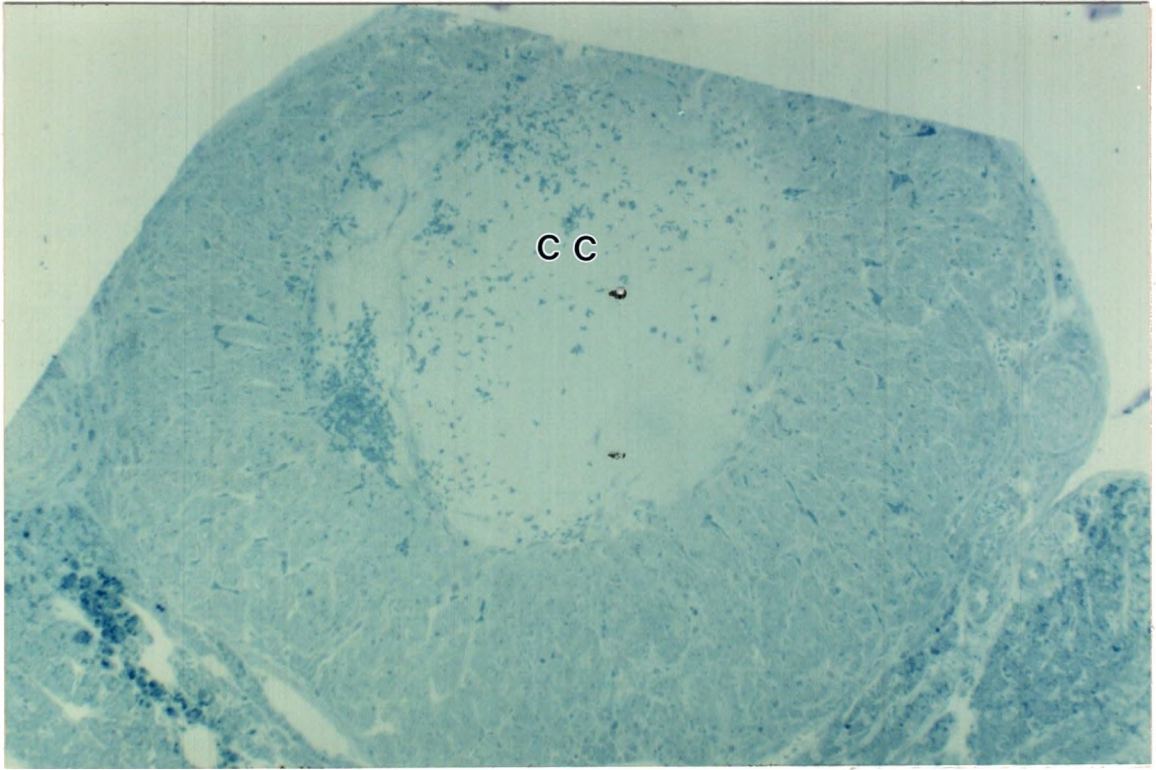


PLATE III

Figure 5. Highpower photomicrograph of a section through a hamster CL at 0900 hours on D2 demonstrating vascular and luteal cell morphology typical of functional capacity. X 1000.

Figure 6. Highpower photomicrographic view of the area directly adjacent to the avascular core of the CL shown in figure 3. A mitotic luteal cell (arrow) and trapped lymphocyte (arrowhead) are lodged next to the luteal parenchyma. X 100.

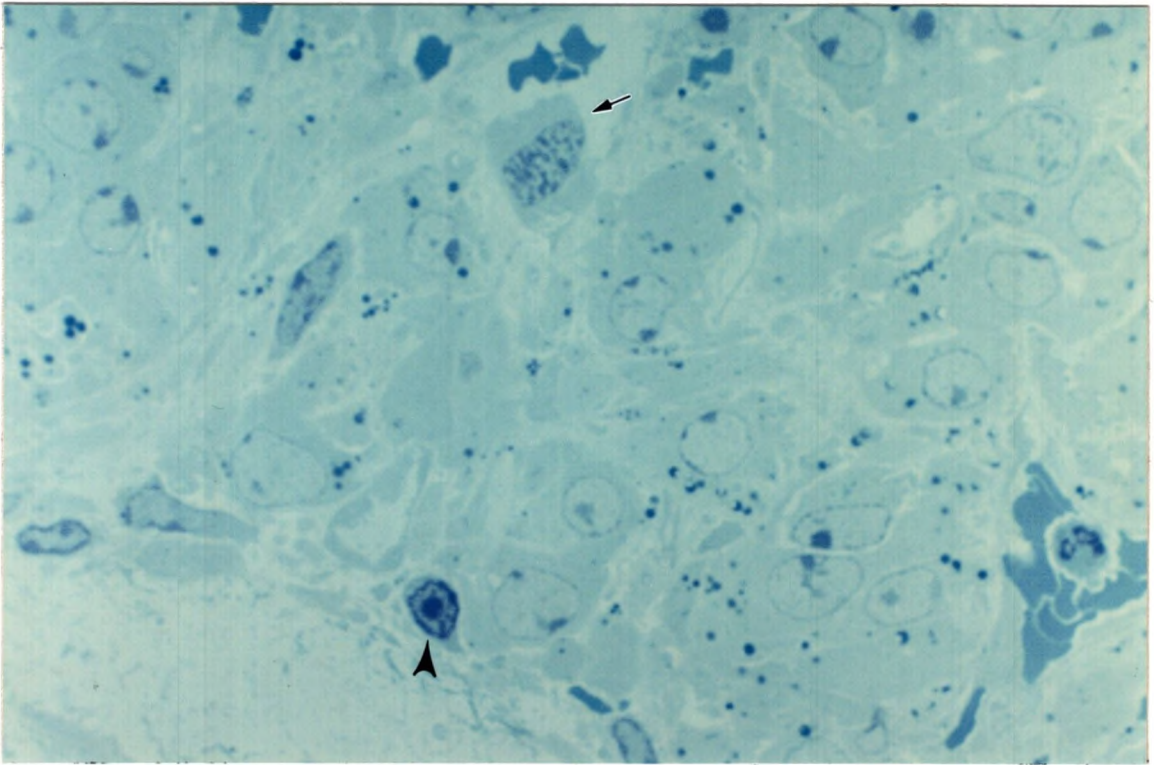
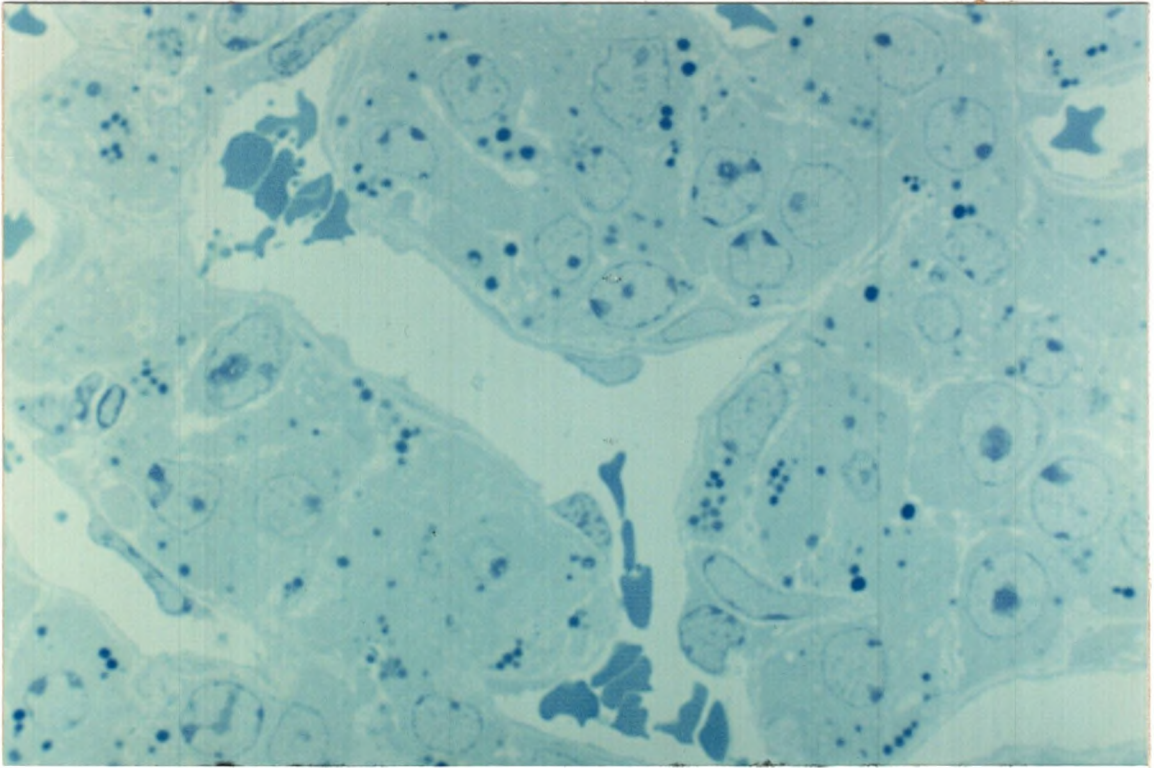


PLATE IV

Figure 7. Highpower photomicrograph of a section through a hamster CL on D2 at 0900 hours. A mitotic endothelial cell is indicated by the arrow. X 1000.

Figure 8. Photomicrograph of a section through a D2 2400 hours hamster CL. This time frame falls within the L-Fs. There is no appreciable morphologic change from that seen prior to the L-Fs. X 400.

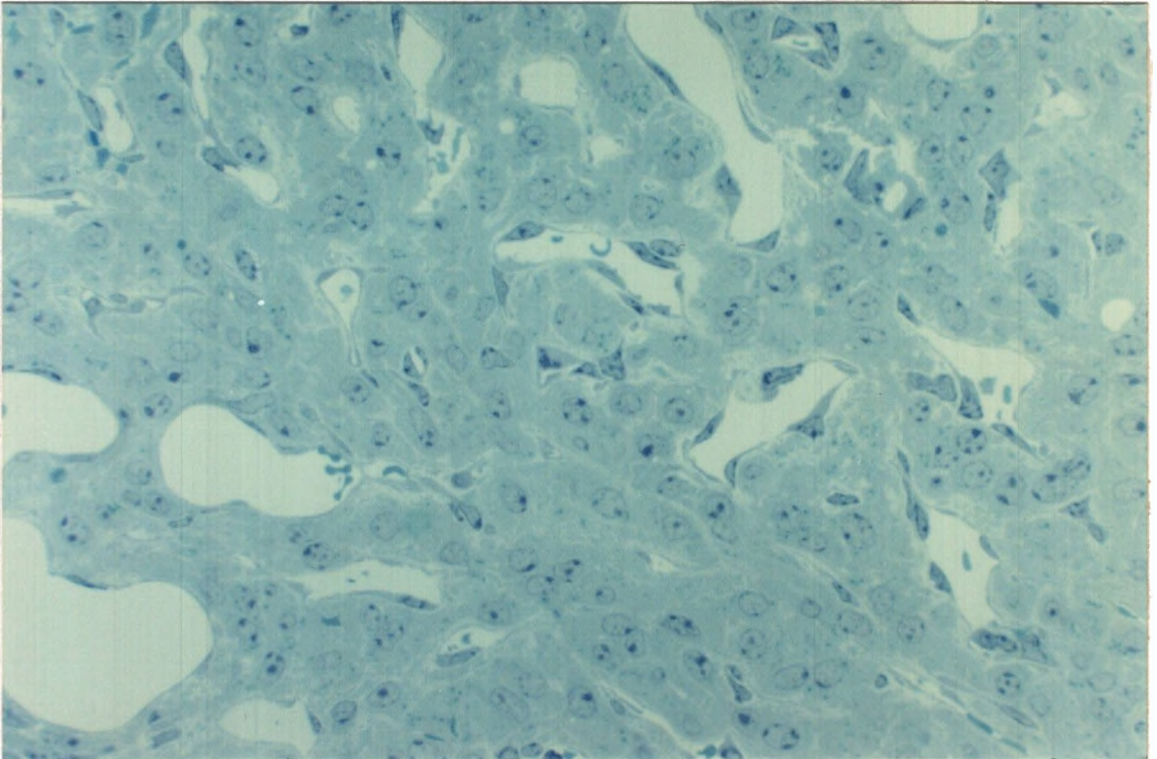
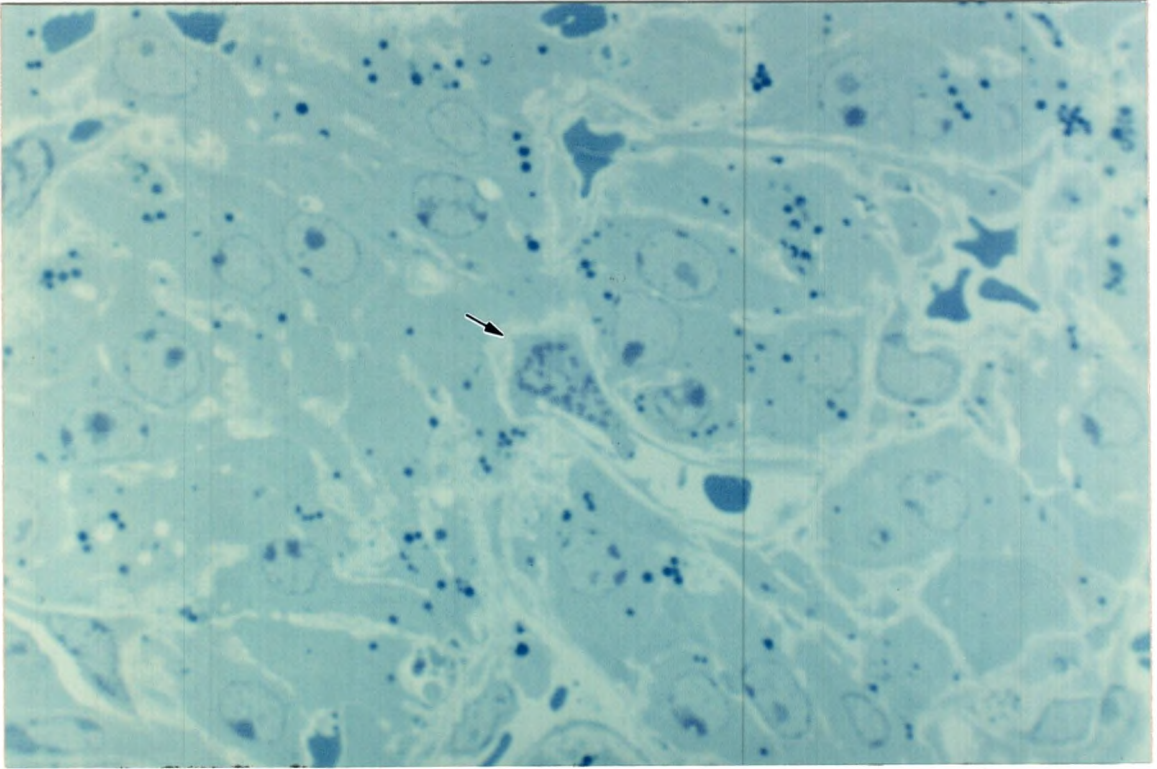


PLATE V

Figure 9. Photomicrograph of a section through a hamster D3 0300 hour CL. The morphology is consistent with that noted on D2 at 2400 hours (see figure 8). X 400.

Figure 10. Photomicrograph of a section through a hamster CL at 0400 hours on D3 which is the end of the L-Fs. The tissue appears healthy and devoid of PMNL. X 400.

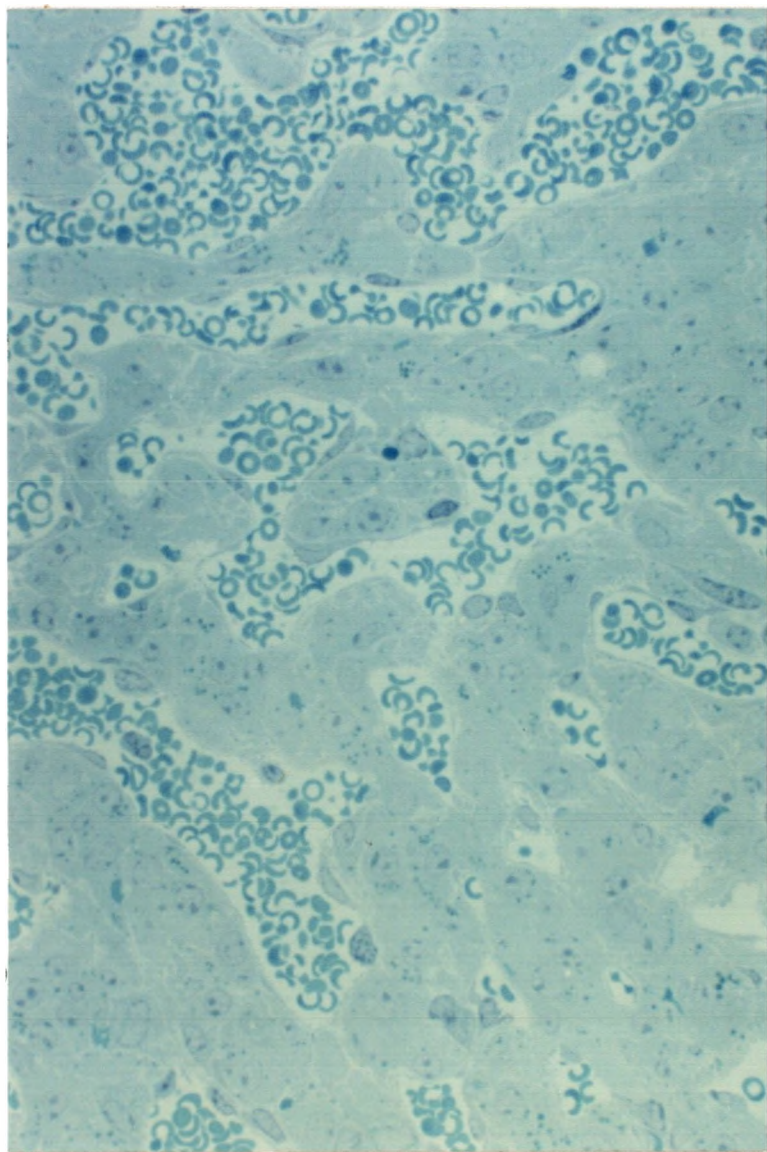
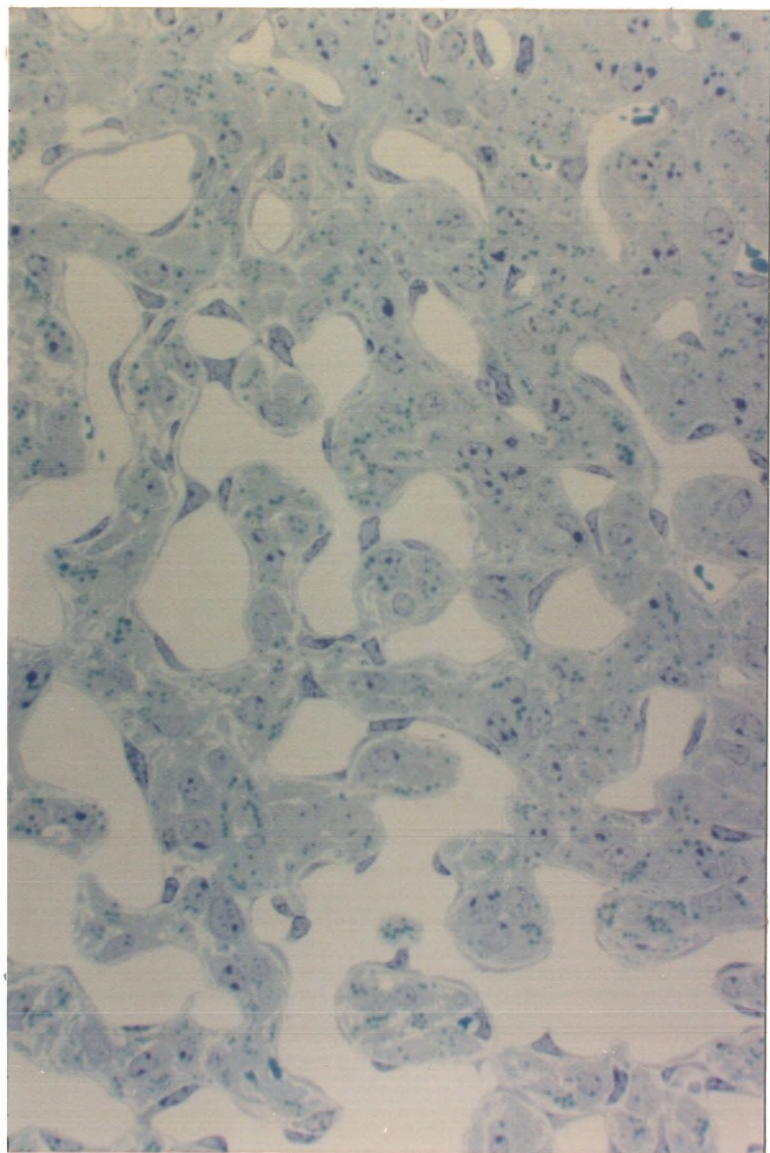


PLATE VI

Figure 11. Photomicrograph of a section through a hamster CL at 0500 hours on D3.
The field is yet devoid of apoptotic figures and PMNL. X 400.

Figure 12. Photomicrograph of a section through a hamster CL at 0500 hours on D3.
No apoptotic changes are yet apparent. However, the presence of a single emigrated PMNL is notable (arrow) within the field. X 400.

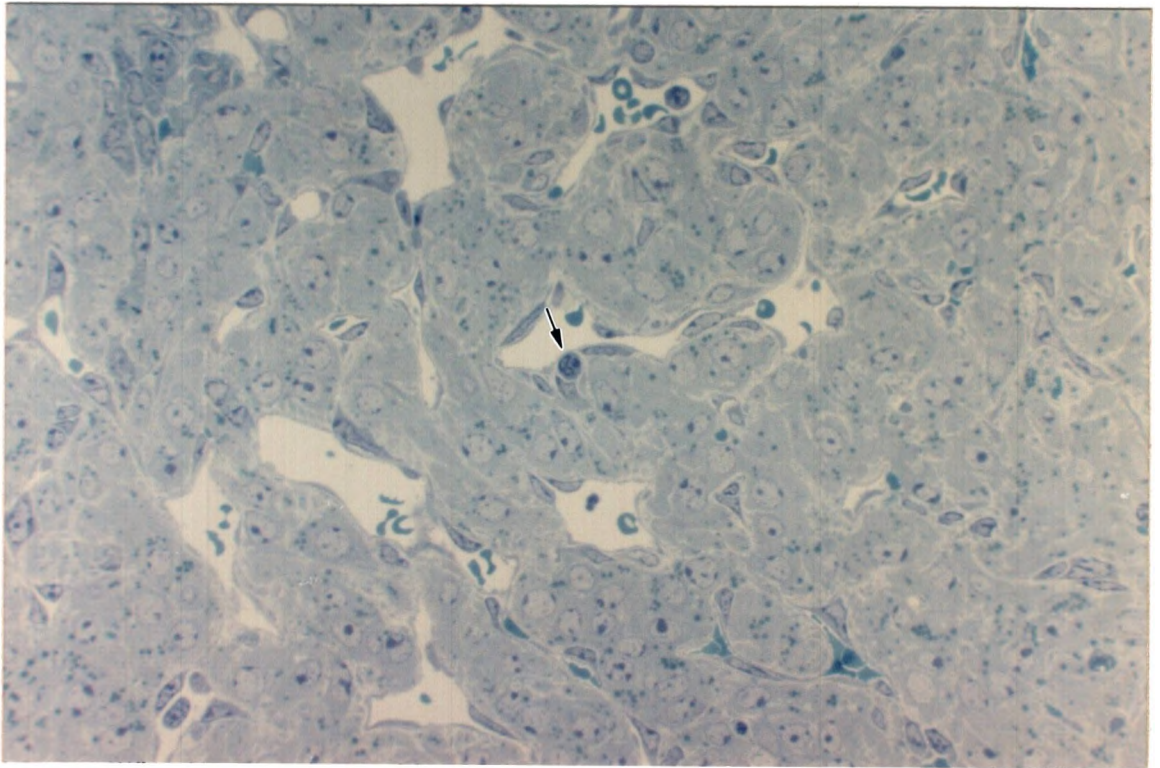
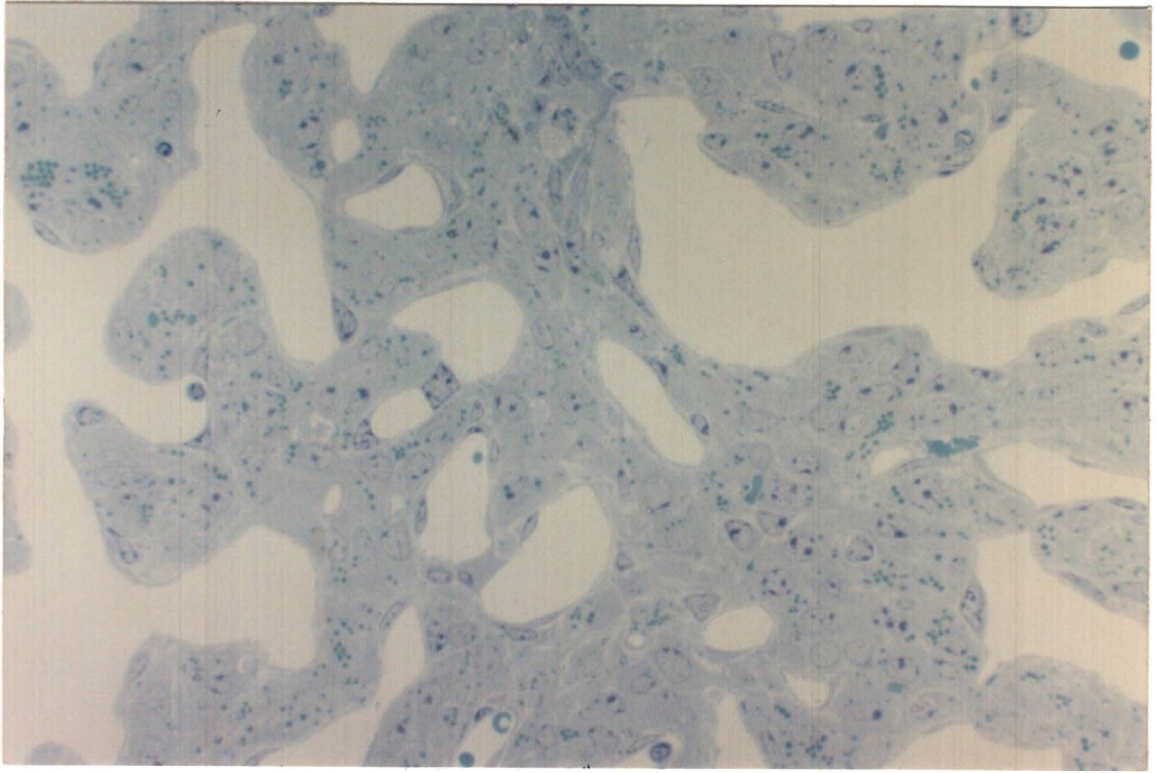


PLATE VII

Figure 13. Photomicrograph of a section through a hamster CL at 0600 hours on D3 at the onset of SL. Numerous recently emigrated PMNL have arrived. X 400.

Figure 14. Highpower photomicrograph of a section through a hamster D3 CL at 0600 hours. Extravascular PMNL are indicated by arrows. X 1000.

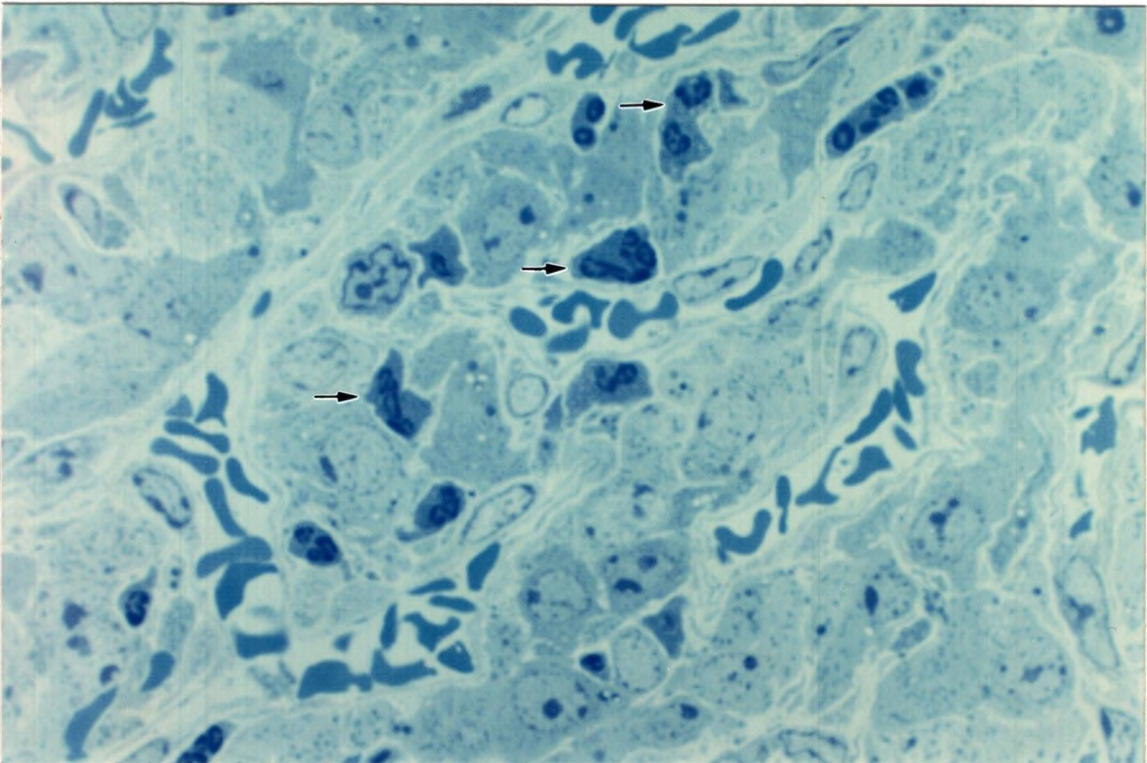
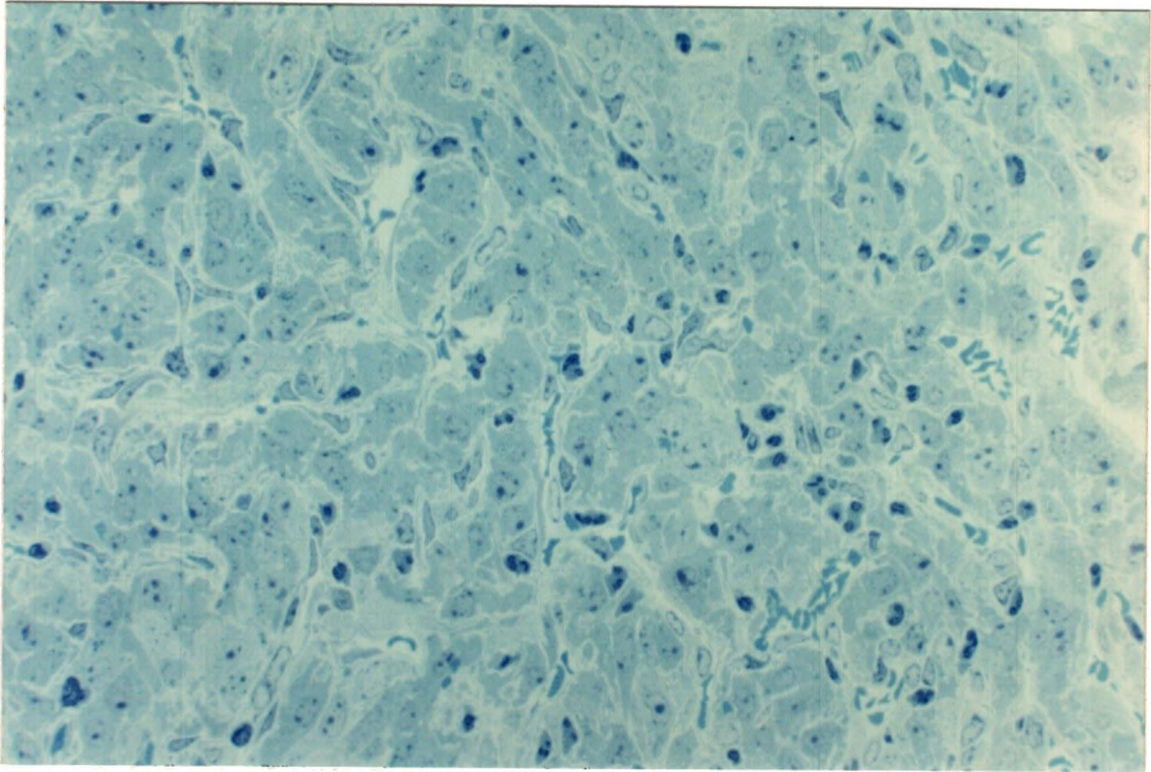


PLATE VIII

Figure 15. Highpower photomicrograph of a section through a hamster CL at 0600 hours on D3. PMNL are located primarily extravascularly while monocytes (arrows) remain intravascular. X 1000.

Figure 16. Highpower photomicrograph of a section through a hamster CL at 0600 hours on D3 at the onset of SL. At this time apoptotic cells can occasionally be seen (arrow). X 1000.

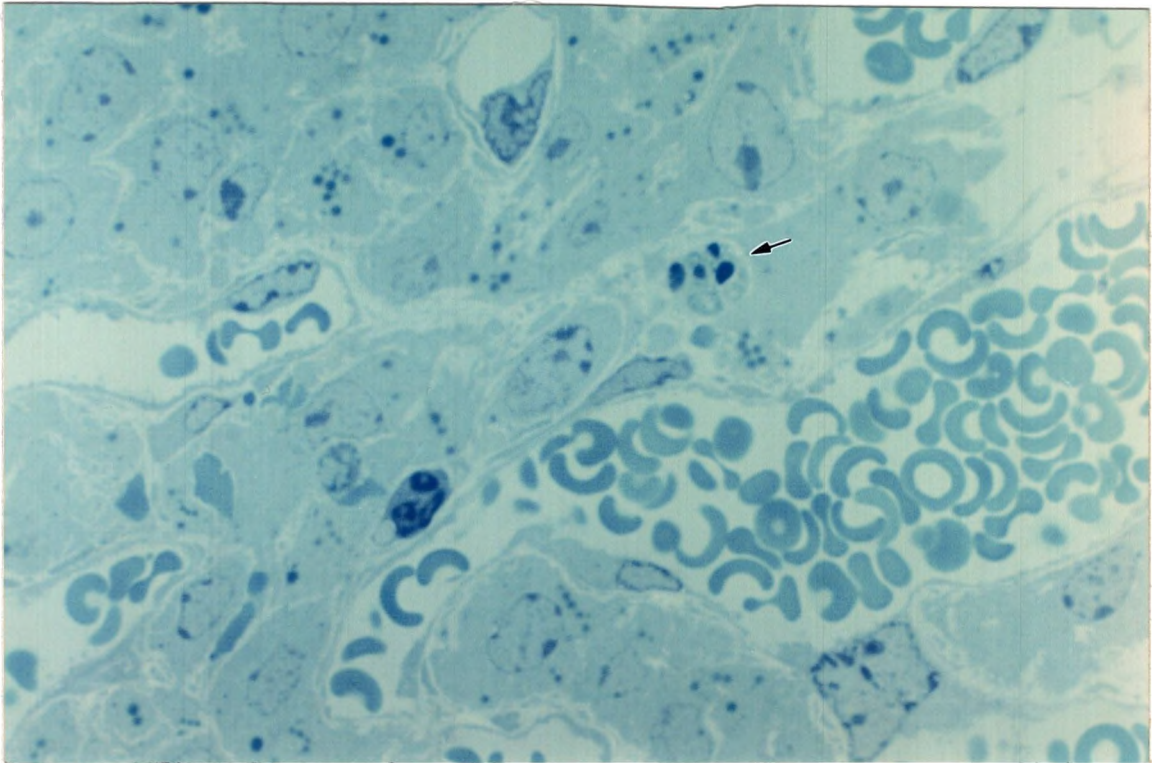
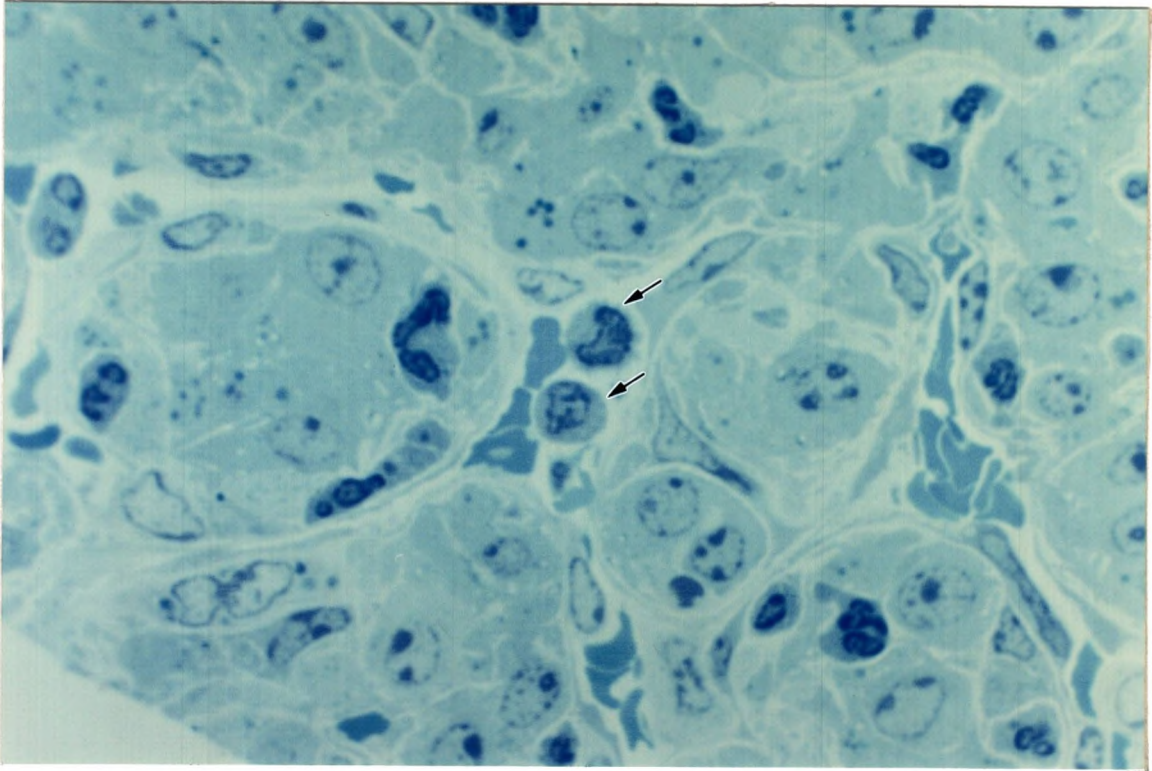


PLATE IX

Figure 17. Highpower photomicrograph of a section through a hamster CL at 0600 hours on D3. An apoptotic cell (arrow) shows crescentic caps of condensed chromatin. X 1000.

Figure 18. Lowpower photomicrograph of a section through a hamster CL at 0900 hours on D3. X 100.

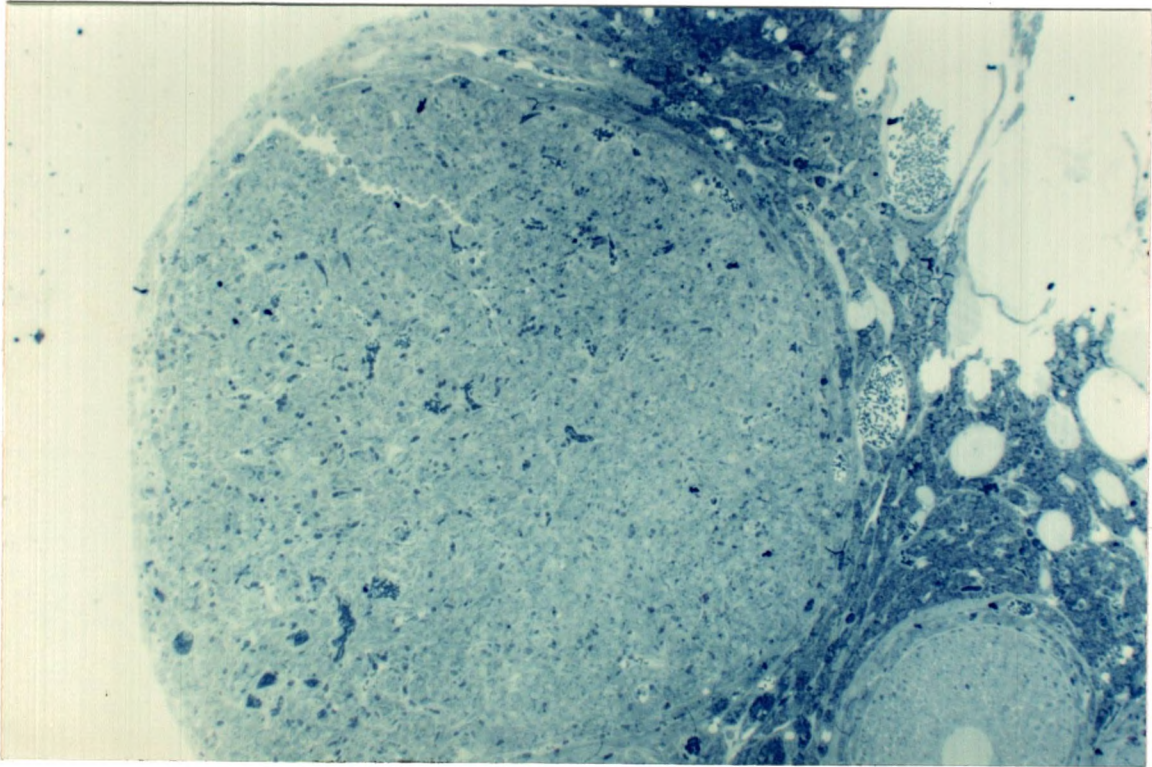
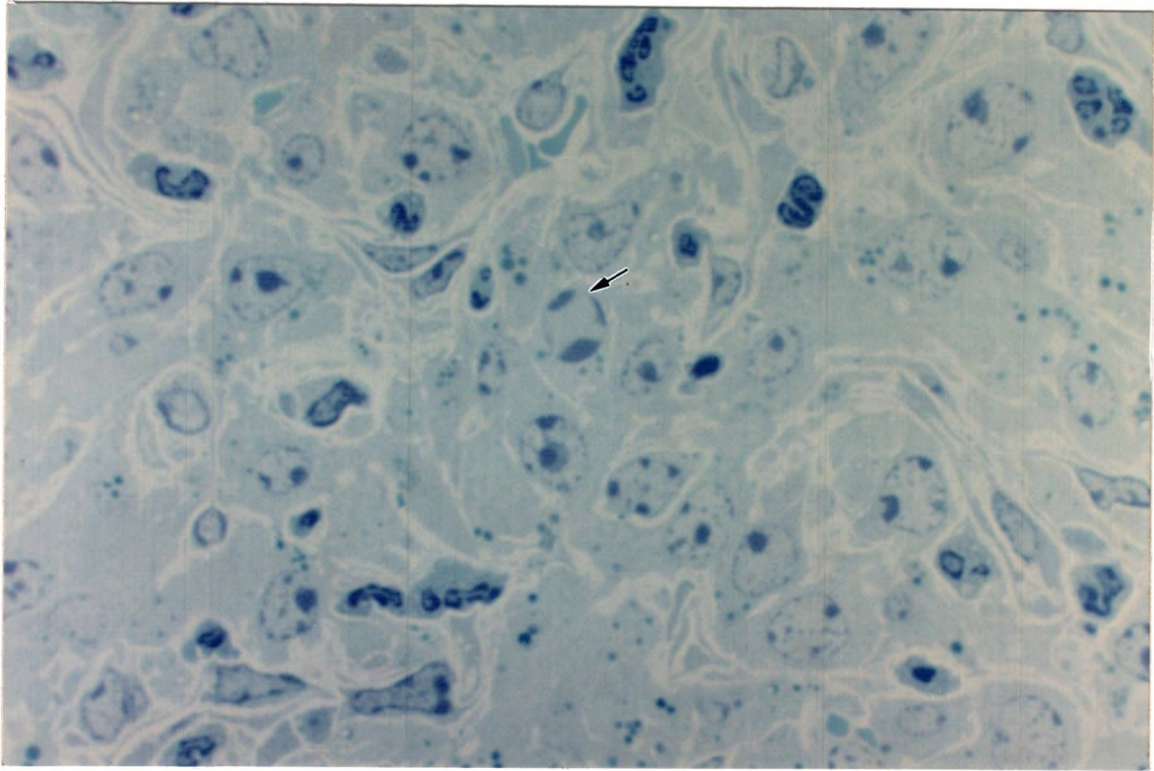


PLATE X

Figure 19. Highpower photomicrograph of a section through a hamster CL at 0900 hours on D3. A classical apoptotic endothelial cell (arrow) shows caps of condensed chromatin. X 1000.

Figure 20. Highpower photomicrograph of a section through hamster luteal tissue at 0900 hours on D3. The arrowhead indicates an apoptotic cell which may be a neutrophil. Arrow, apoptotic body. X 1000.

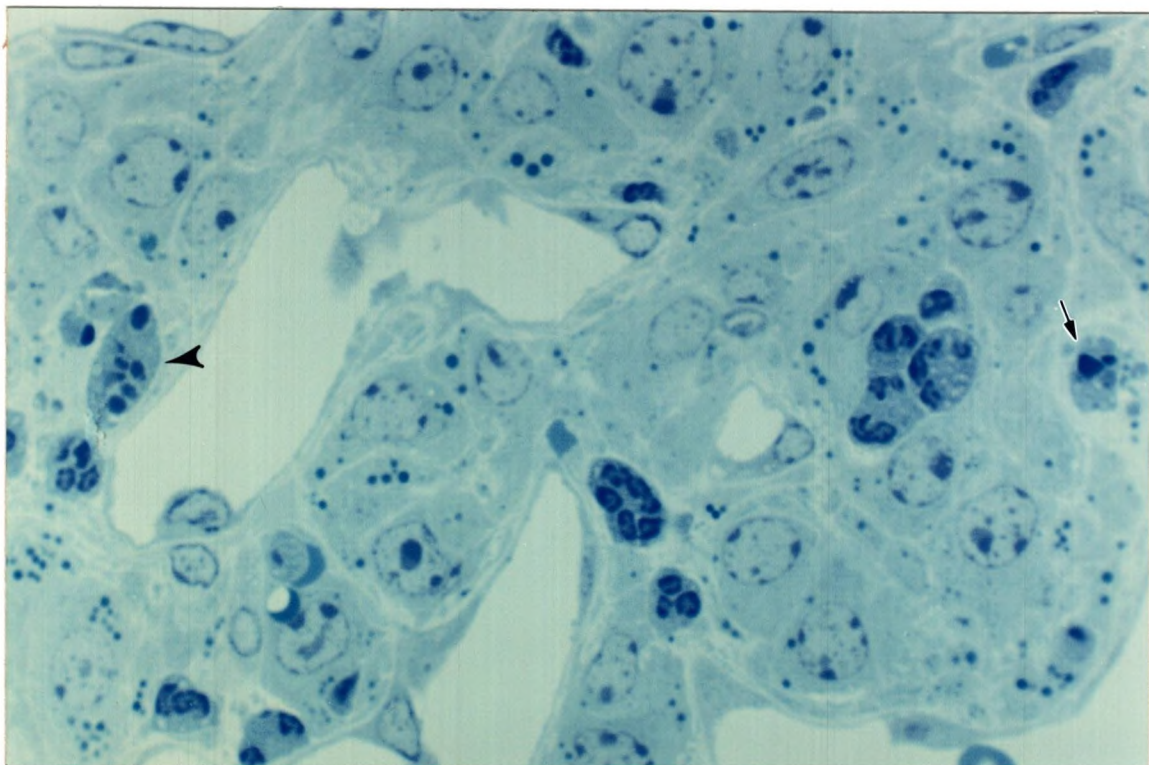
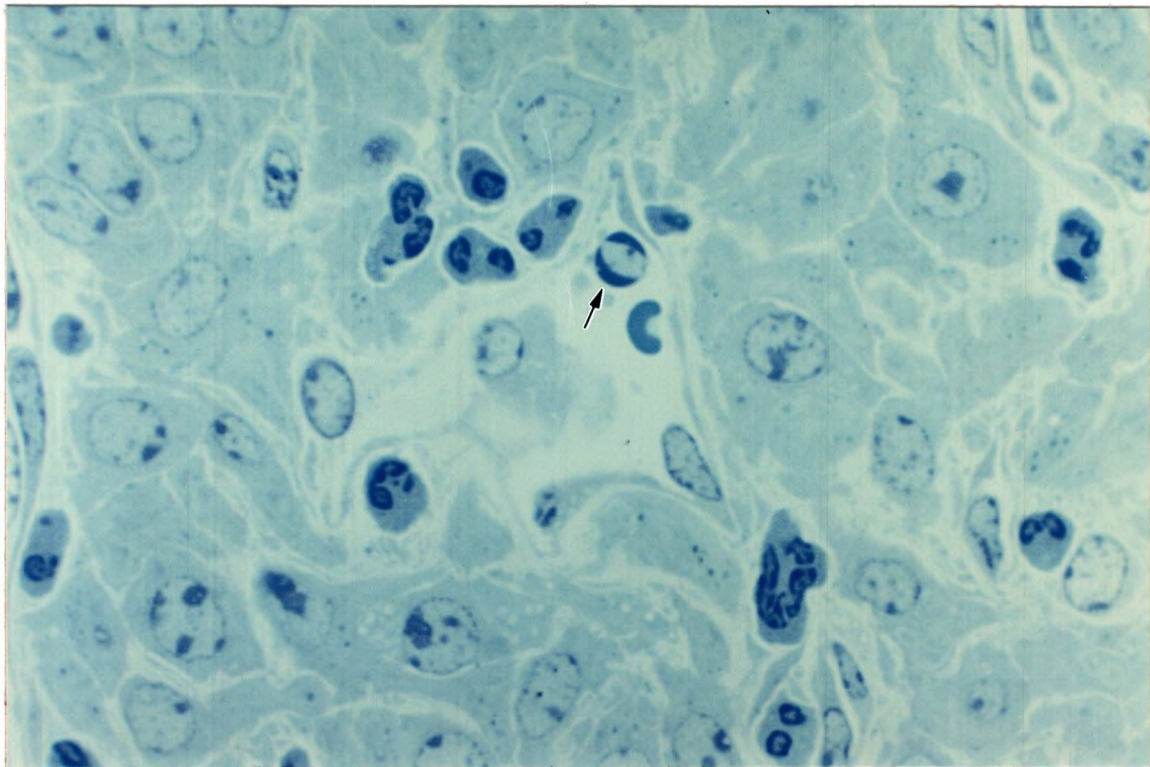


PLATE XI

Figure 21. Highpower photomicrograph of a section through a hamster CL at 0900 hours on D3. Endothelial apoptotic bodies (arrow) are sloughing into the lumen of a large venule. X 1000.

Figure 22. Highpower photomicrograph of a section through D3 hamster luteal tissue at 0900 hours. An apoptotic endothelial cell similar to the one in figure 21 is indicated by the arrow. X 1000.

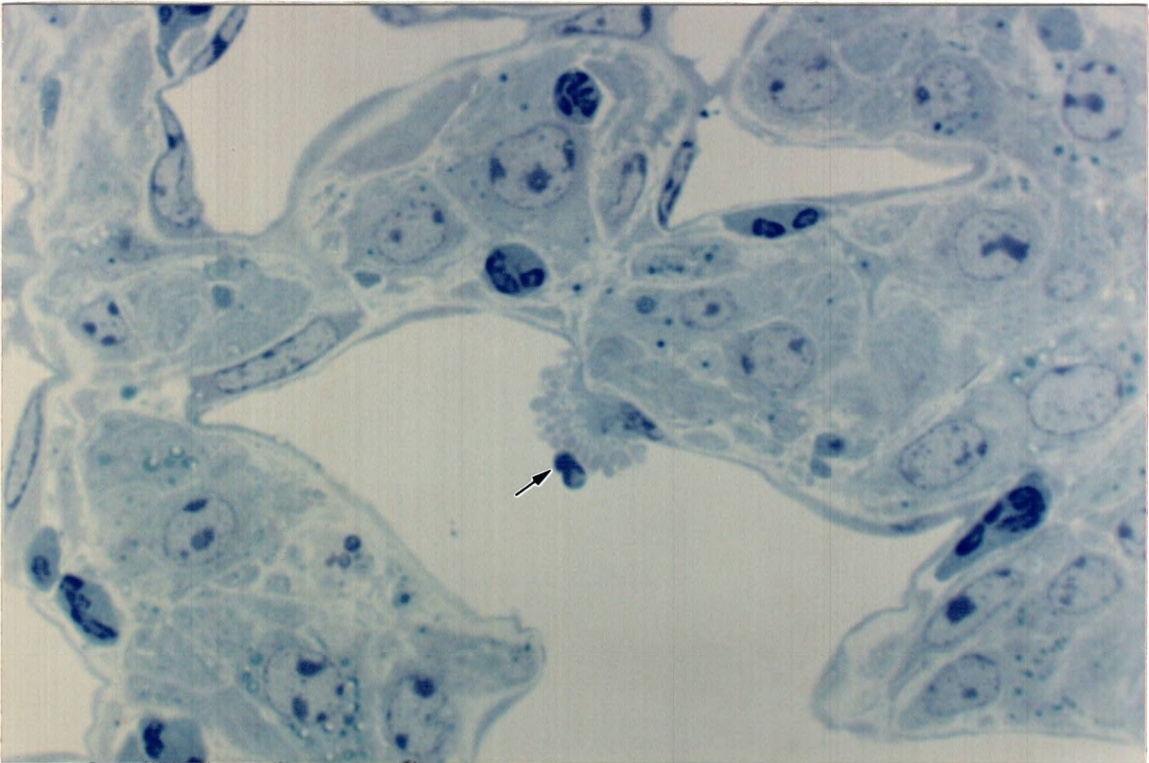
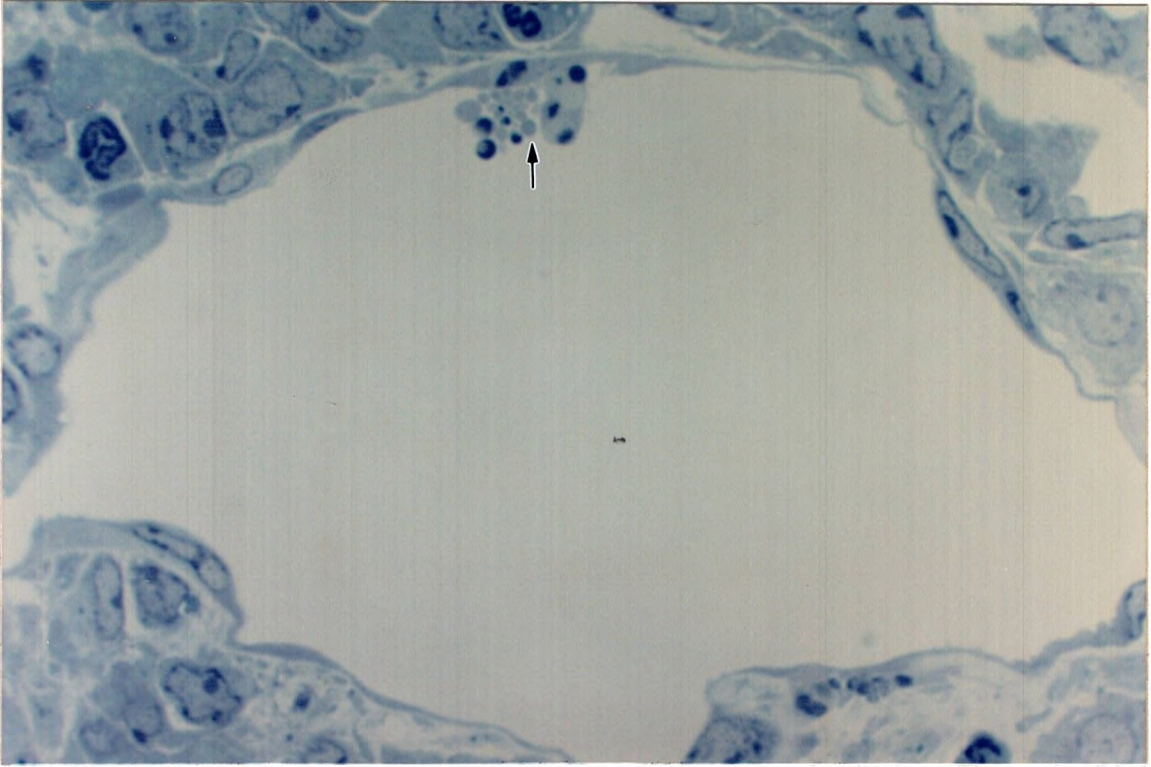


PLATE XII

Figure 23. Highpower photomicrograph of a section through a D3 CL at 0900 hours demonstrating a mitotic figure (arrow). This phenomenon is enigmatic. X 1000.

Figure 24. Highpower photomicrograph of a section through hamster luteal tissue at 0900 hours on D3. Note the odd endothelial baffle-like formations (arrows). X 1000.

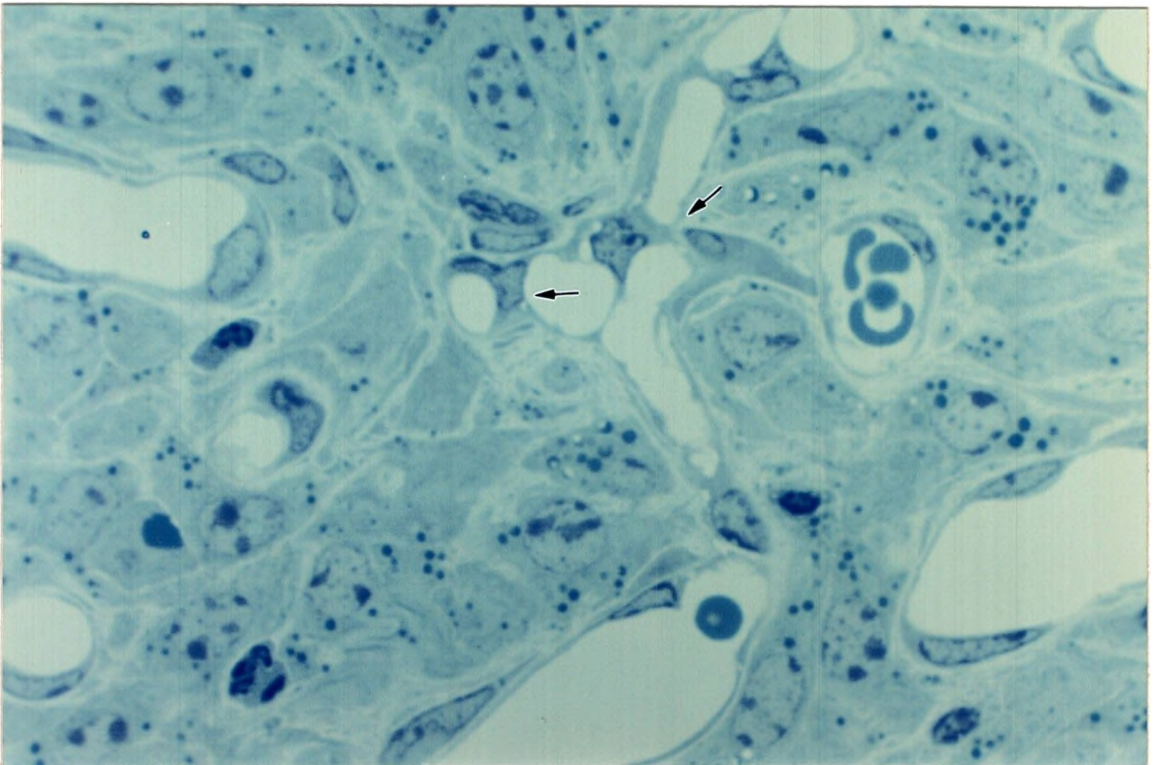
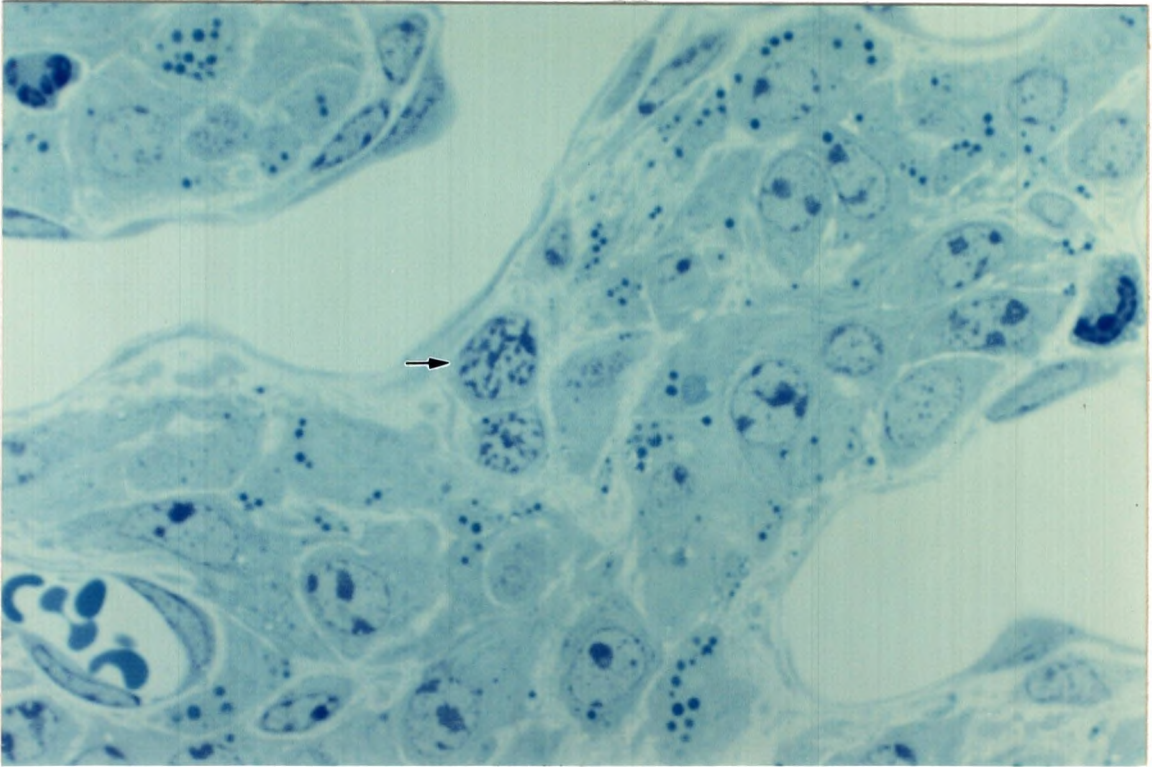


PLATE XIII

Figure 25 Highpower photomicrograph of a section through a hamster CL at 0900 hours on D3. A luteal cell appears to have transformed into a phagocyte as indicated by the accumulated apoptotic debris in its cytoplasm (arrow). This nucleus shows no chromatin condensation as is typical of apoptosis. X 1000.

Figure 26. Photomicrograph of a section through a hamster CL at 1300 hours on D3 taken at highpower. Many capillaries appear to have collapsed at this time. Also vacuolation and increased lipid accumulation is evident. Apoptotic cells, (arrows). X 1000.

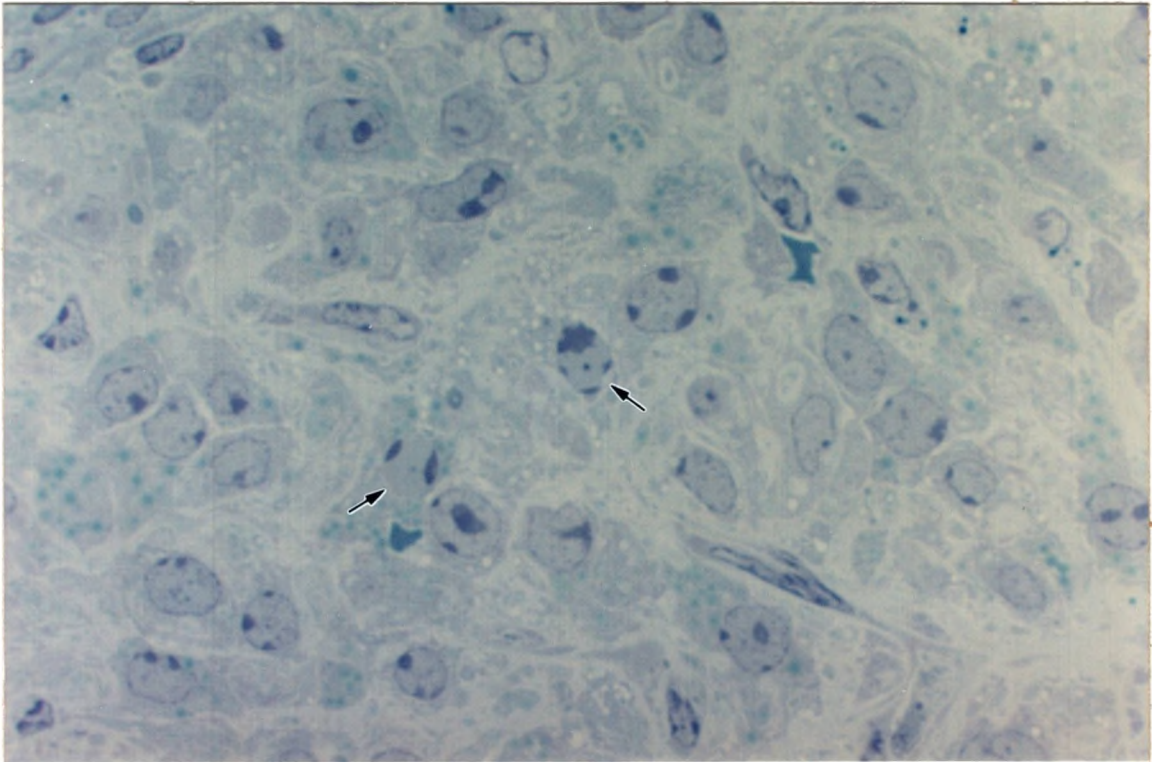
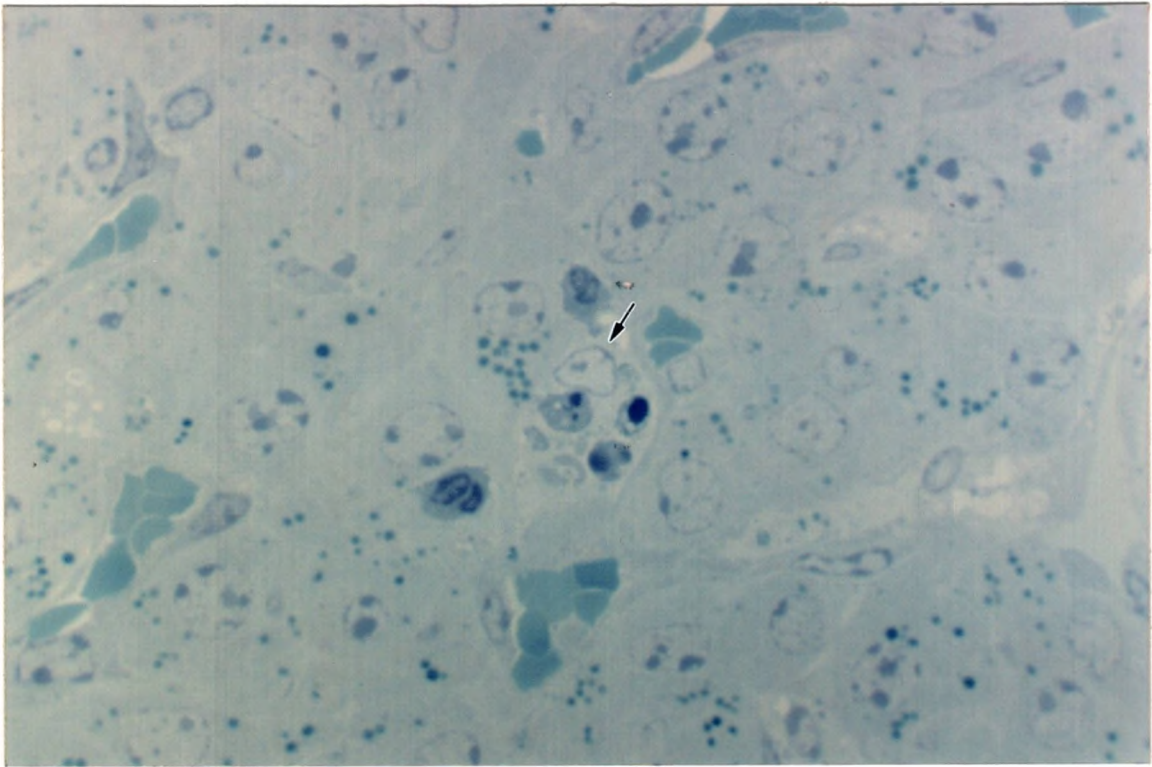


PLATE XIV

Figure 27. Highpower photomicrograph of a section through hamster luteal tissue at 1300 hours on D3. Cellular vacuolation and lipid accumulation is evident as is increased interstitial space. Apoptotic debris is accumulated in the interstitial space (arrows). X 1000.

Figure 28. Highpower photomicrograph of a section through a hamster CL at 1300 hours on D3. A significant amount of apoptotic endothelial debris is present in the capillary in the center of the field (arrows). X 1000.

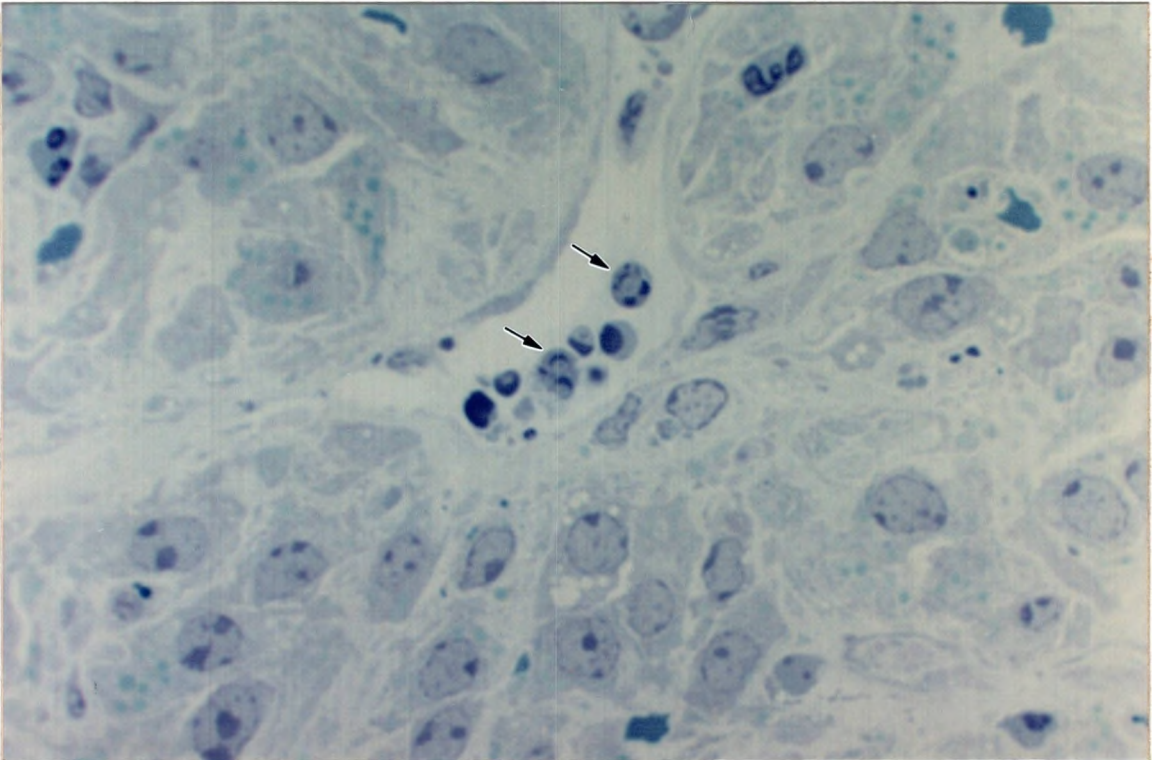
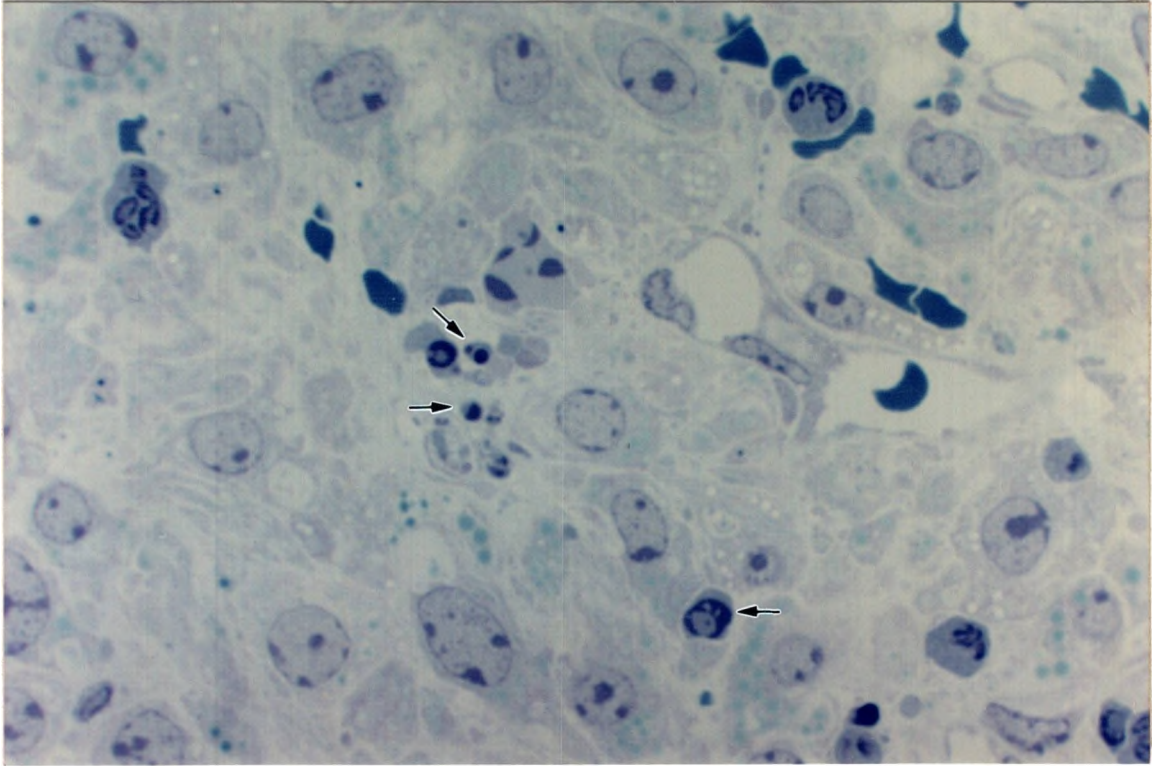


PLATE XV

Figure 29. Photomicrograph of a section through hamster 1300 hour luteal tissue on D3 taken at high power. An occluded capillary is indicated by the arrow. Many apoptotic luteal cells are present (arrowheads). X 1000.

Figure 30. Highpower photomicrograph of a section through a hamster CL at 1300 hours on D3. Capillary occlusion is evident (arrows) and lipid is accumulated in many luteal cells. X 1000.

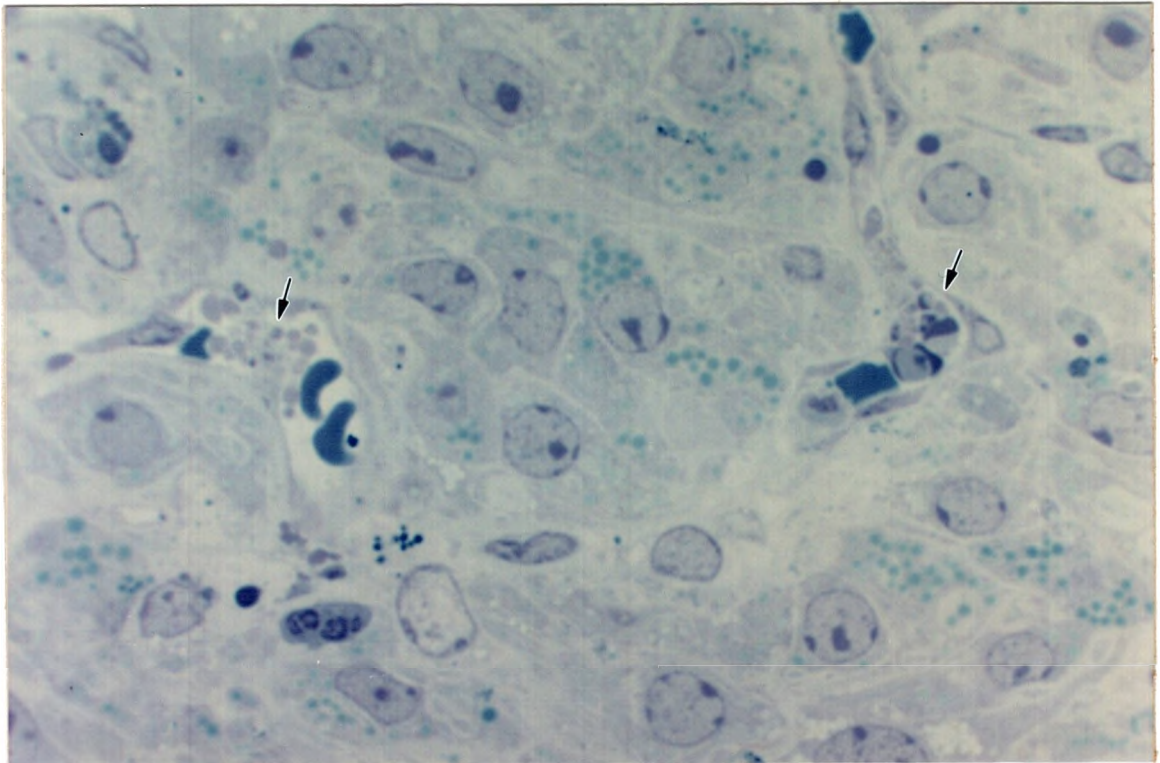
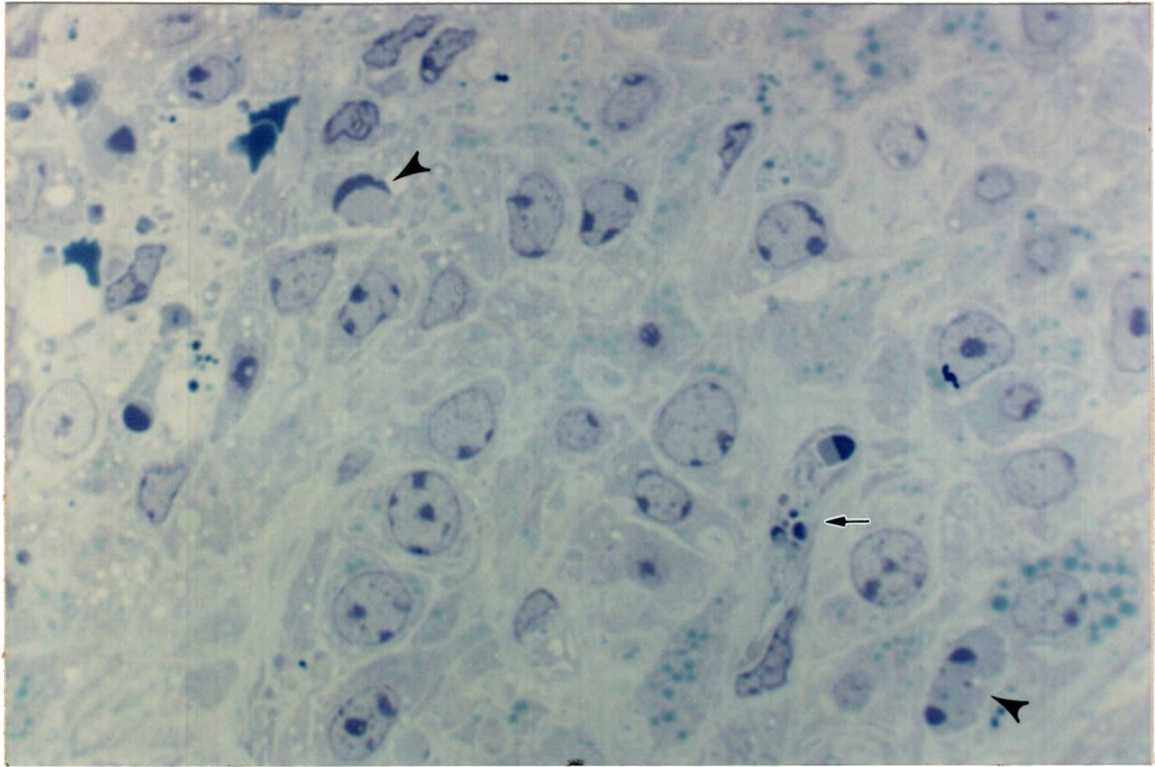


PLATE XVI

Figure 31. Highpower photomicrograph of a section through a hamster CL at 1300 hours on D3. Numerous apoptotic bodies are formed by fragmentation of the endothelial cell in the center of the field (arrow). X 1000.

Figure 32. Photomicrograph of a section through hamster luteal tissue at 1300 hours on D3 taken at highpower. Degeneration of endothelium by apoptosis and transcapillary baffling (arrows) compromises vascular integrity. X 1000.

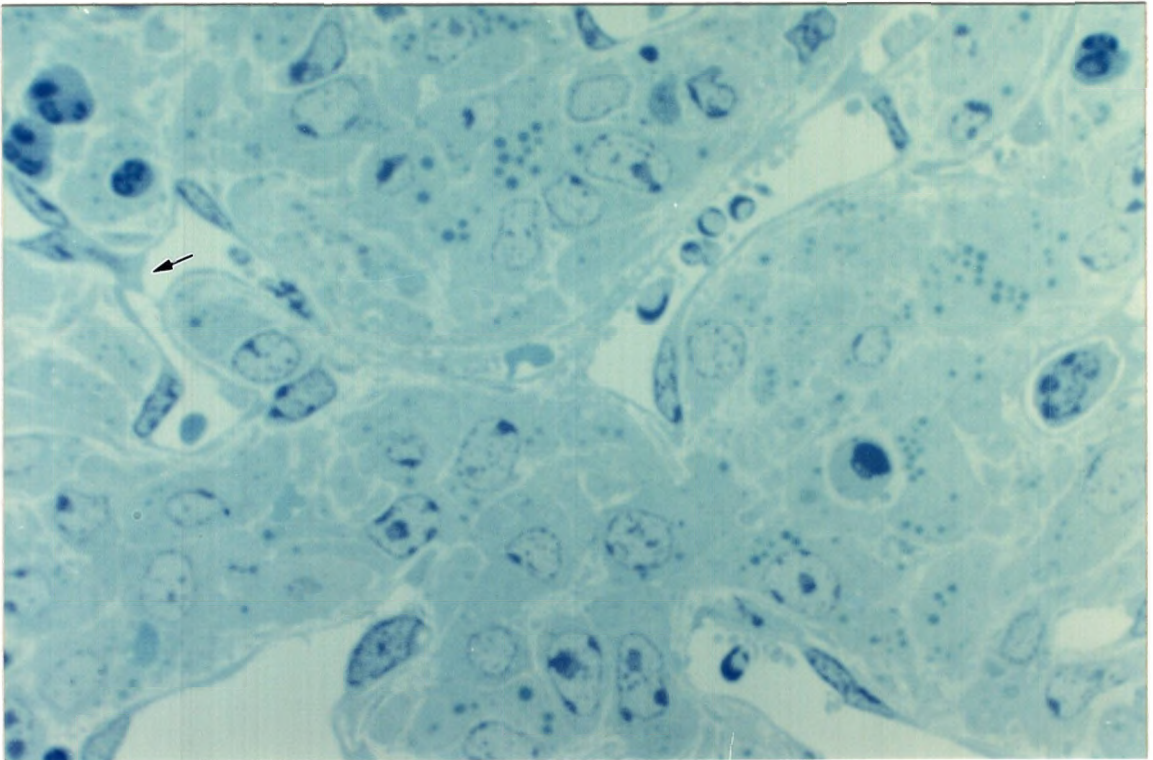
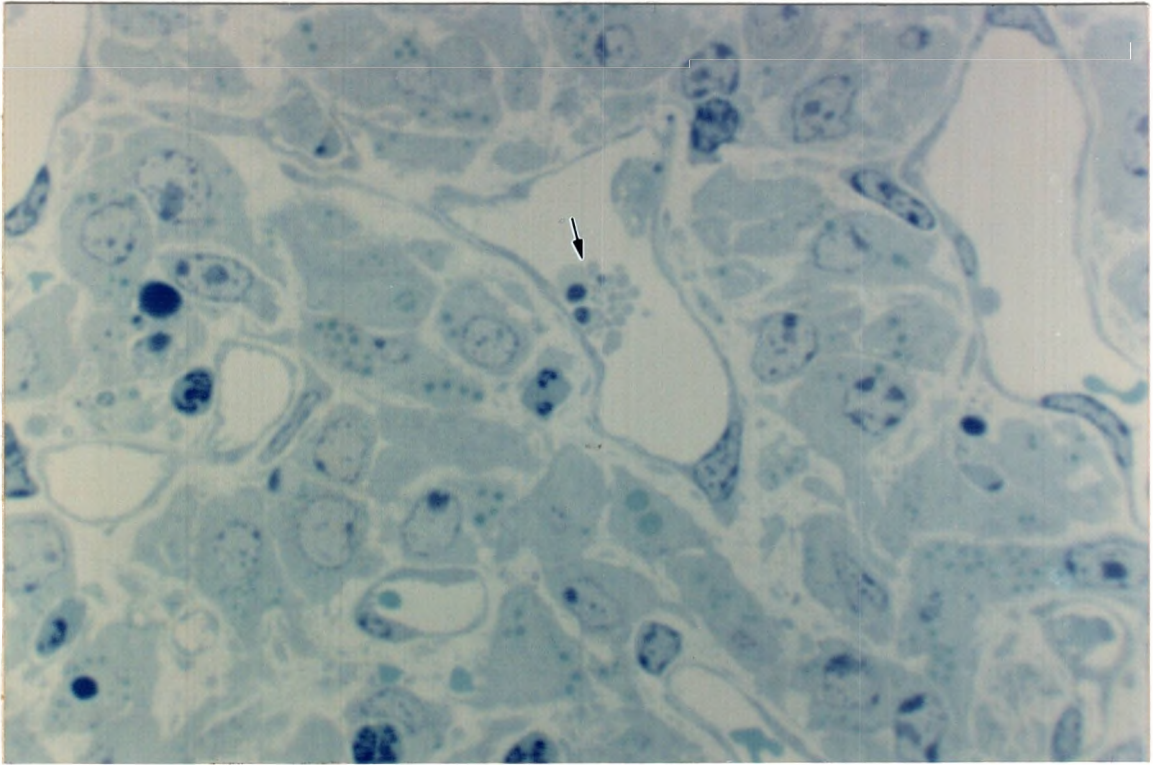


PLATE XVII

Figure 33. Highpower photomicrograph of a section through a hamster CL at 1530 hours on D3. Capillary degeneration (arrows) and luteal apoptosis (arrowheads) is evident. X 1000.

Figure 34. Photomicrograph of a section through hamster luteal tissue on D3 at 1530 hours taken at highpower demonstrating pronounced vascular degeneration. Apoptotic luteal cells (arrows), cellular vacuolation, and lipid accumulation are pronounced. X 1000.

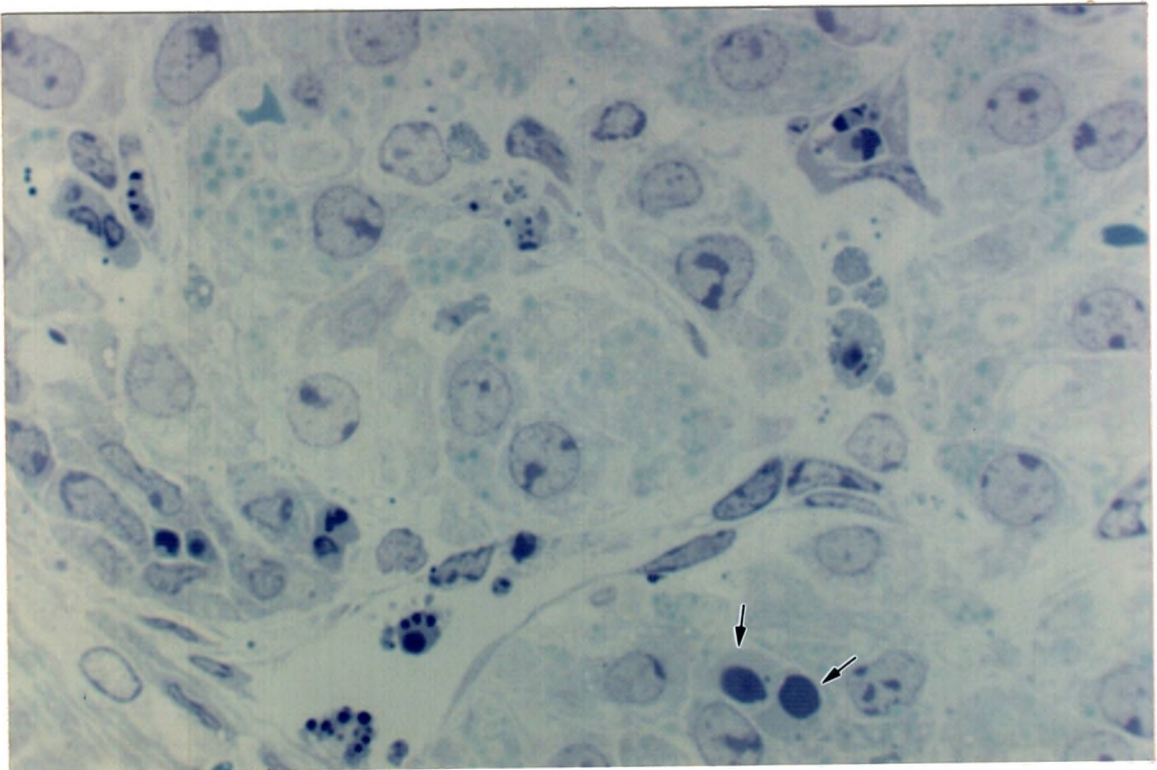
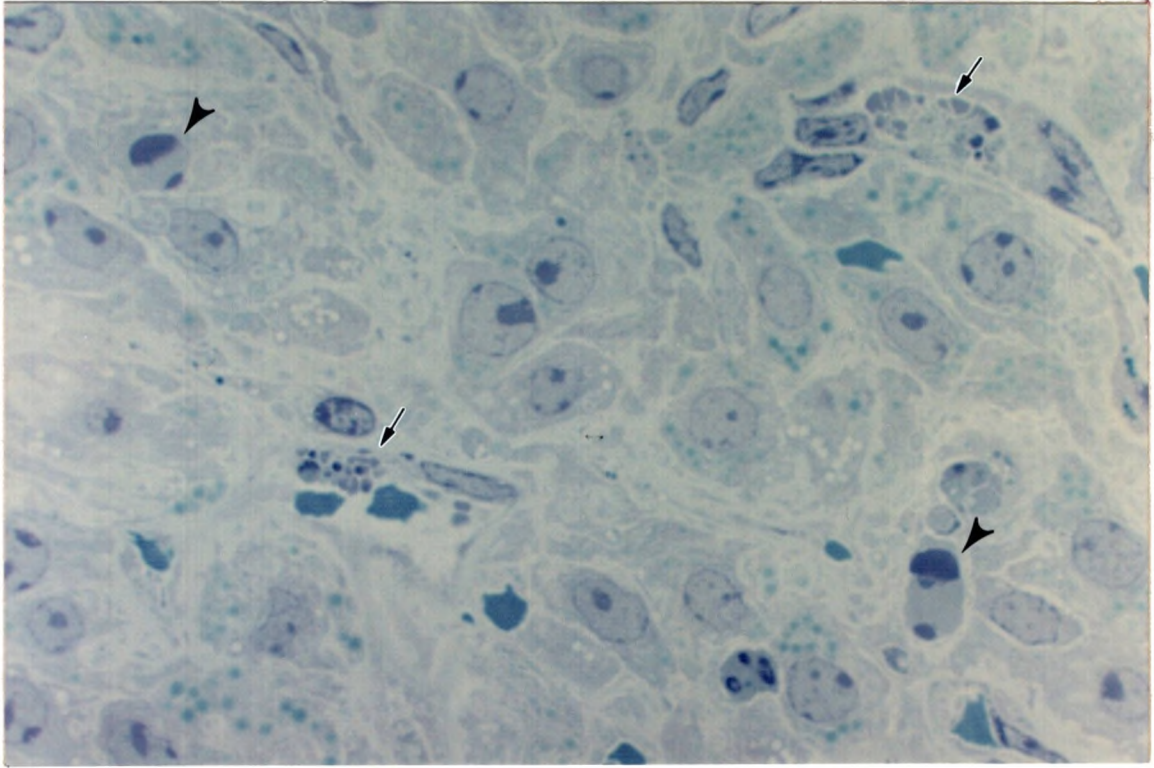


PLATE XVIII

Figure 35 Highpower photomicrograph of a section through a hamster CL at 1530 hours on D3. There is much apoptotic cell death. Arrow, transformed luteal cell. X 1000.

Figure 36 Highpower photomicrograph of a section through hamster luteal tissue at 1530 hours on D3. A mitotic cell (arrow) is shown surrounded by degenerating tissue. X 1000.

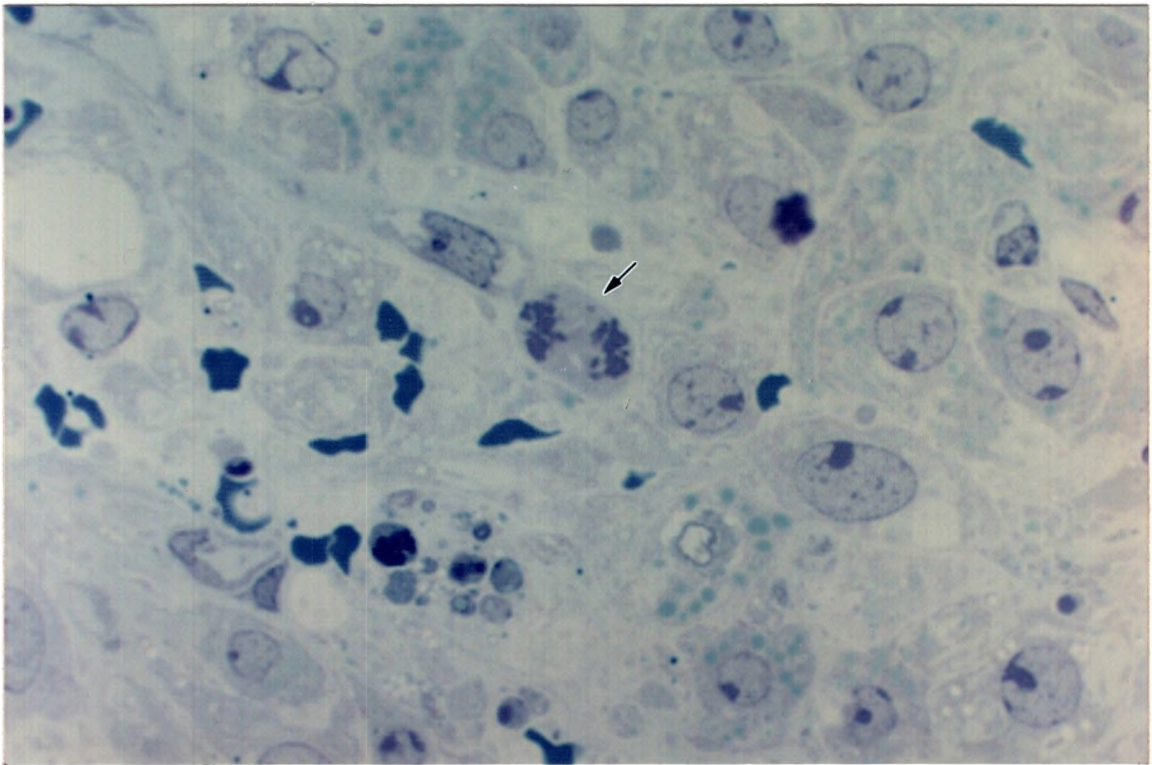
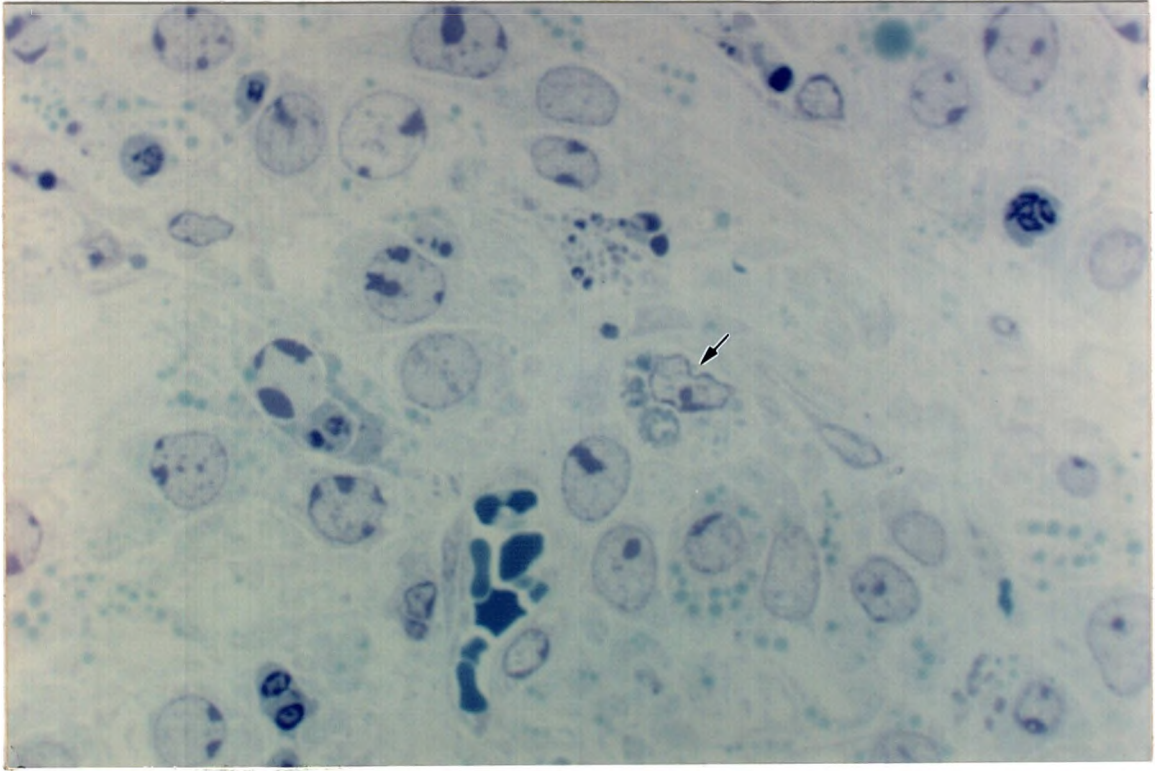


PLATE XIX

Figure 37. Lowpower photomicrograph of section through a hamster CL at 0900 hours on D4. The gland has shrunken and is avascular in character as compared to 0900 hours on D3 (figure 18). X 100.

Figure 38. Photomicrograph of a section through a hamster CL at 0900 hours on D4 demonstrating the morphology of advanced luteolysis. Thecal cells are located near the margin and appear to accumulate less lipid than granulosa cells. Arrows indicate the theca lutein area. X 400.

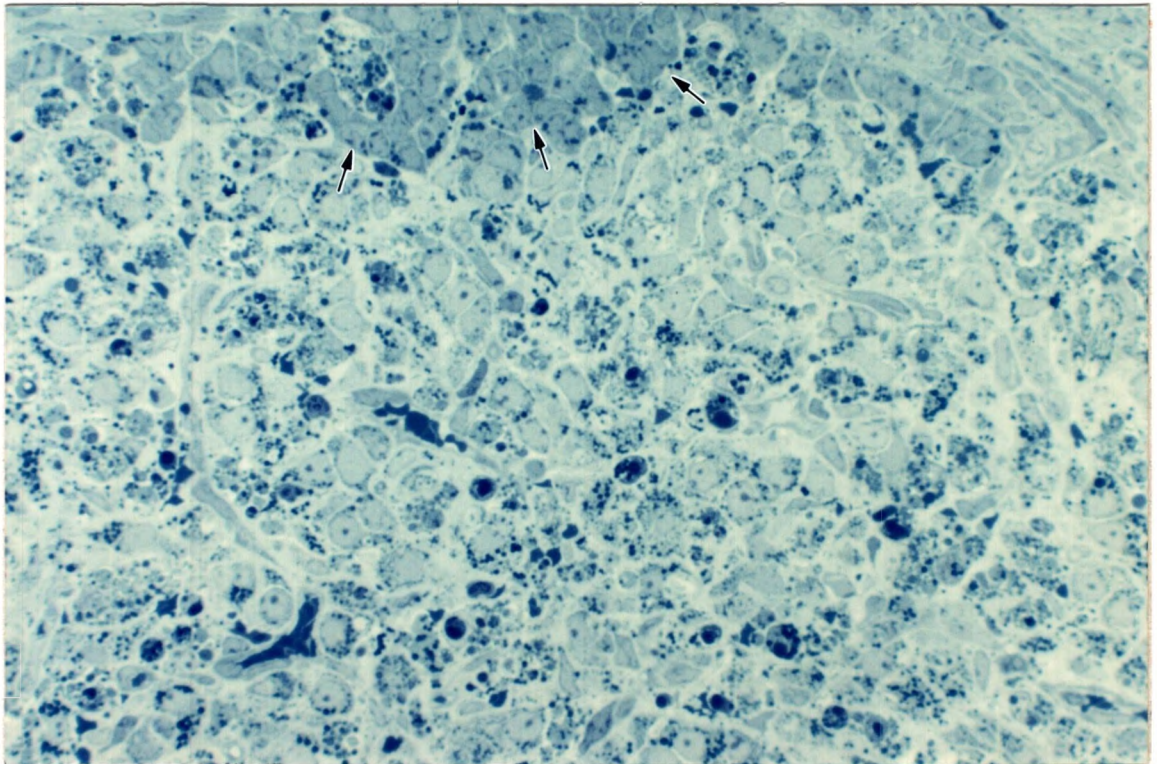
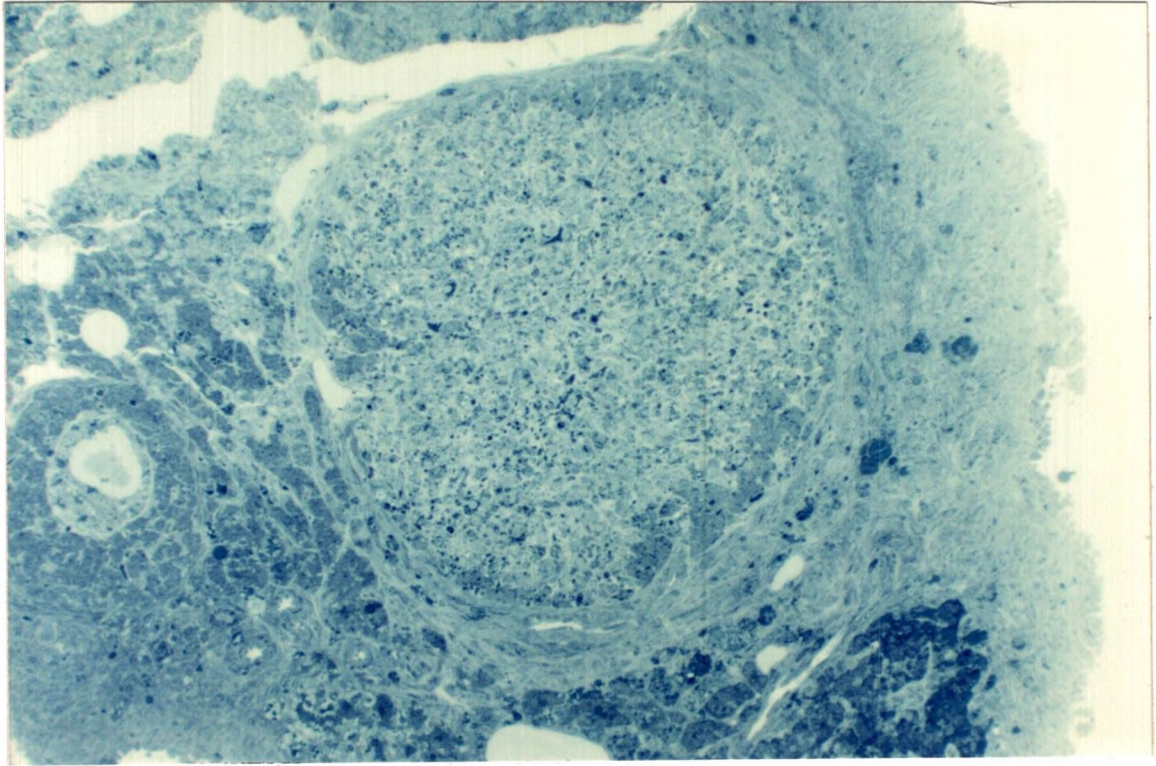


PLATE XX

Figure 39. Highpower photomicrograph of a section through hamster luteal tissue at 0900 hours on D4. Considerable lipid accumulation and scattered apoptotic bodies are present. The arrow indicates one such large apoptotic body. X 1000.

Figure 40. Highpower photomicrograph of a section through hamster luteal tissue in advanced luteolysis at 0900 hours on D4. Disorganization of luteal structure characterizes the tissue. A transformed luteal cell is indicated by the arrow. X 1000.

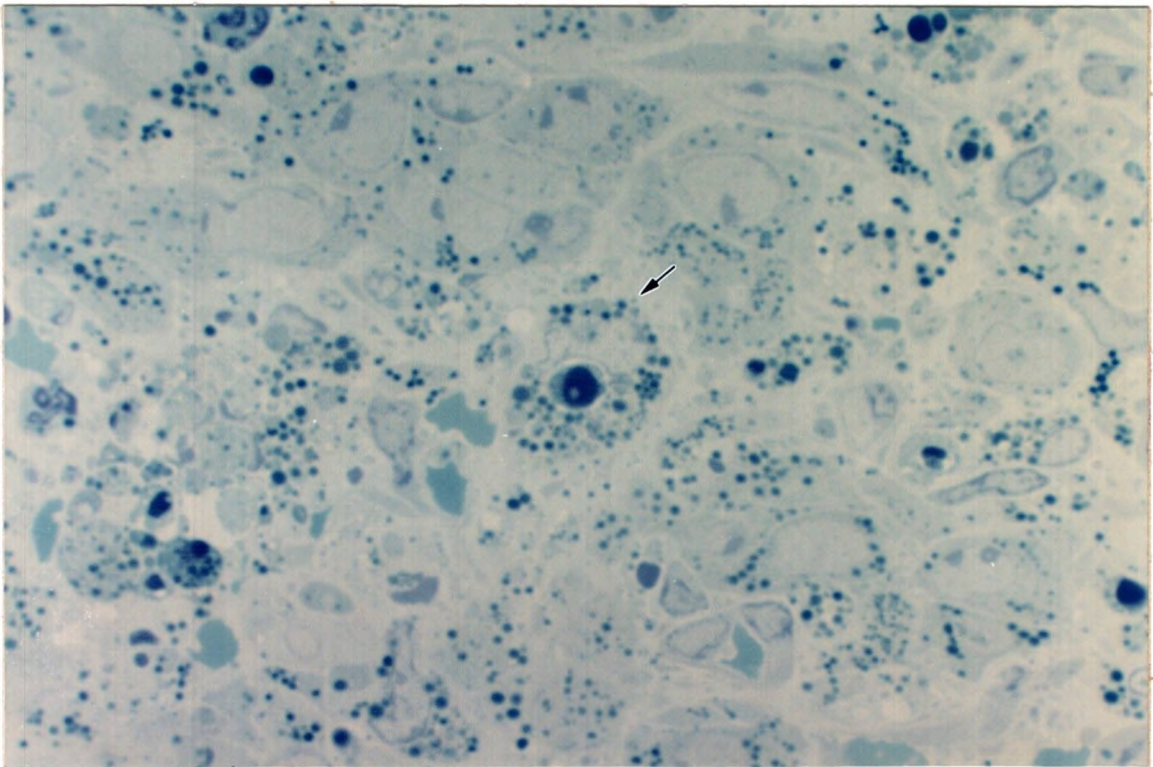
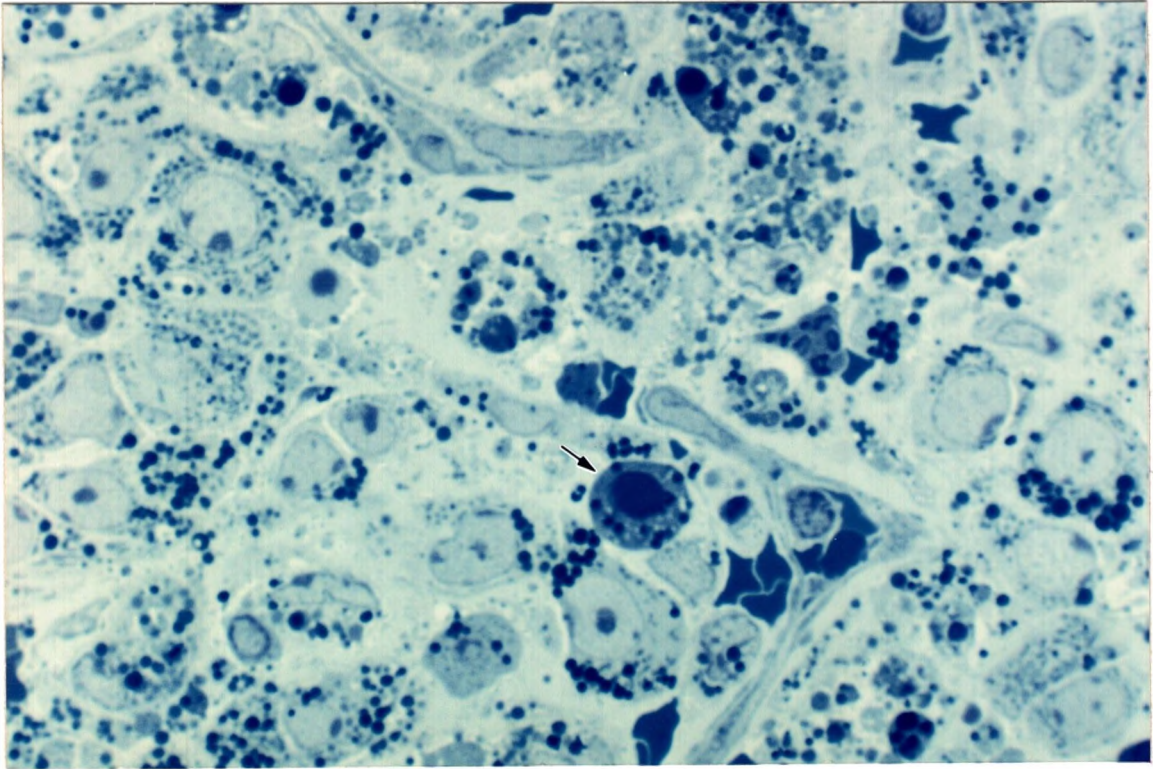


PLATE XXI

Figure 41. Highpower photomicrograph of a section through a 0900 hour hamster CL on D4. A transformed luteal cell is shown at the tip of the arrow. X 1000.

Figure 42 Highpower photomicrograph of section through a hamster CL at 0900 hours on D4 demonstrating a transformed luteal cell with an abundance of apoptotic debris in its cytoplasm (arrow). X 1000.

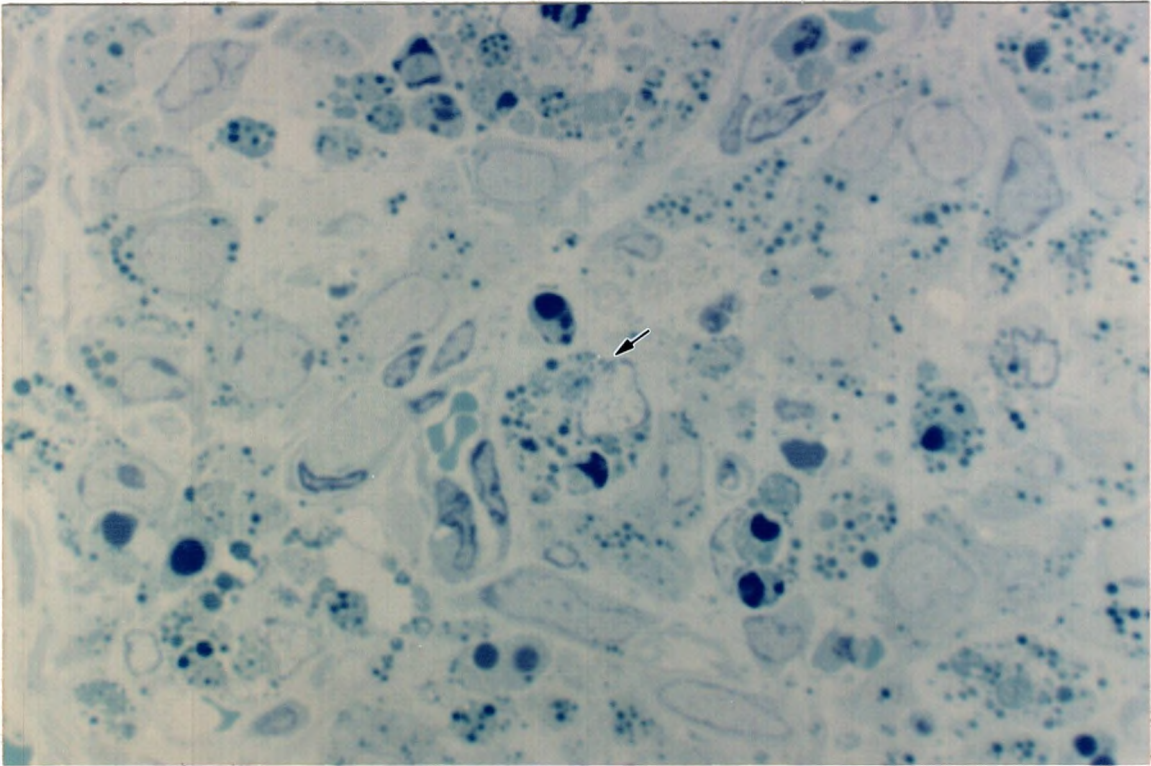
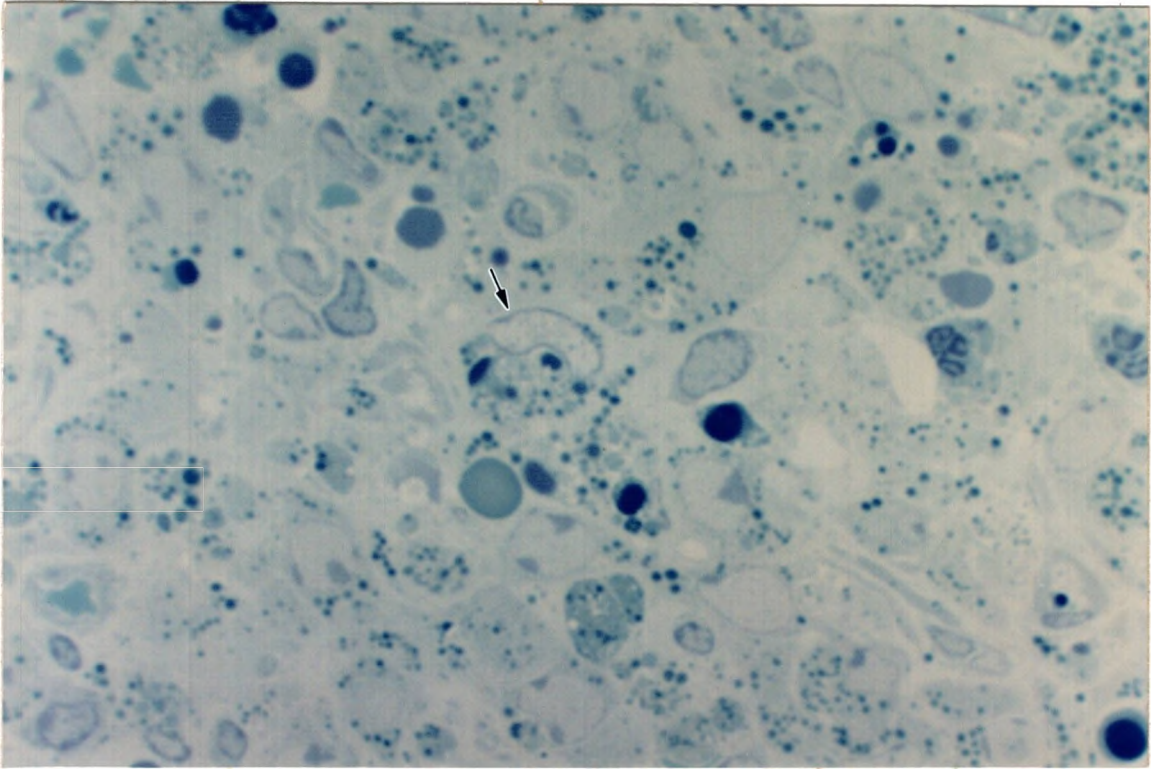


PLATE XXII

Figure 43. Highpower photomicrograph of a section through hamster luteal tissue at 0900 hours on D4. In the field are two phagocytic transformed luteal cells (arrows) which may account, in part, for the dampened inflammatory response seen in hamster luteolysis. X 1000.

Figure 44. Lowpower photomicrograph of a section through an 0900 hour hamster ovary on D1 demonstrating the tiny remnants (cr) of three degenerated CL from the previous cycle. X 100.

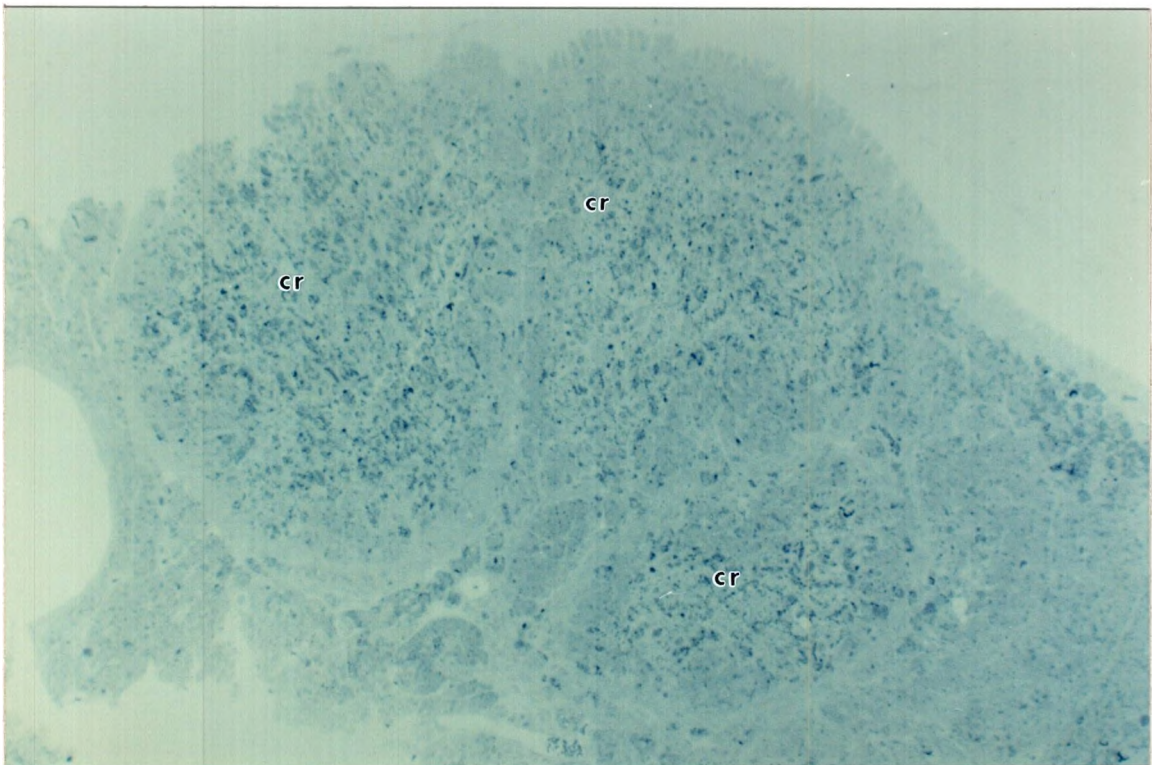
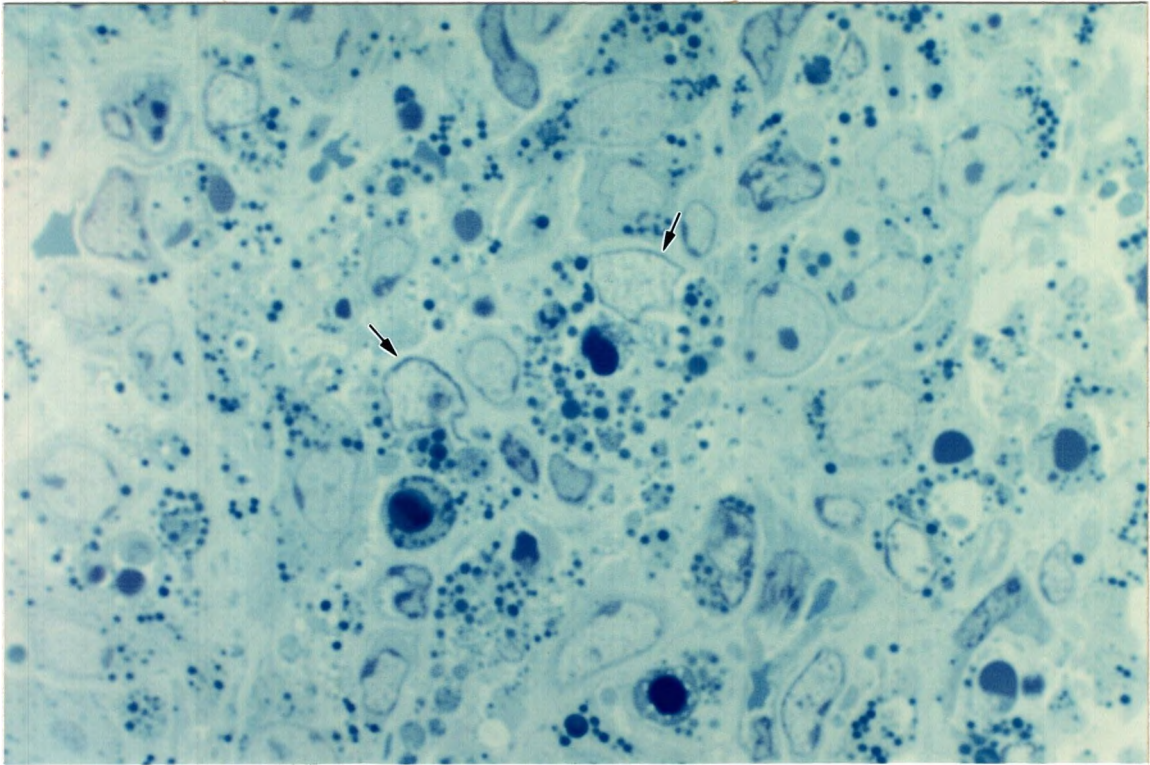


PLATE XXIII

Figure 45. Electronmicrograph of section through D1 0900 hour hamster granulosa lutein cells. There are few intercellular junctions (arrows) but many large extracellular spaces with numerous microvillus processes. Mitochondria (m) appear dense. The microvascular network has not yet developed throughout the gland. X 7,500.

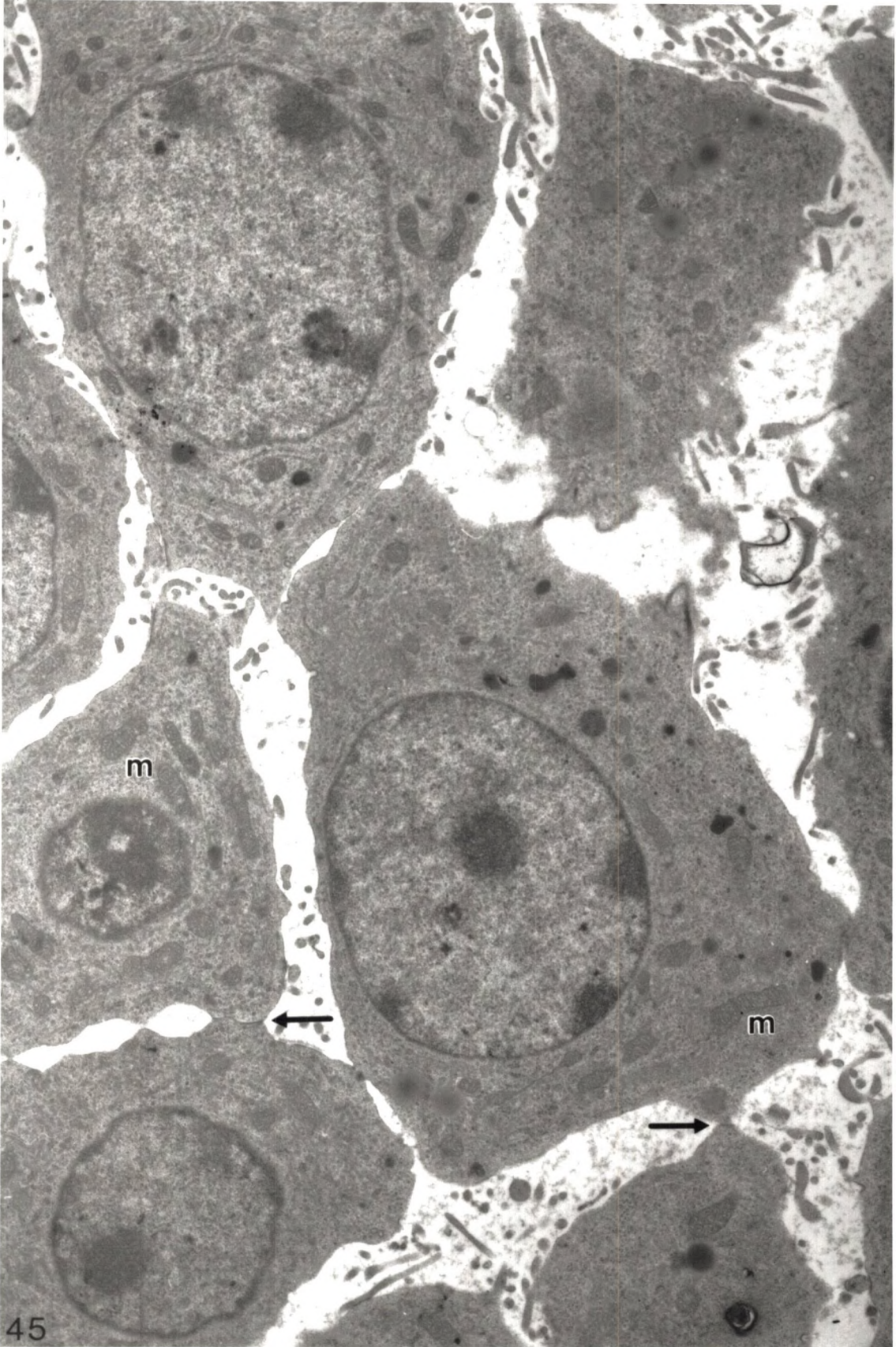


PLATE XXIV

Figure 46 Electronmicrograph of a section through hamster D2 0900 hour luteal tissue. The extracellular space is reduced from D1 (figure 45) and the luteal cells approximate one another. There are numerous cell-cell junctions. The mitochondria (m) are swollen with rarified matrices and the amount of SER (ser) is markedly increased from D1. There are scattered lipid droplets within the luteal cell cytoplasm and there is a rich blood supply such that no luteal cell is more than a cell width away from a capillary. X 7,500.

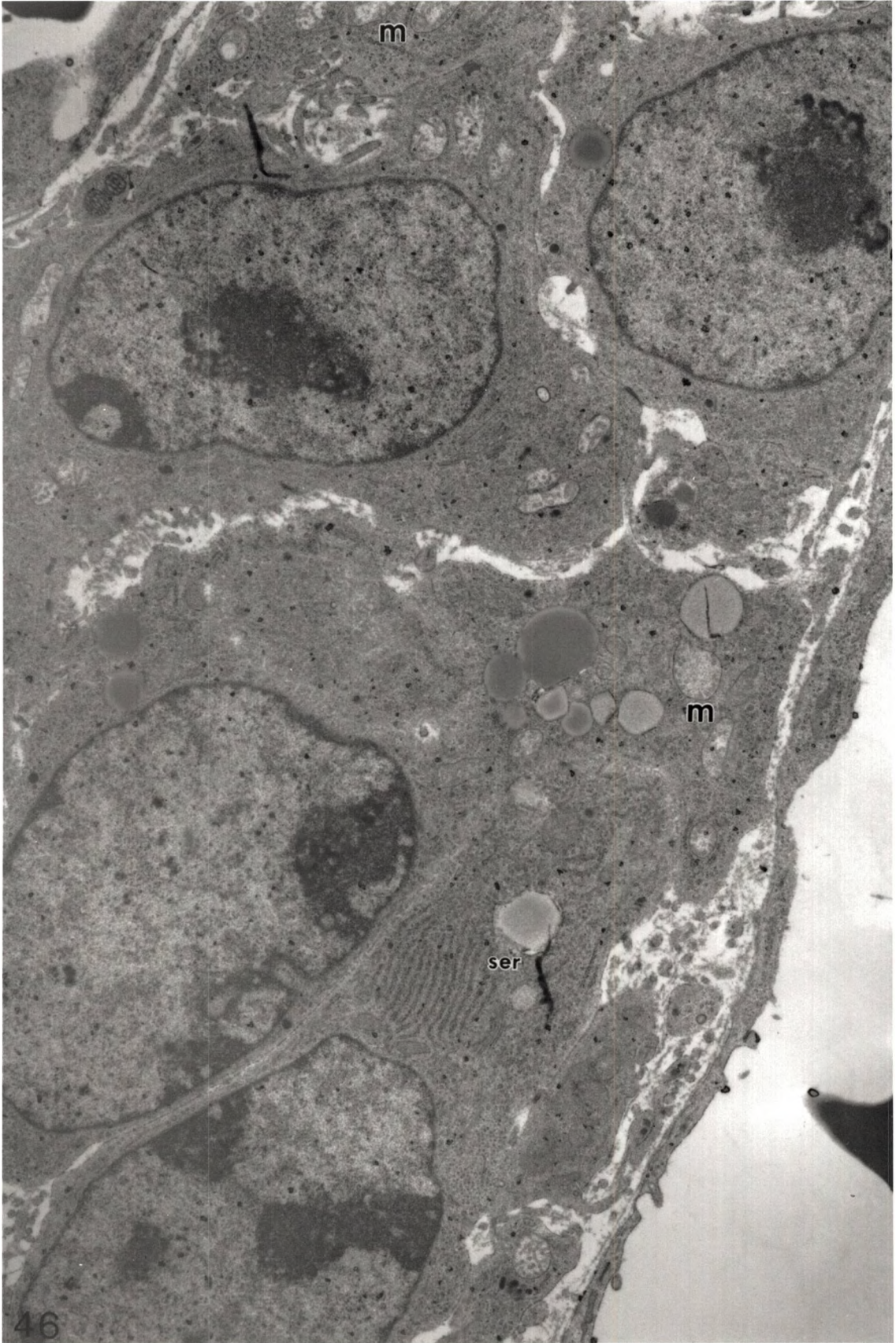


PLATE XXV

Figure 47. Electronmicrograph of a section through hamster luteal tissue at 2400 hours on D2, the midpoint of the L-Fs. The most obvious changes from 0900 hours are the formation of areas containing extracellular membranous debris (arrow) and the more compact and electron dense appearance of the mitochondria (m), similar to D1. X 5,600.

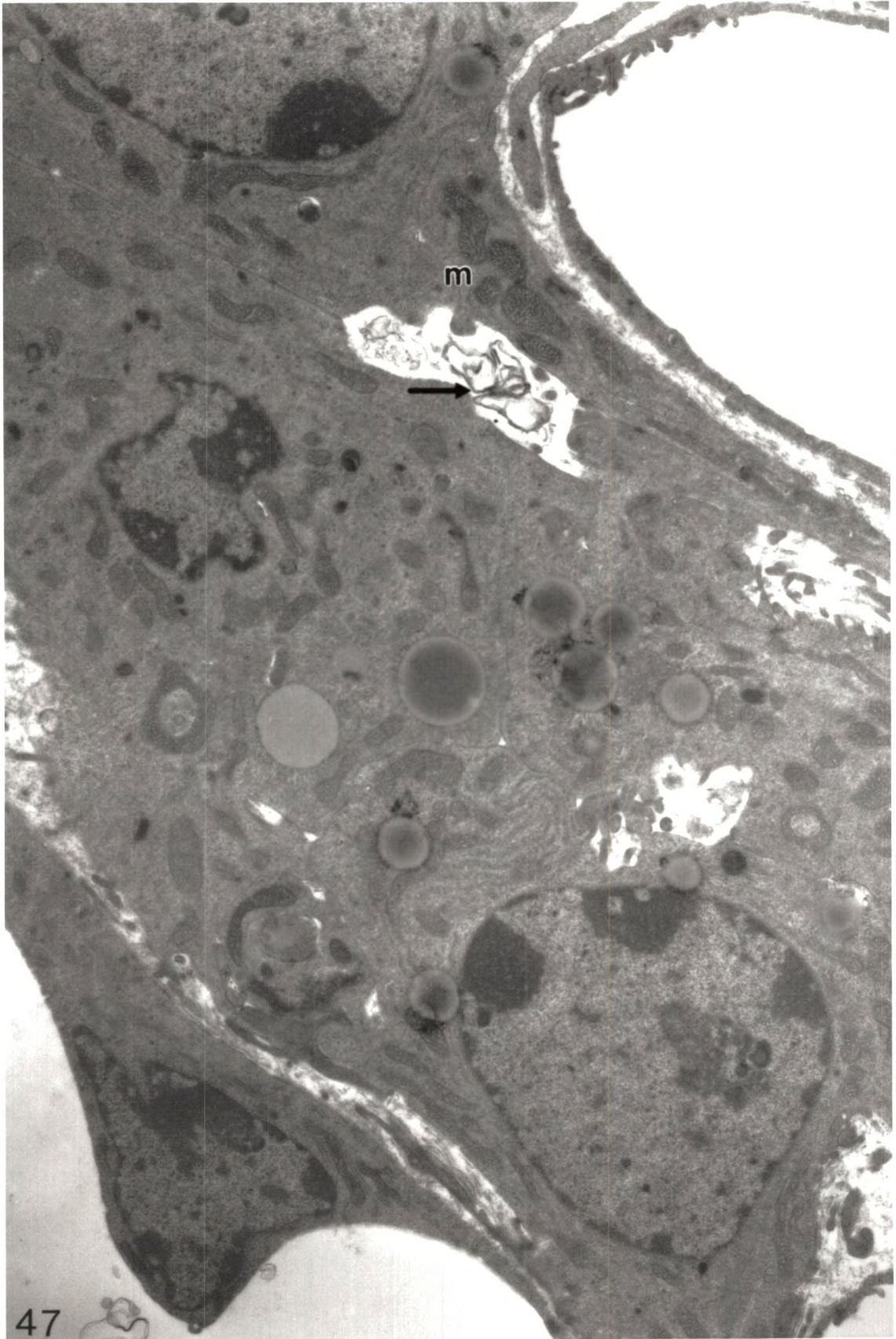


PLATE XXVI

Figure 48. Electronmicrograph of a section through D3 0300 hour hamster luteal tissue. Increased detached membranous structures or myelin figures (mf) are evident in the extracellular space. Endothelial vesicles (arrows) and myelin figures (mf) are present in the intravascular space. X 10,500.

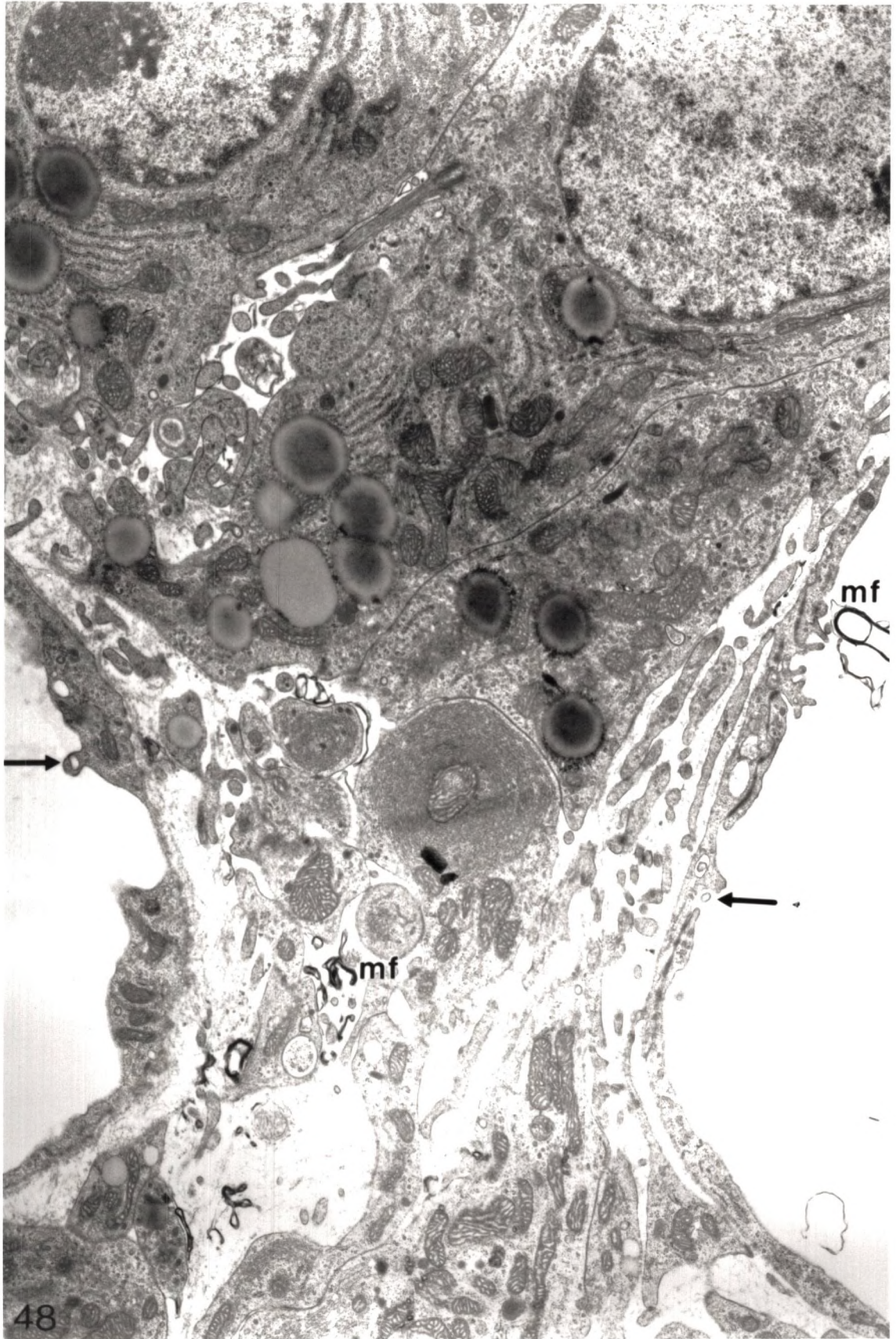
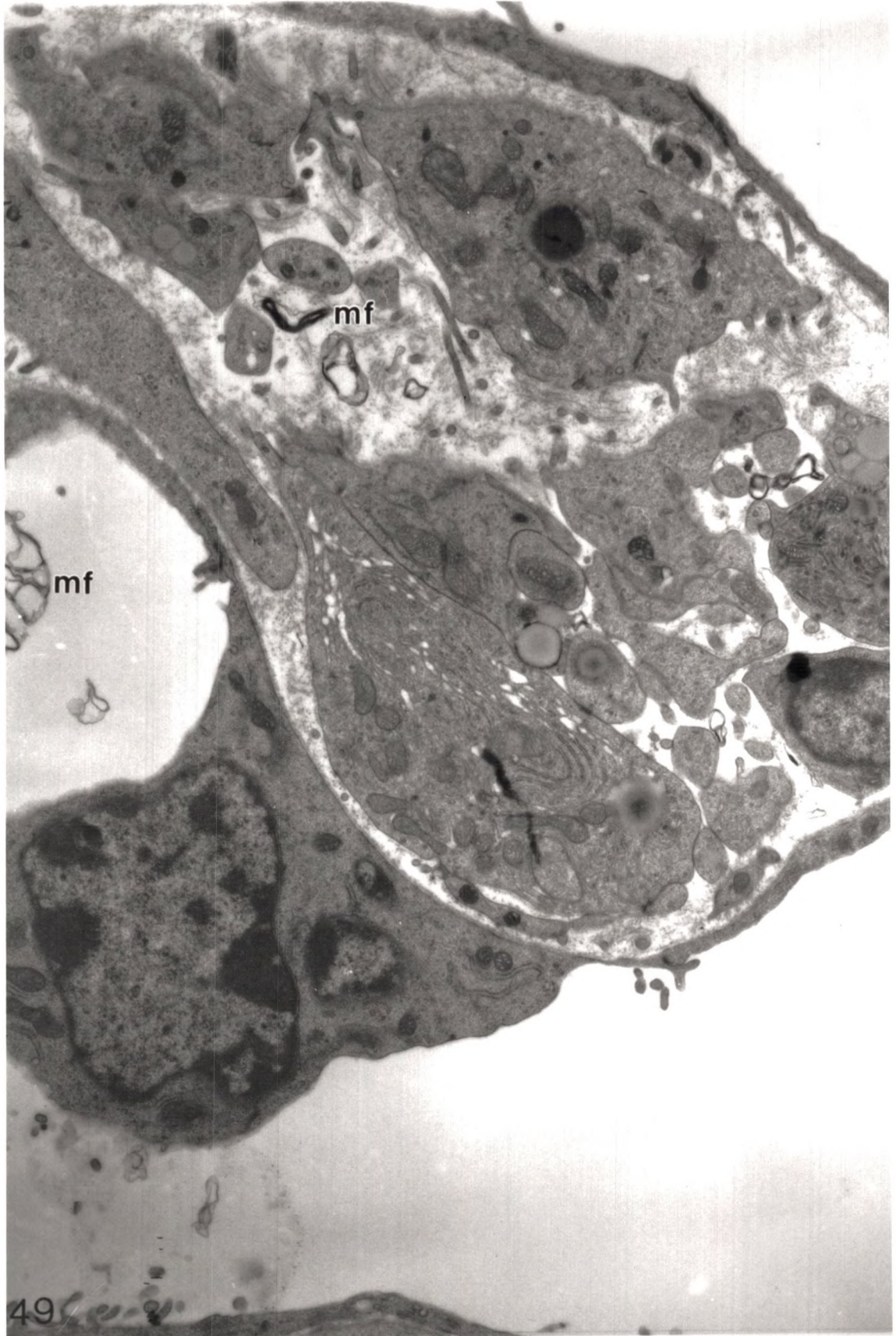


PLATE XXVII

Figure 49. Electronmicrograph of a section through hamster luteal tissue at 0300 hours on D3. Features are similar to figure 48. Myelin figures, (mf). X 10,700.



mf

mf

PLATE XXVIII

Figure 50. Electronmicrograph of a section through 0300 hour hamster luteal tissue on D3. Intravascular myelin figures are evident as are lysosomes (L) within luteal cells. Most lysosomes are relatively small but some are quite large, (arrowhead). X 10,700.

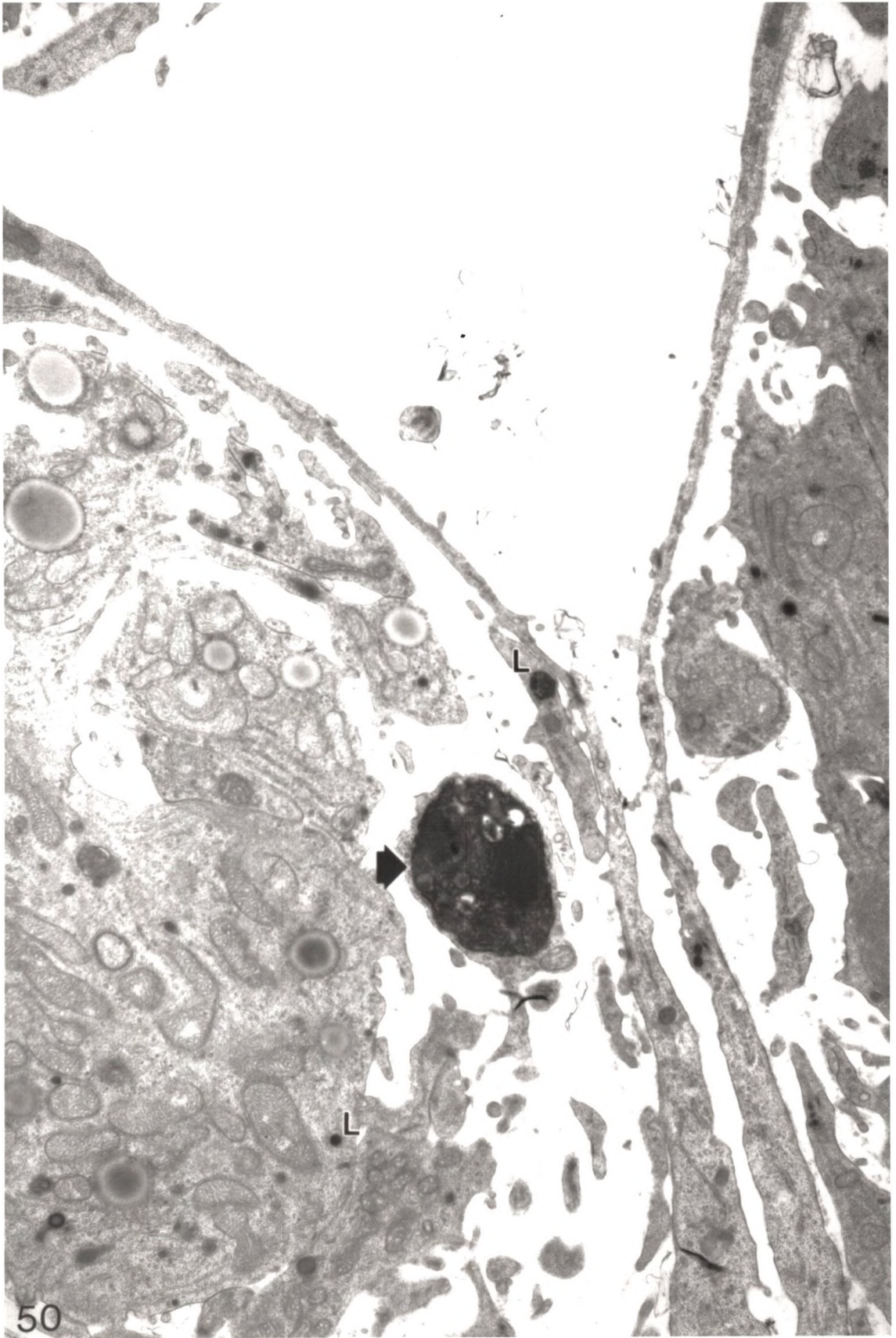


PLATE XXIX

Figure 51. Electronmicrograph of a section through 0600 hour luteal cells on D3. Large lysosomes (L) and lipid droplets (LD) are present in some cells. Extracellular myelin figures (mf) are evident. There is abundant SER (ser) in many luteal cells and some RER (er) as well. X 20,800.

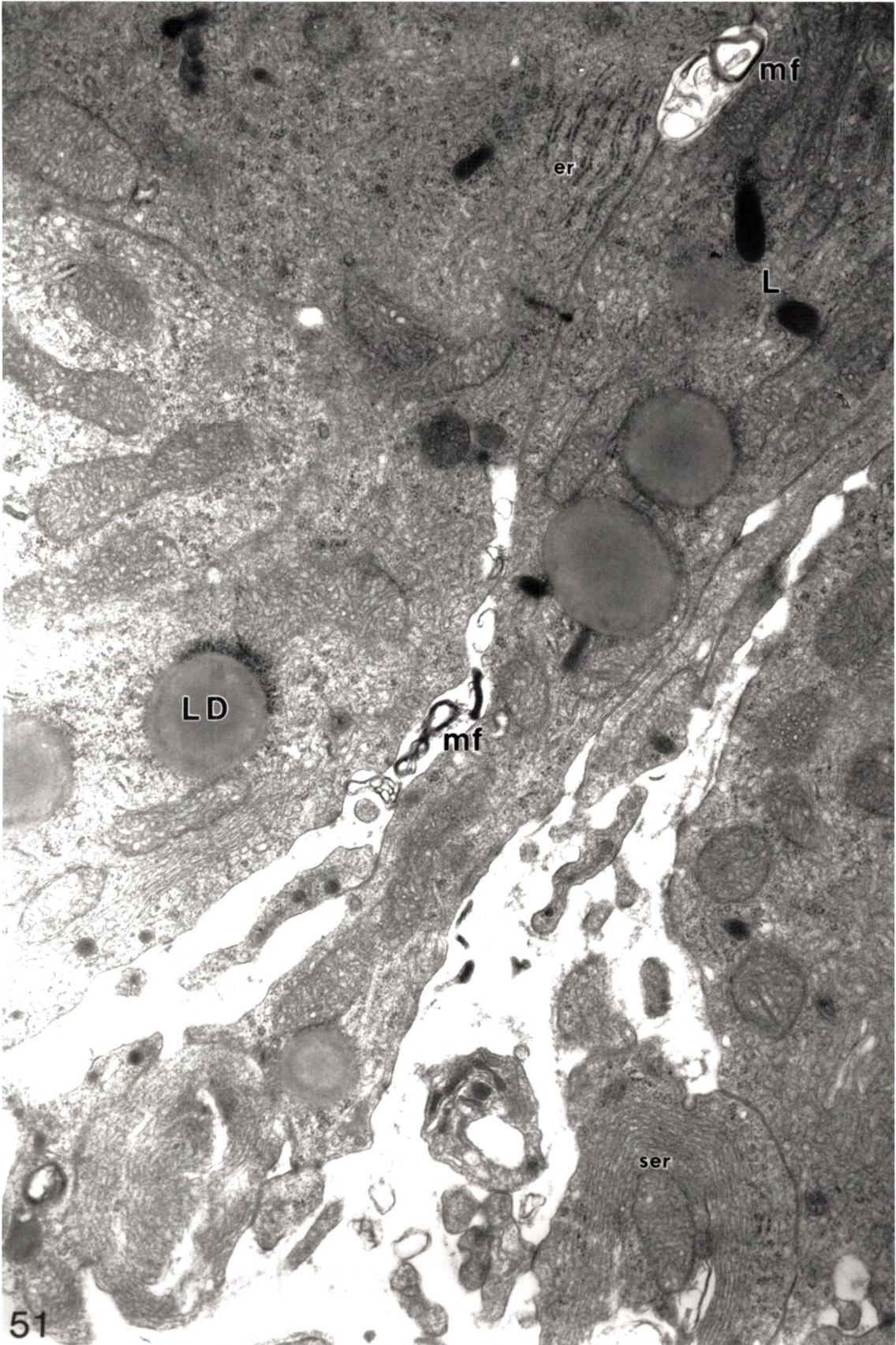


PLATE XXX

Figure 52. Electronmicrograph of a section through hamster luteal tissue at 0600 hours on D3. An emigrated neutrophil is present (arrowheads) X 7,500.

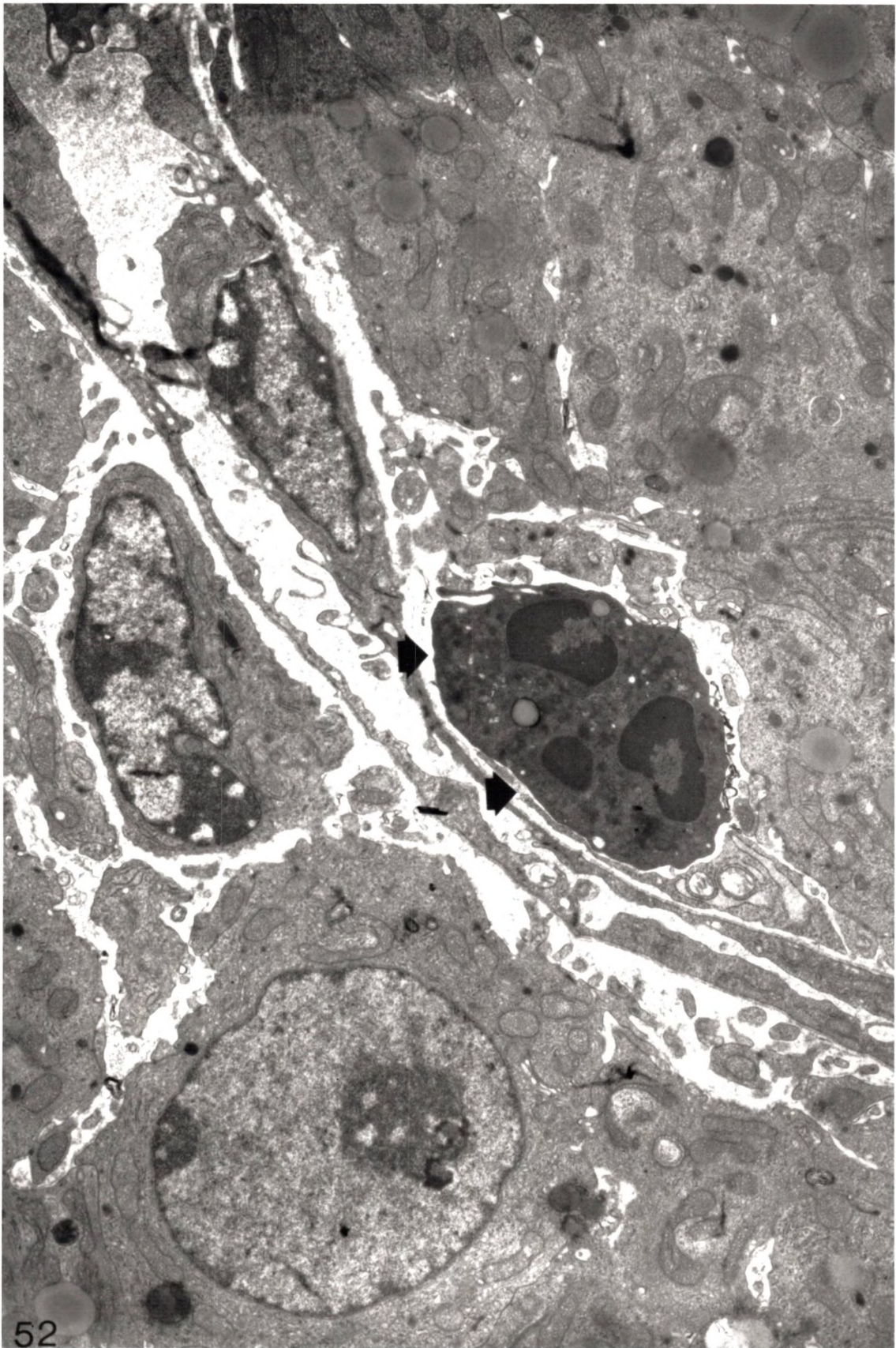
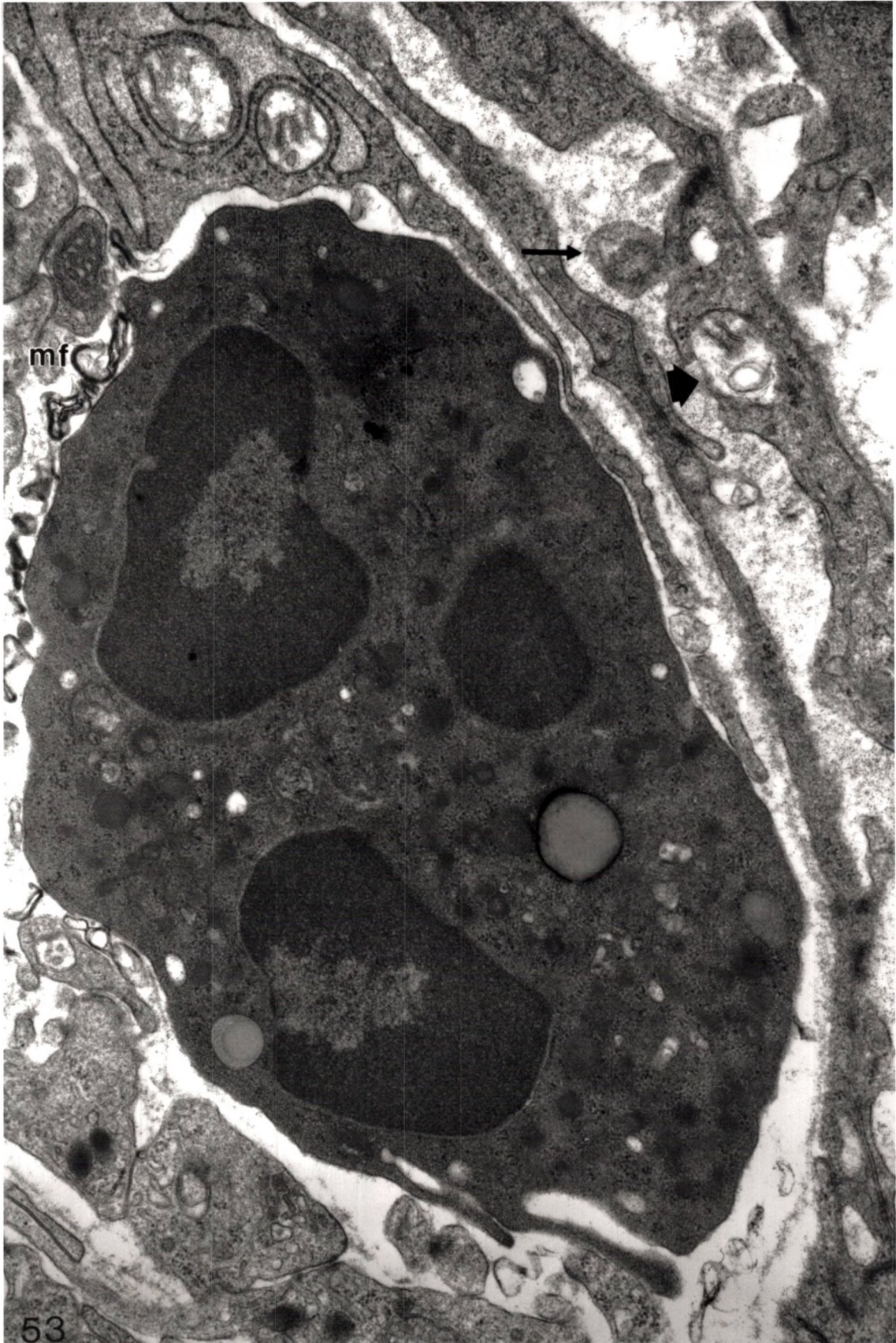


PLATE XXXI

Figure 53. Higherpower electronmicrograph of the field seen in figure 52. An extravascular PMNL and myelin figures (mf) are evident. Luminal endothelial endocytosis (arrowhead) and blebs protruding from the endothelial surface (arrow) are also notable. X 23,000.



mf

PLATE XXXII

Figure 54. Electronmicrograph of a section through hamster luteal tissue at 0900 hours on D3. Many cells are diminished in size due to marked reduction in SER content. This coincides with increased extracellular space. Atrophic debris and myelin figures are seen in the extracellular space. X 12,000.

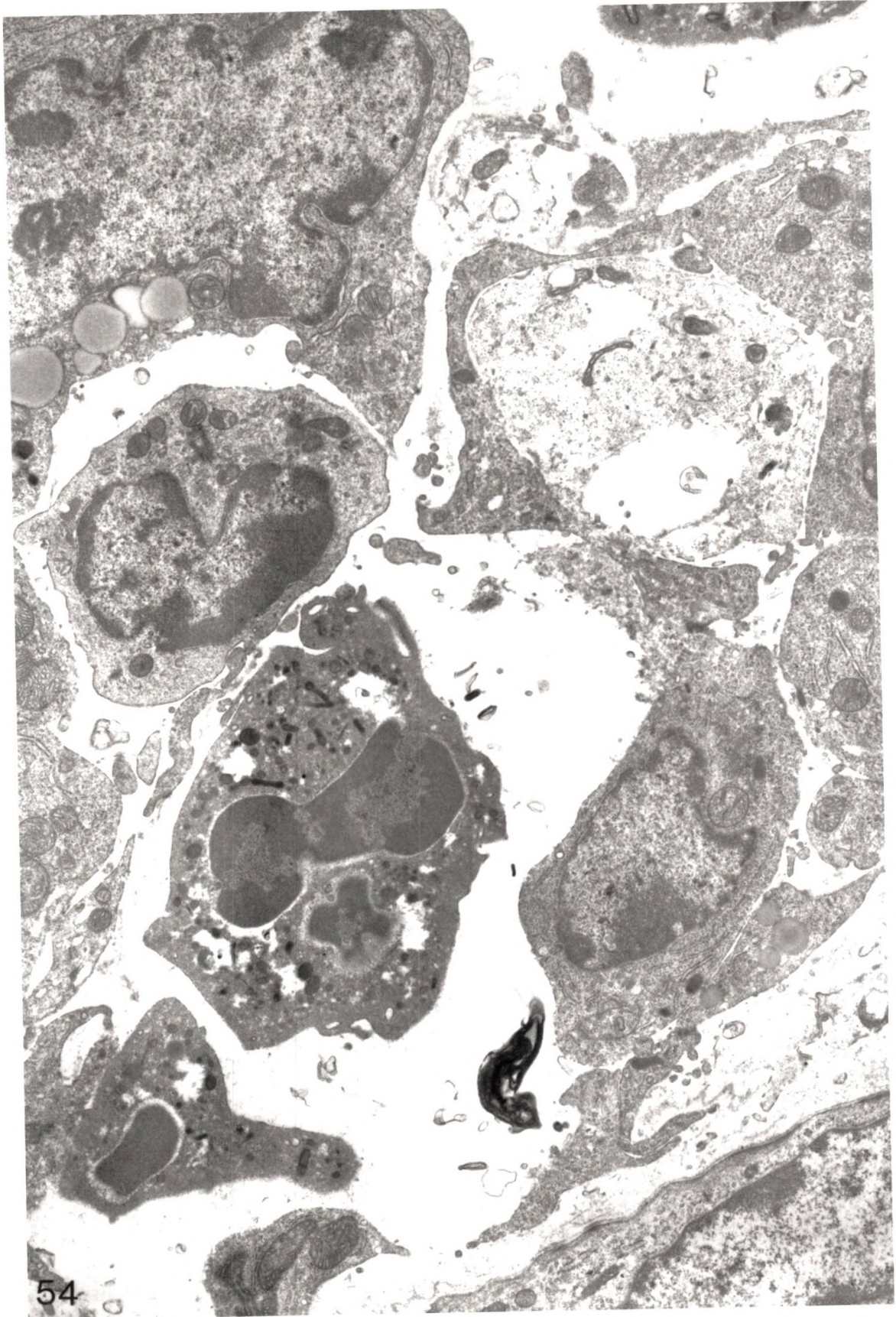


PLATE XXXIII

Figure 55. Electronmicrograph of a section through hamster luteal tissue at 0900 hours on D3. Myelin figures (mf), transcytotic endothelial vesicles (arrowheads) and PMNL phagosomes (arrows) are detectable. A = artifact. X 8,200.

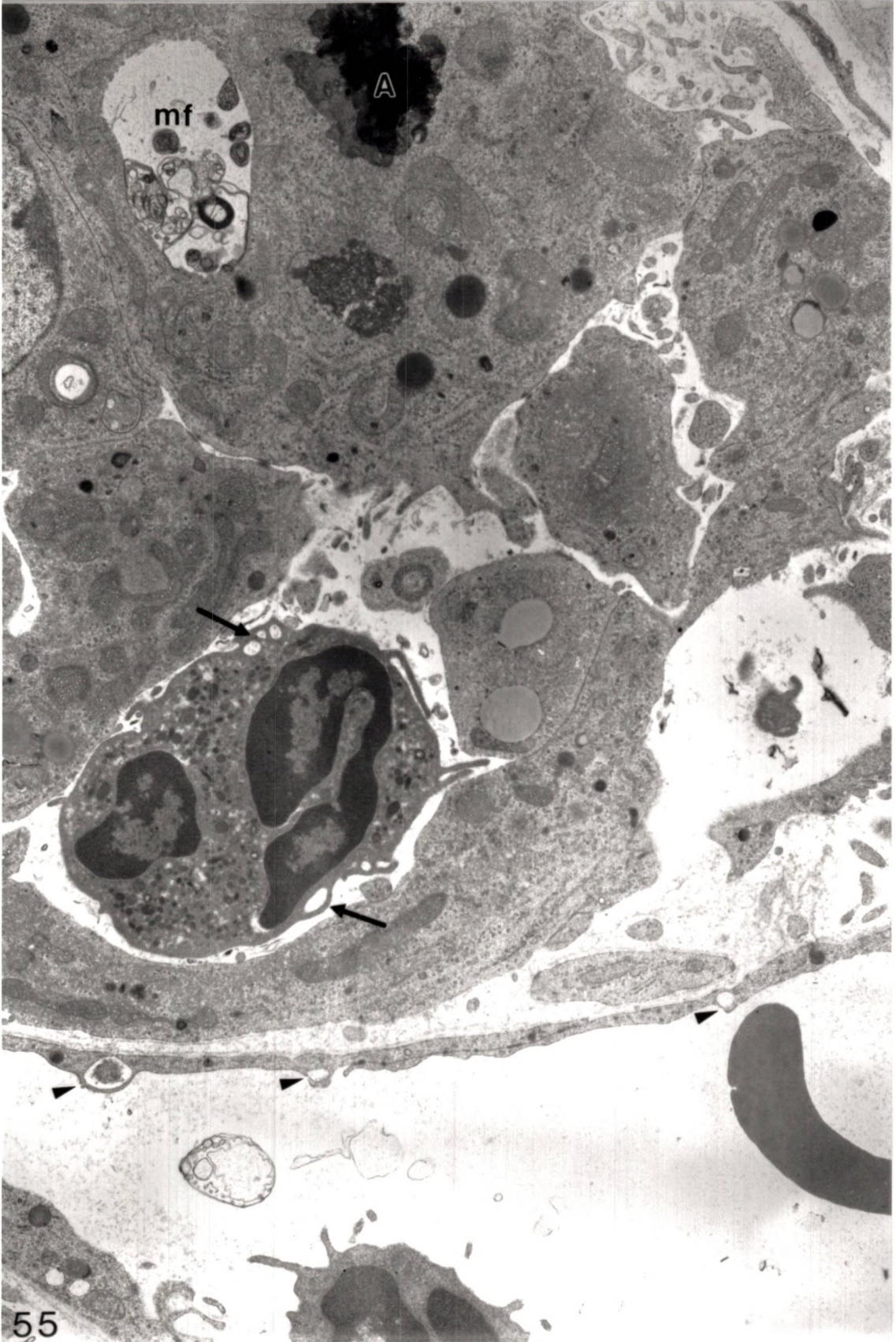


PLATE XXXIV

Figure 56. Electronmicrograph of a section through hamster luteal tissue at 0900 hours on D3. An odd endothelial baffle-like formation in the capillary lumen (arrowhead) and blebs (arrows) are shown. X 7,600.

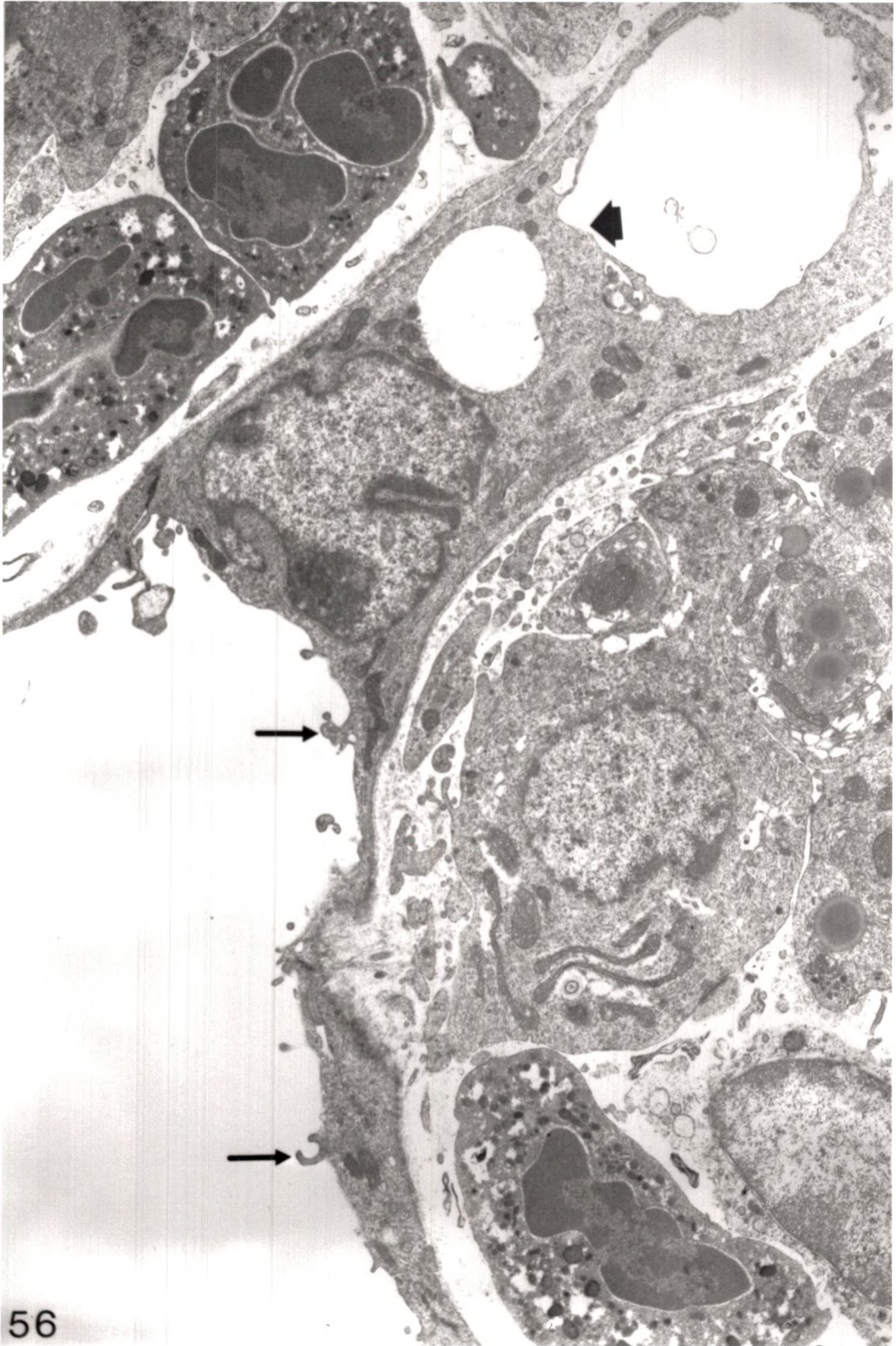


PLATE XXXV

Figure 57. Electronmicrograph of a section through hamster luteal tissue on D3 at 0900 hours. A large number of detached endothelial blebs are free in the capillary lumen (arrows). X 7,700.

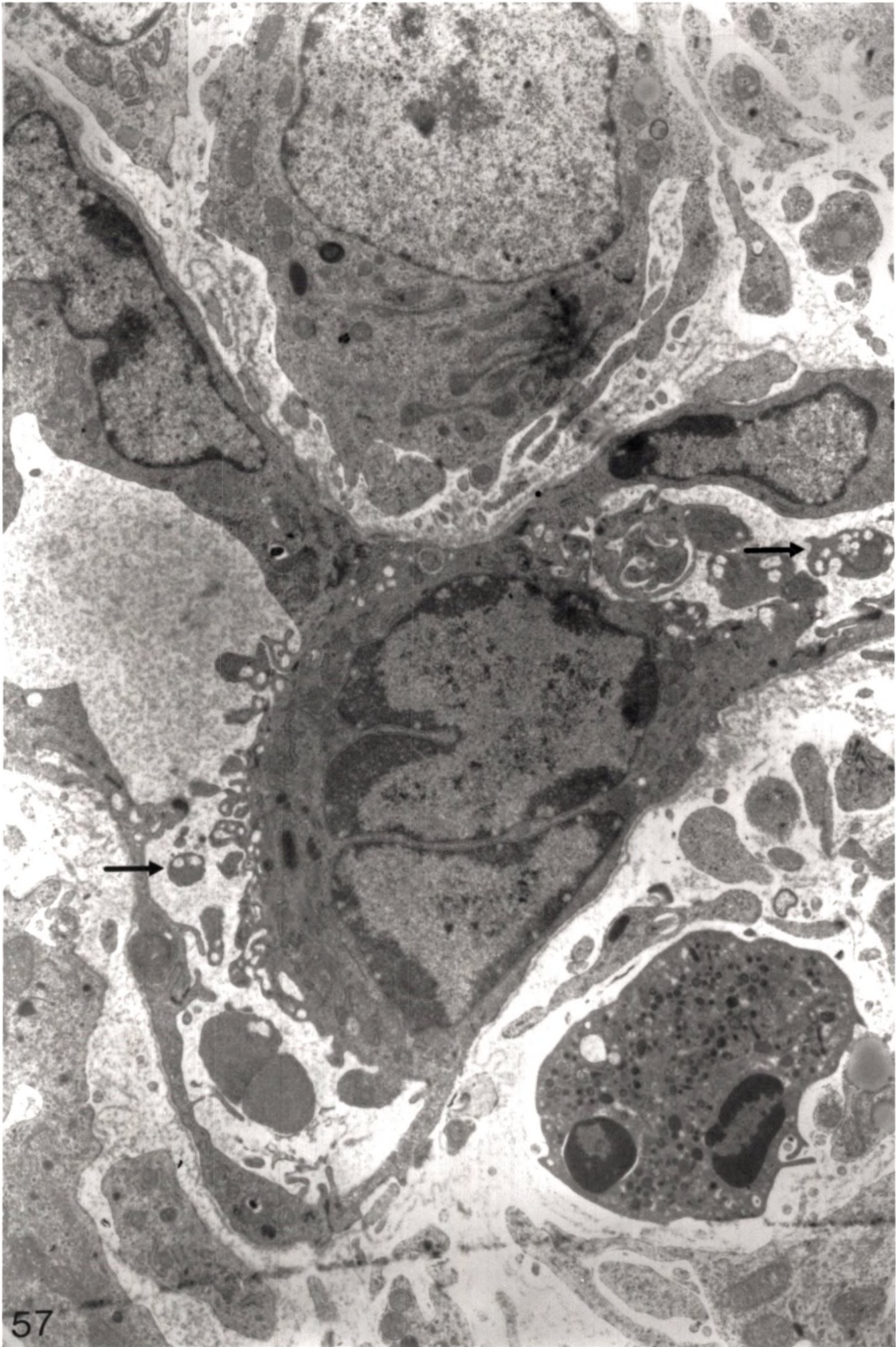


PLATE XXXVI

Figure 58. Electronmicrograph of a section through hamster luteal cells at 1300 hours on D3. Lipid droplet (LD) accumulation in some cells is abundant. Elongated, dumbbell-shaped mitochondria (m) are present in many cells. X 7,500.

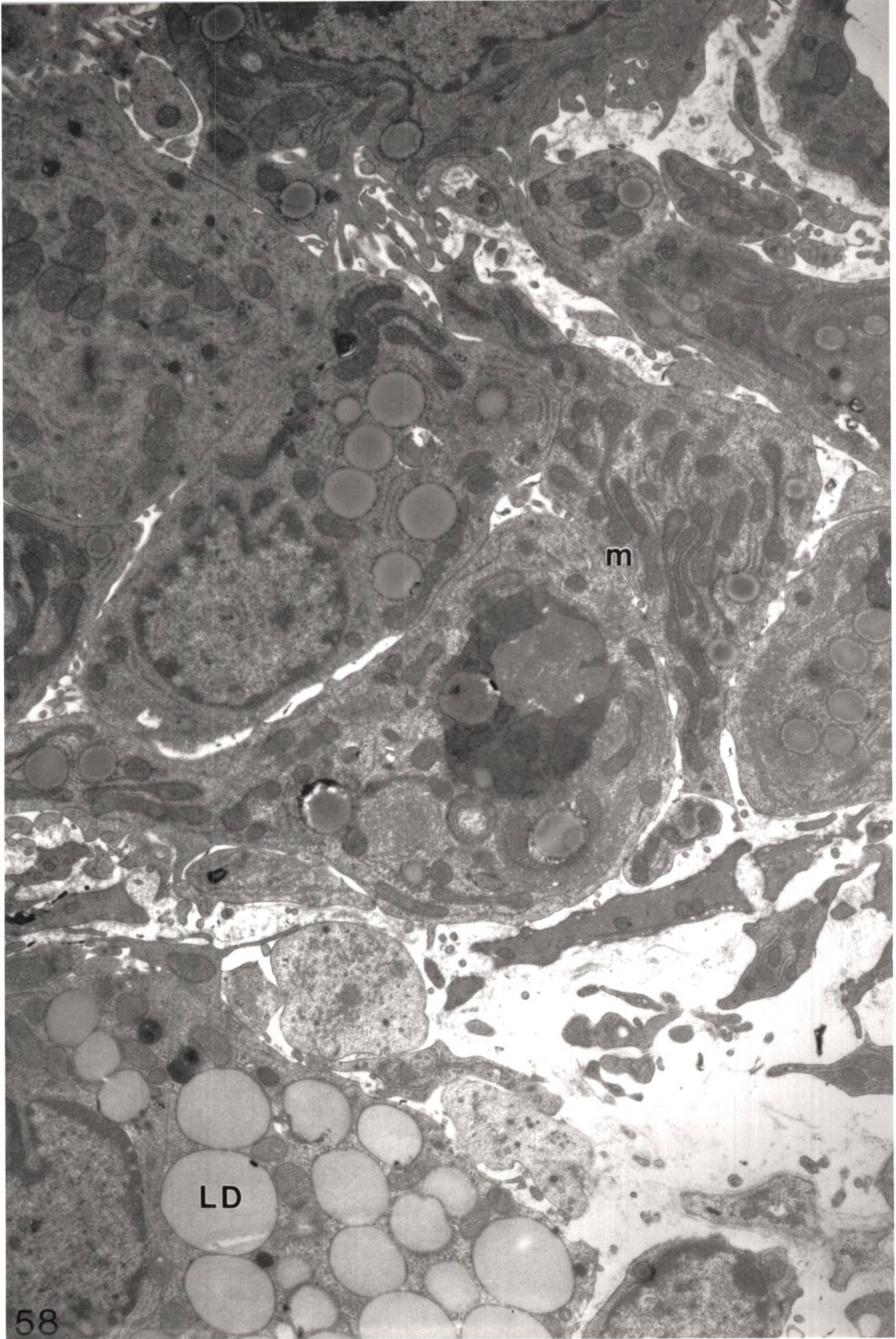


PLATE XXXVII

Figure 59. Electronmicrograph of a section through hamster luteal cells at 1300 hours on D3. A transformed luteal cell (TC) has engulfed apoptotic bodies and myelin figures. The apoptotic bodies (ab) have already begun disintegrating. X 16,700.

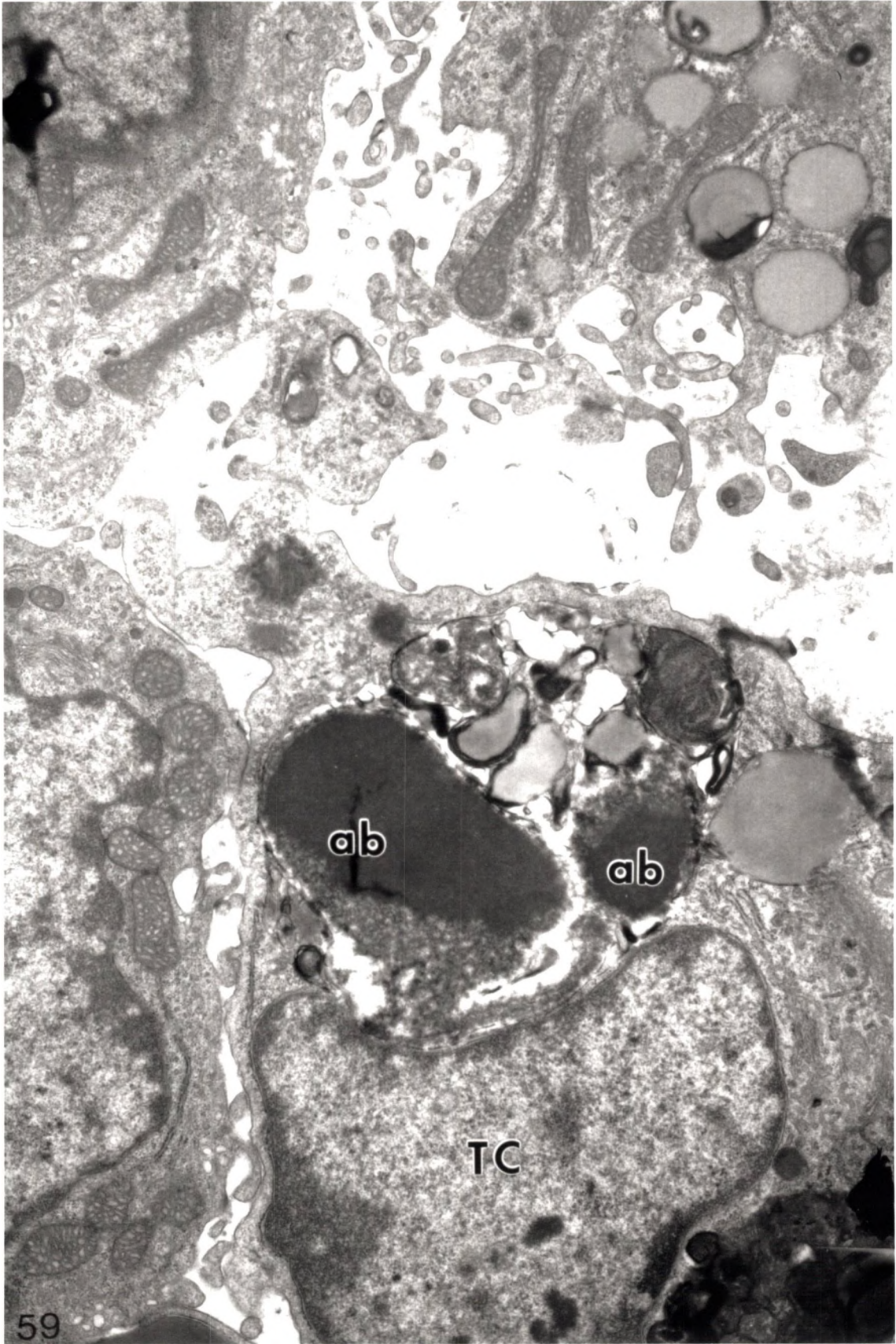


PLATE XXXVIII

Figure 60. Electronmicrograph of a section through hamster luteal tissue at 1200 hours on D3. An extravasated PMNL and extravascularly accumulated india ink carbon particles are shown. X 8,700.

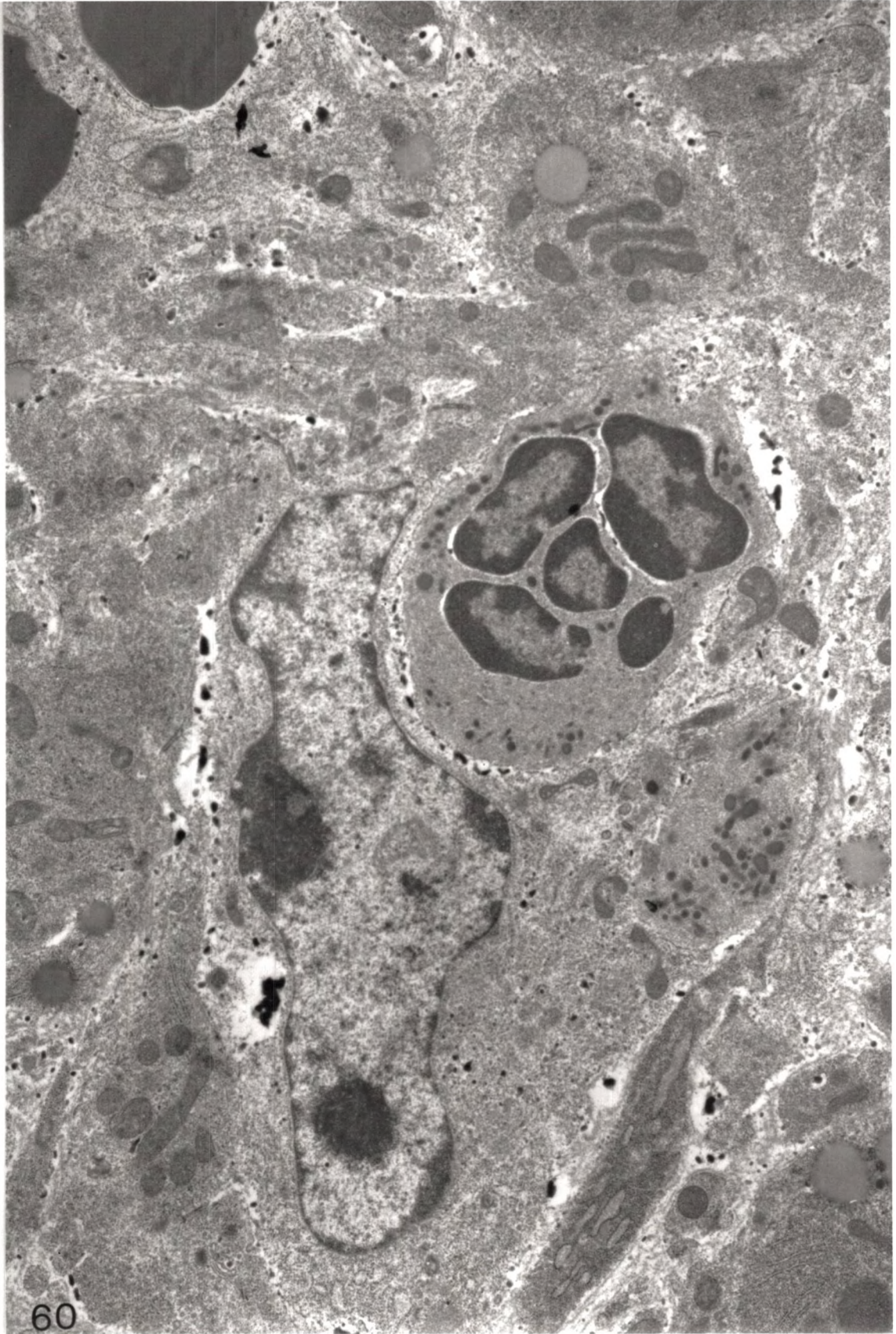
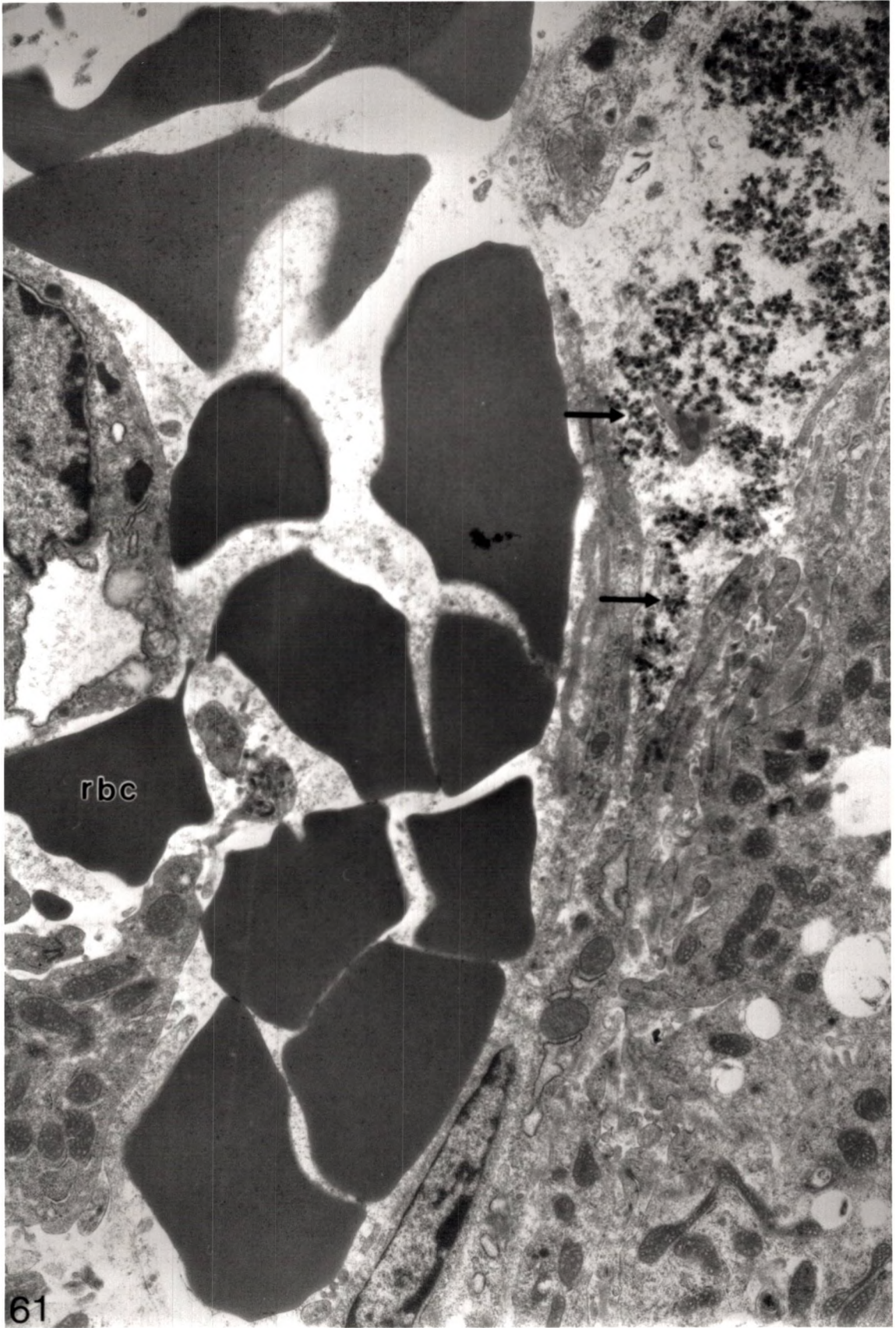


PLATE XXXIX

Figure 61. Electronmicrograph of a section through hamster luteal tissue at 1200 hours on D3. Accumulation of india ink carbon particles outside the vessel boundary (arrows) is demonstrated. An extravasated erythrocyte (rbc) is also shown. X 9,300.



rbc

PLATE XL

Figure 62. Electronmicrograph of a section through hamster luteal tissue on D3 at 1300 hours. In the field is a capillary in which apoptotic changes are occurring. An apoptotic body (ab) is located in the lower left corner of the field. An endothelial nucleus (Nu) is bulging into the lumen at the upper right margin of the field. X 7,500.

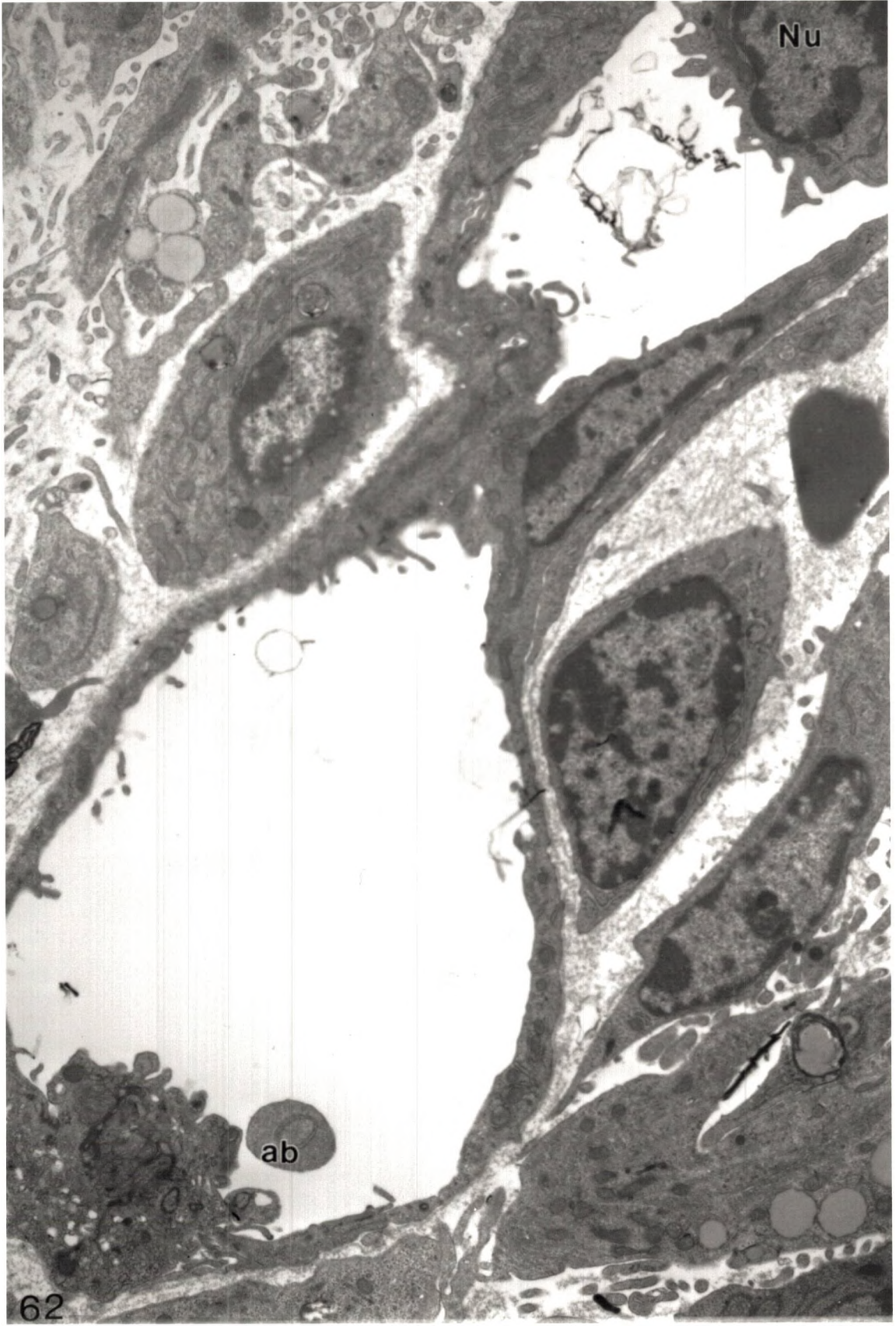


PLATE XLI

Figure 63. Electronmicrograph of a section through hamster luteal tissue on D3 at 1300 hours. A disintegrating capillary at the center of the field (cap) is notable. Portions of erythrocytes (rbc) have hemorrhaged into the regressing luteal parenchyma. X 7,900.

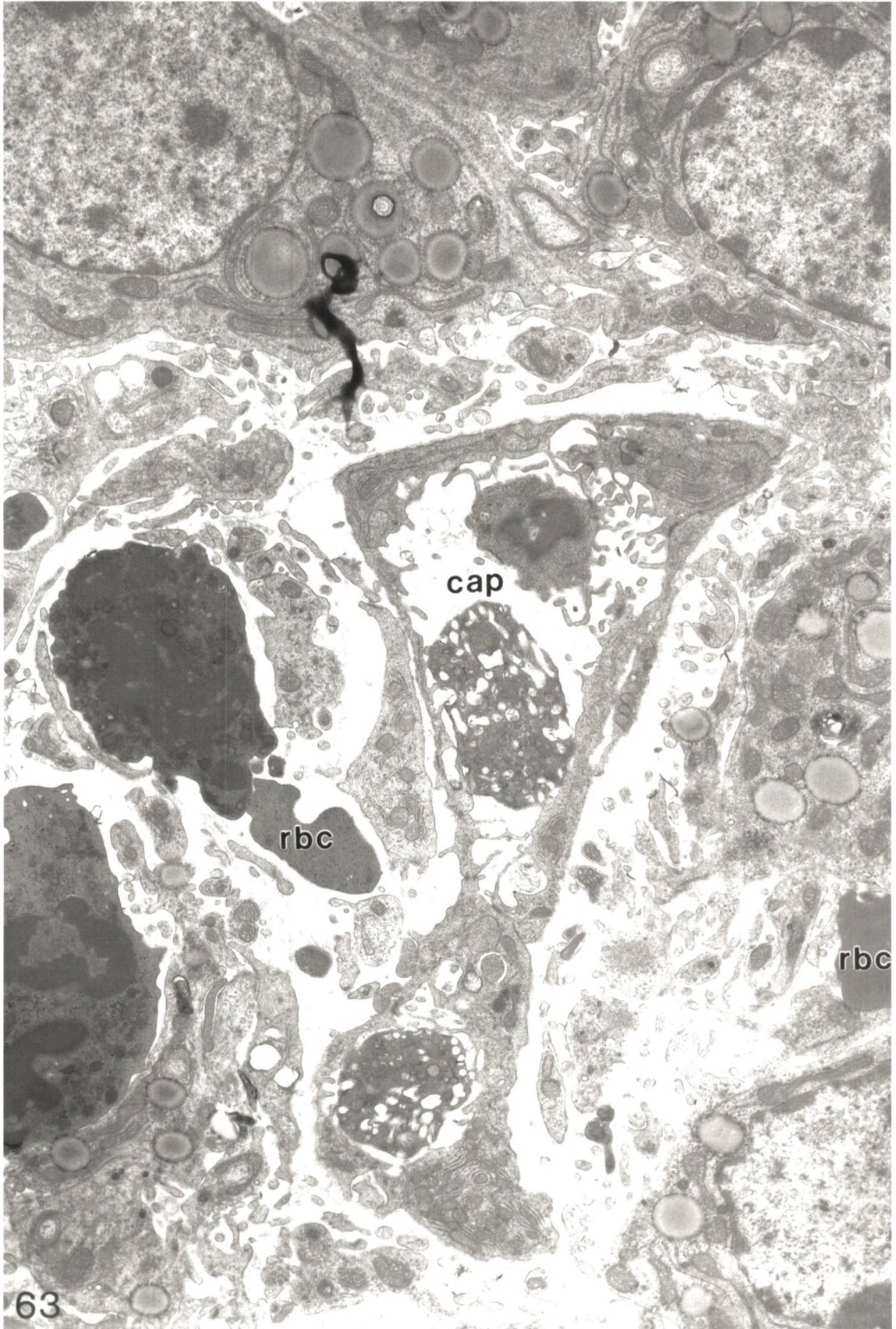


PLATE XLII

Figure 64. Electronmicrograph of a section through 1300 hour hamster luteal tissue on D3. Highlighted in the field is the presence of (classic) apoptotic bodies from a dying endothelial cell (arrows). X 9,000.

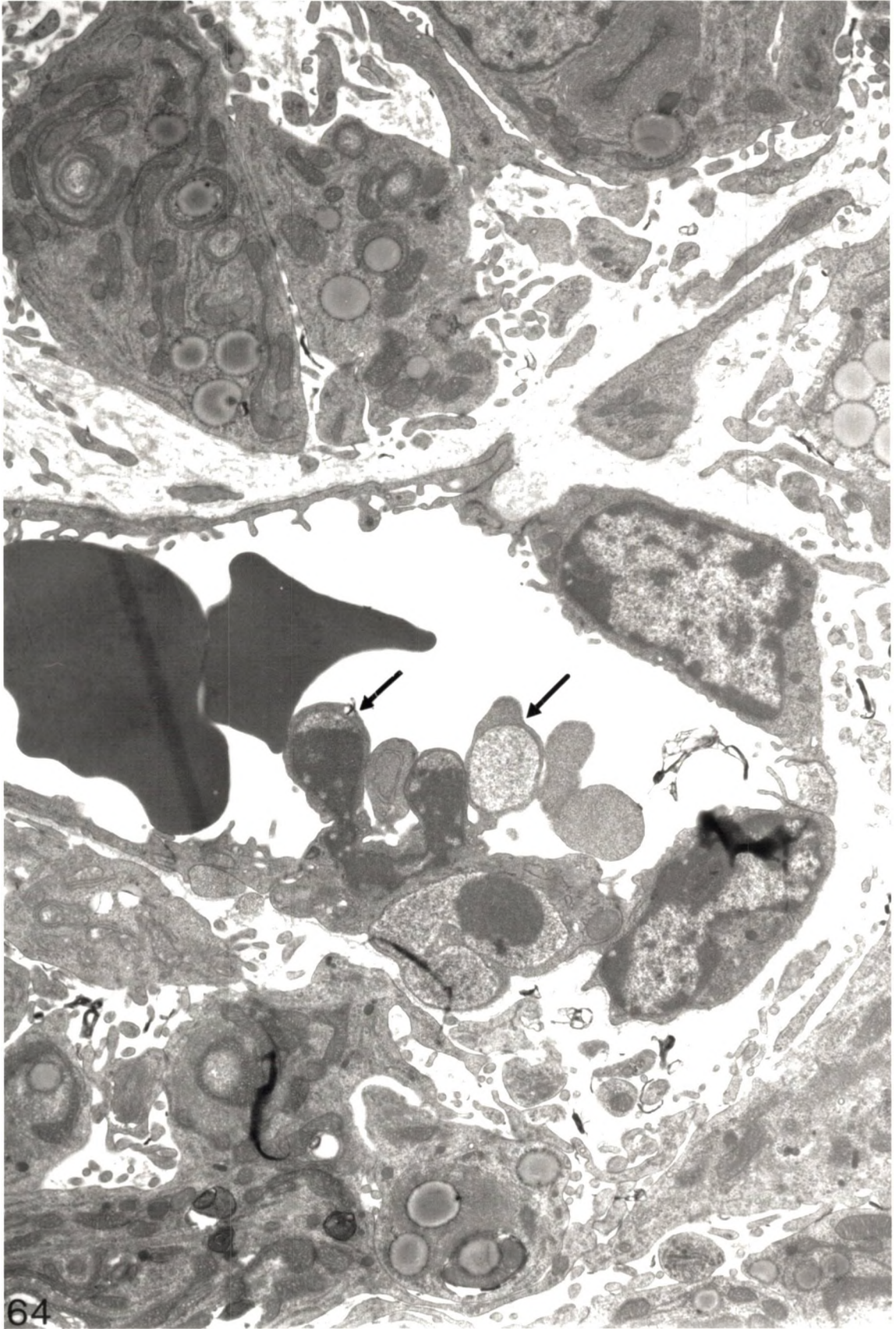


PLATE XLIII

Figure 65. Electronmicrograph of a section through hamster luteal tissue at 1300 hours on D3. Large apoptotic bodies (ab) are demonstrated. An occluded capillary (cap) is filled with an apoptotic cell (arrowhead). X 8,100.

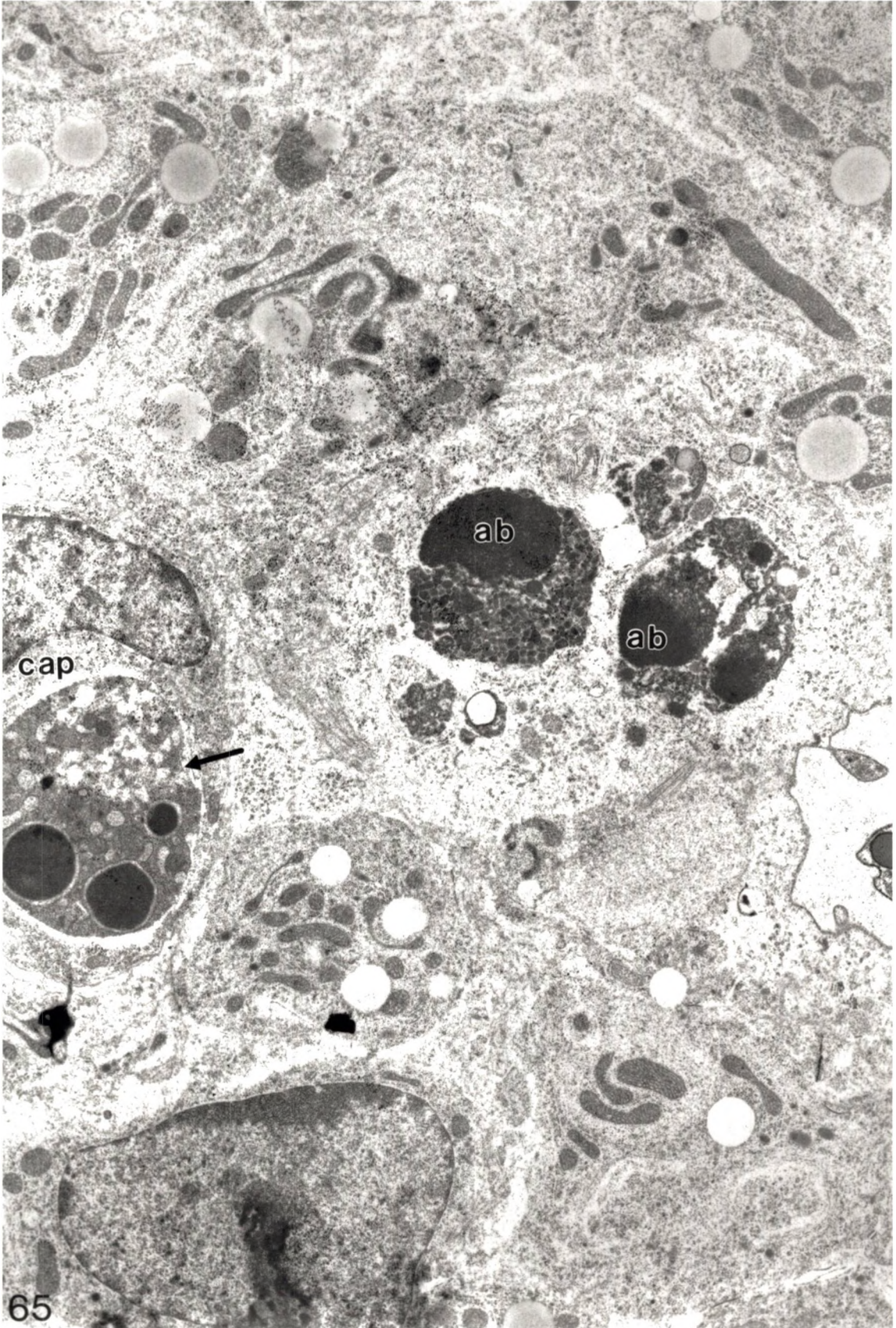


PLATE XLIV

Figure 66. Electronmicrograph of a section through hamster luteal tissue on D3 at 1530 hours. A classic apoptotic body (ab) is shown. X 14,000.

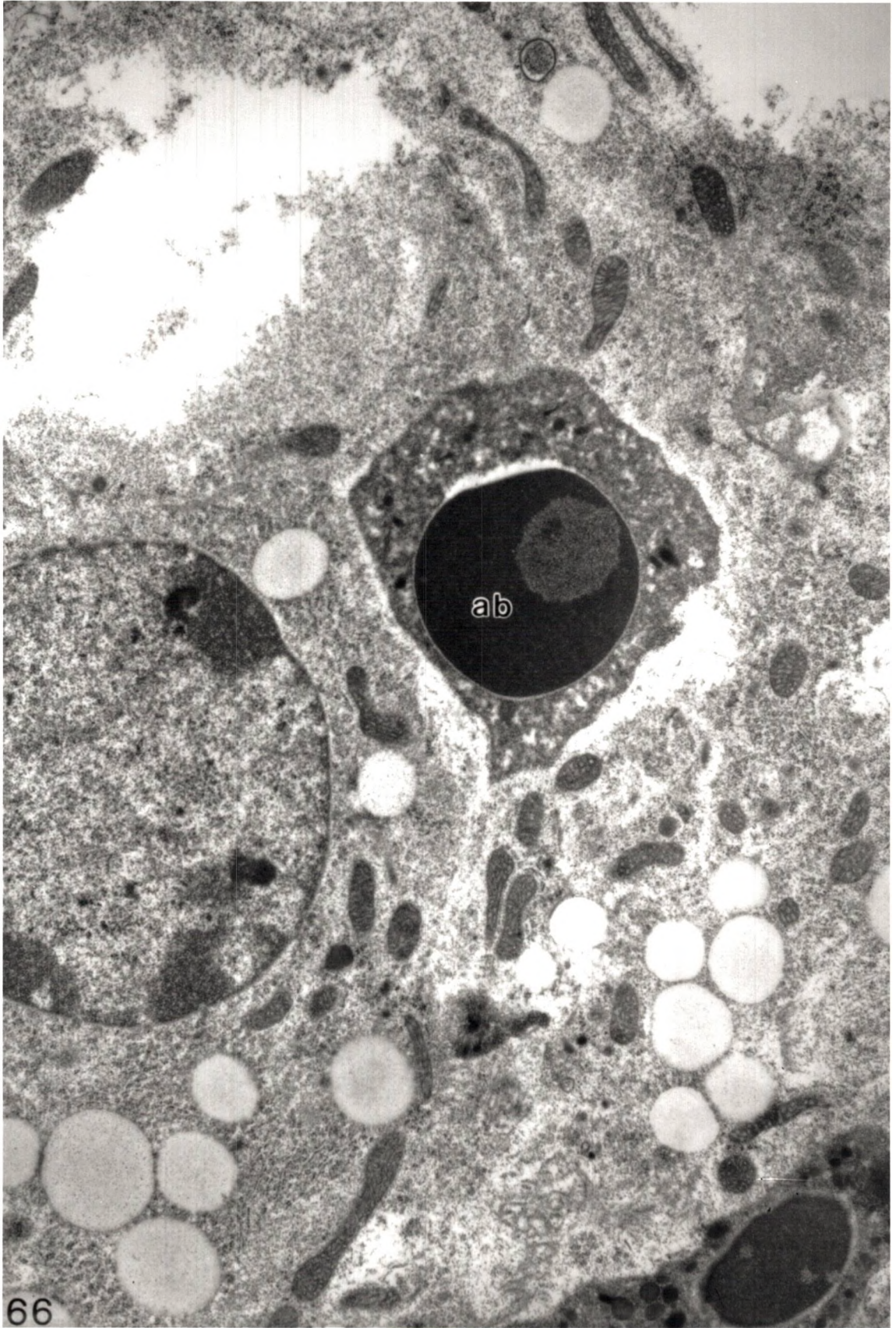


PLATE XLV

Figure 67. Electronmicrograph of a section through hamster luteal cells at 0900 hours on D4. A viable luteal has engulfed an apoptotic body (ab). X 10,300.

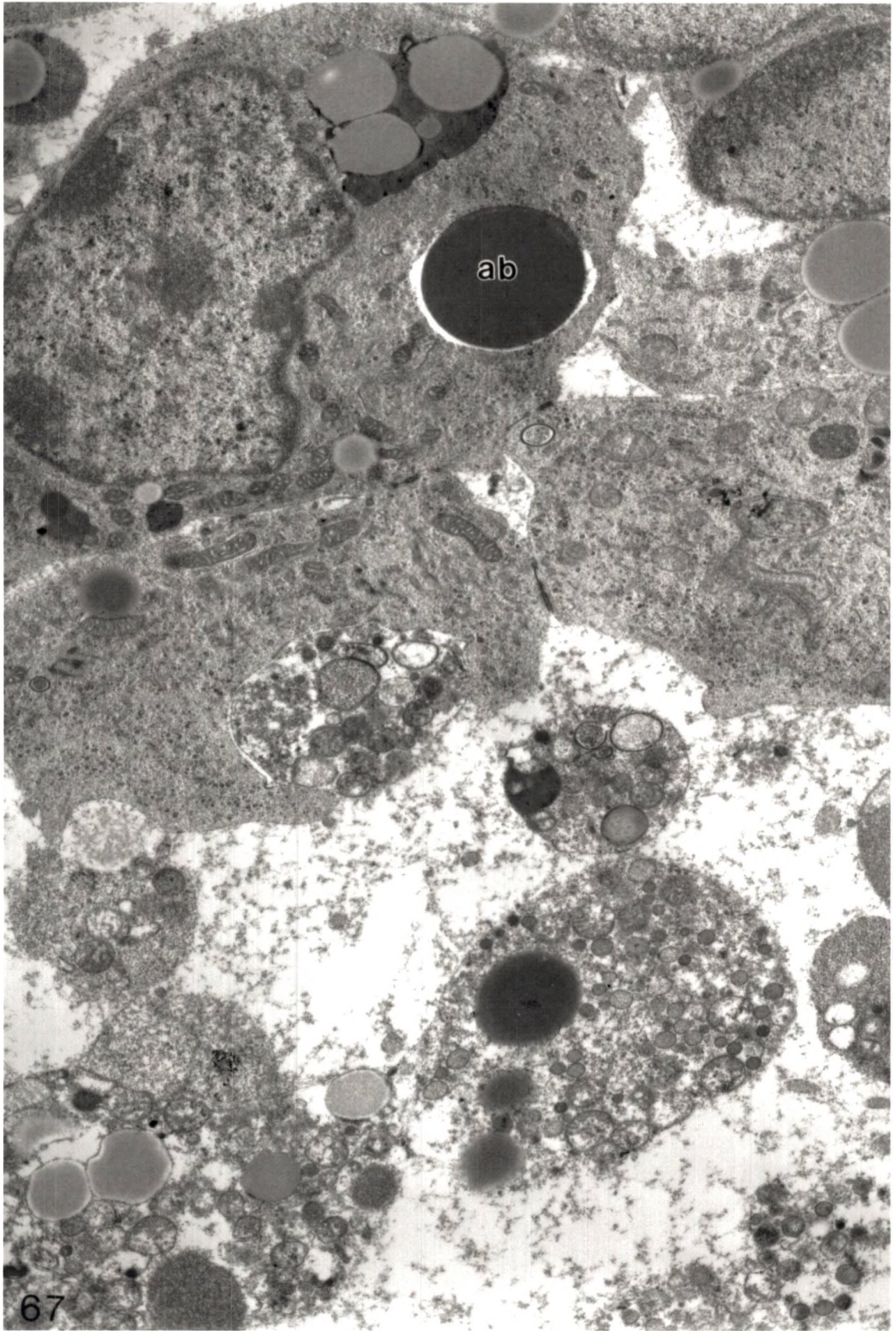


PLATE XLVI

Figure 68. Electronmicrograph of a section through hamster luteal cells at 0900 hours on D4. Viable cells contain little lipid (in this field) and their mitochondria appear dense. The nuclei are large and euchromatic. Apoptotic bodies (ab) are present and encased in a surrounding membrane (arrows). A = artifact. X 10,000.

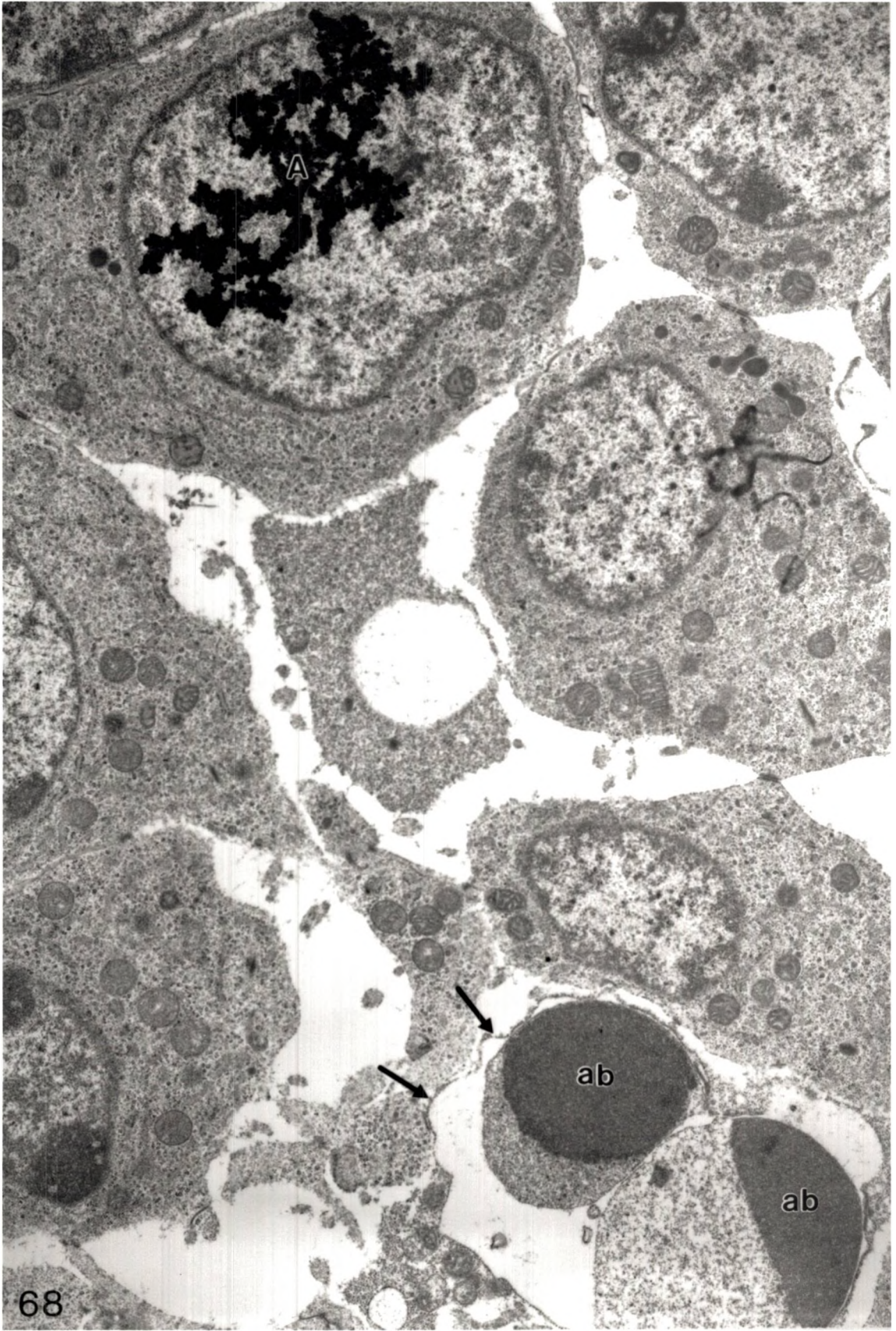
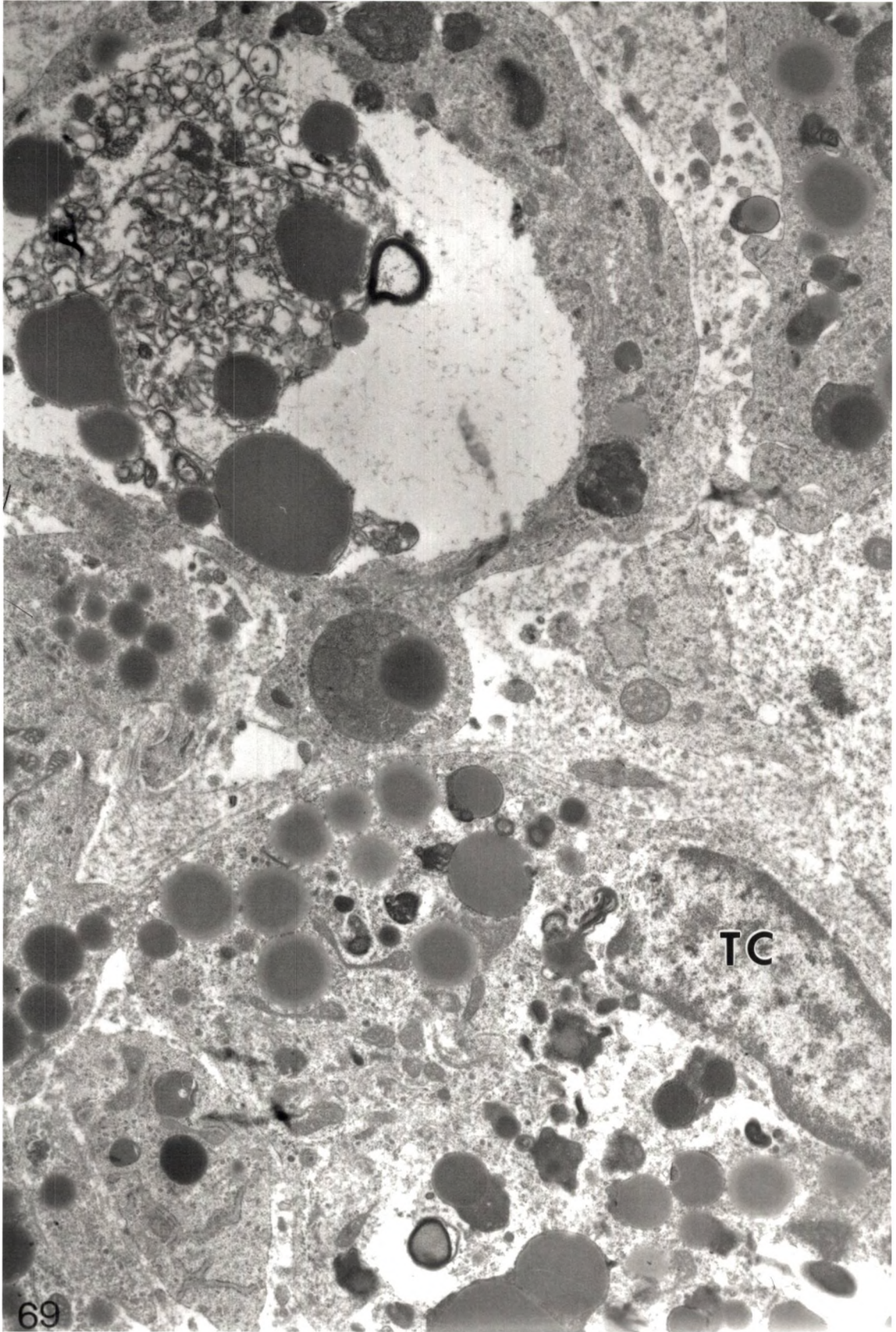


PLATE XLVII

Figure 69. Electronmicrograph of luteal cells at 0900 hours on D4. Tissue histology appears disorganized with a transformed luteal cell (TC) present that has accumulated much degenerating debris within its cytoplasm. X 10,000.



TC

PLATE XLVIII

Figure 70. Electronmicrograph of a section through hamster luteal tissue on D4 at 0900 hours. A large transformed-phagocytic luteal cell (TC) is shown. Its nucleus is obstructed from view by several distinct apoptotic bodies (ab) and other engulfed debris within its cytoplasm. X 10,000.

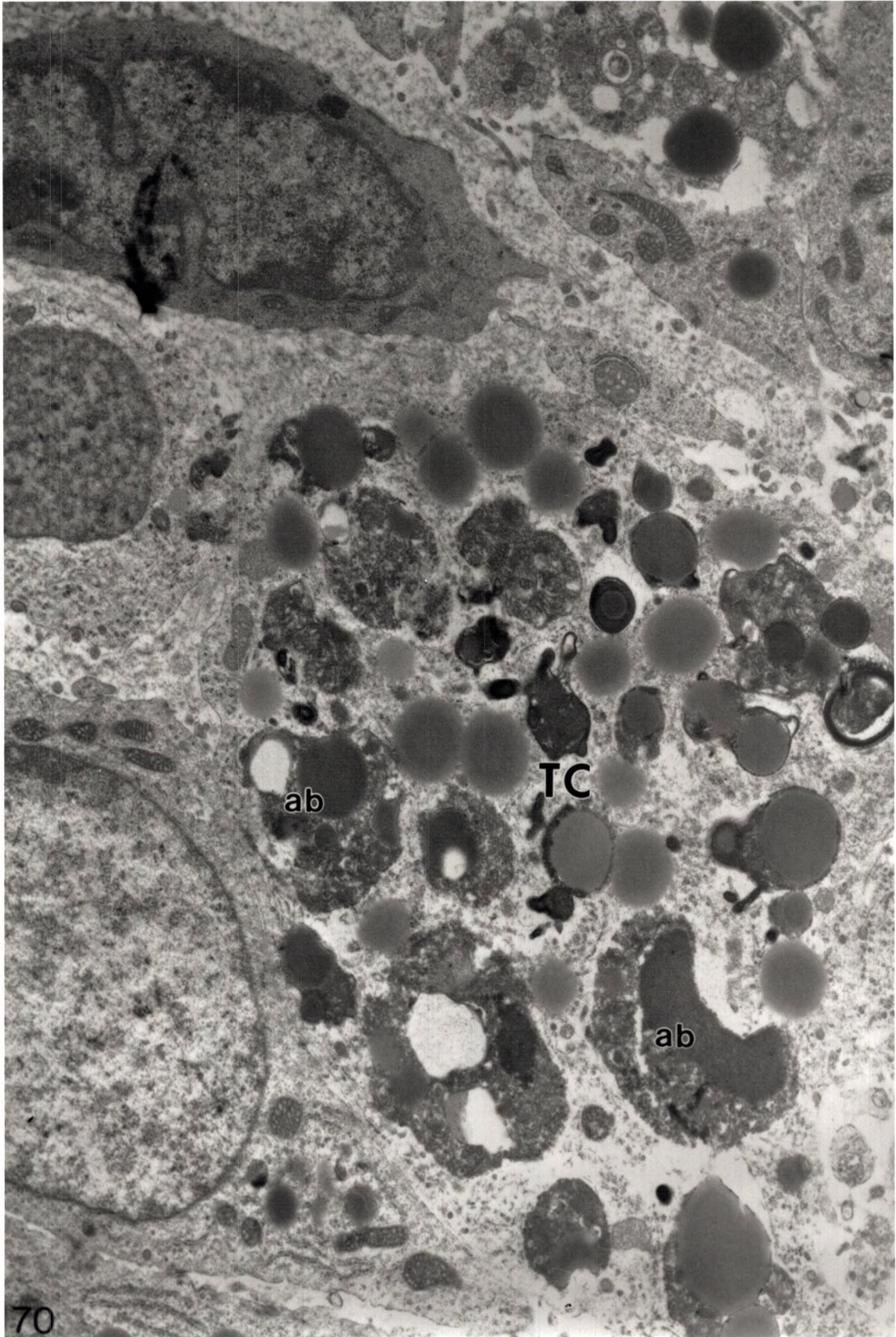


PLATE XLIX

Figure 71. Electronmicrograph of a section through hamster luteal tissue at 0900 hours on D4. Several viable lipid-laden cells are present with large euchromatic nuclei. Portions of two PMNL are also visible (arrows). X 8,1000.

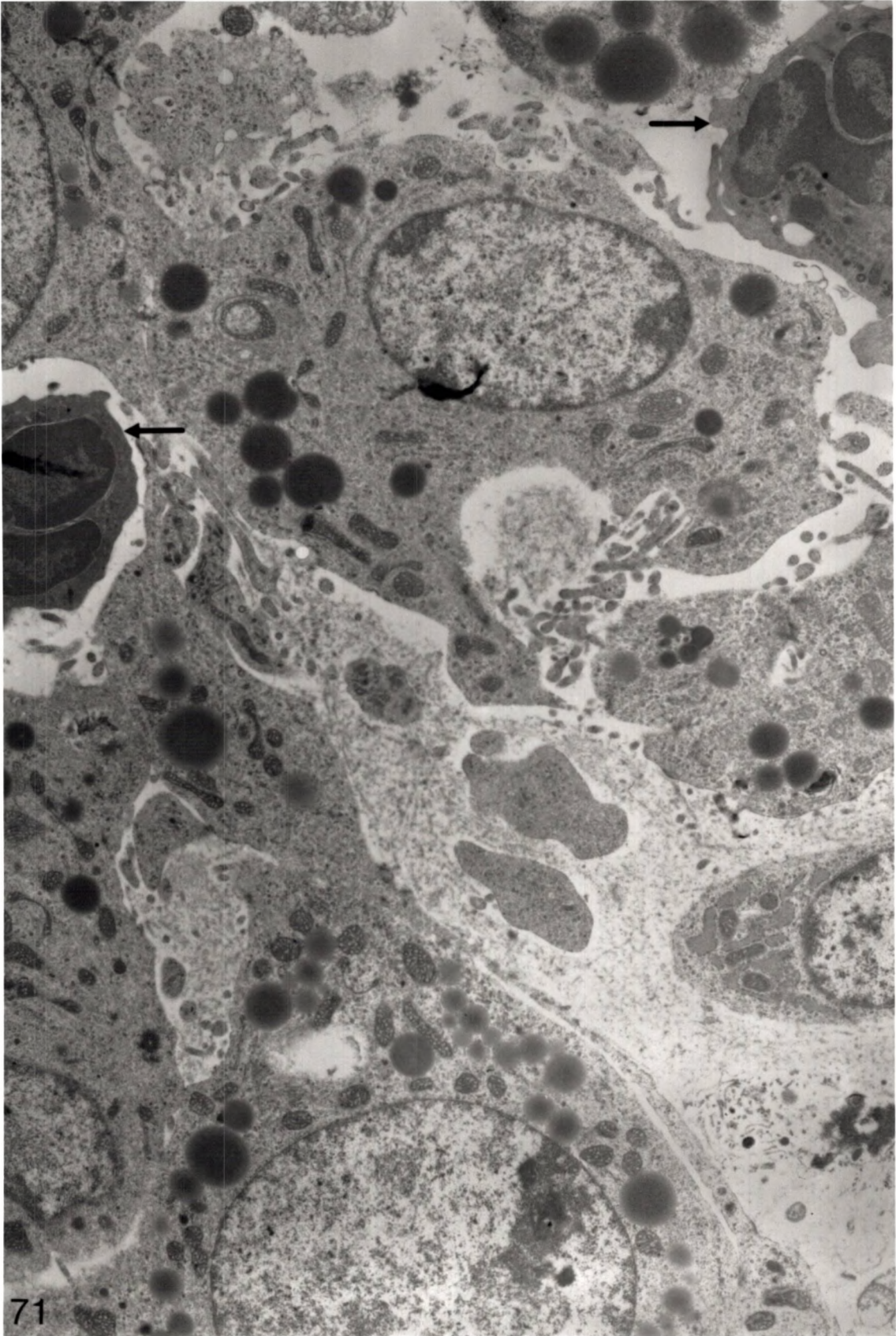


PLATE L

Figure 72. Electronmicrograph of a section through hamster luteal tissue on D4 at 0900 hours. A capillary lumen (cap) is filled with apoptotic debris (ad), typical of remaining identifiable vessels. X 13,200.

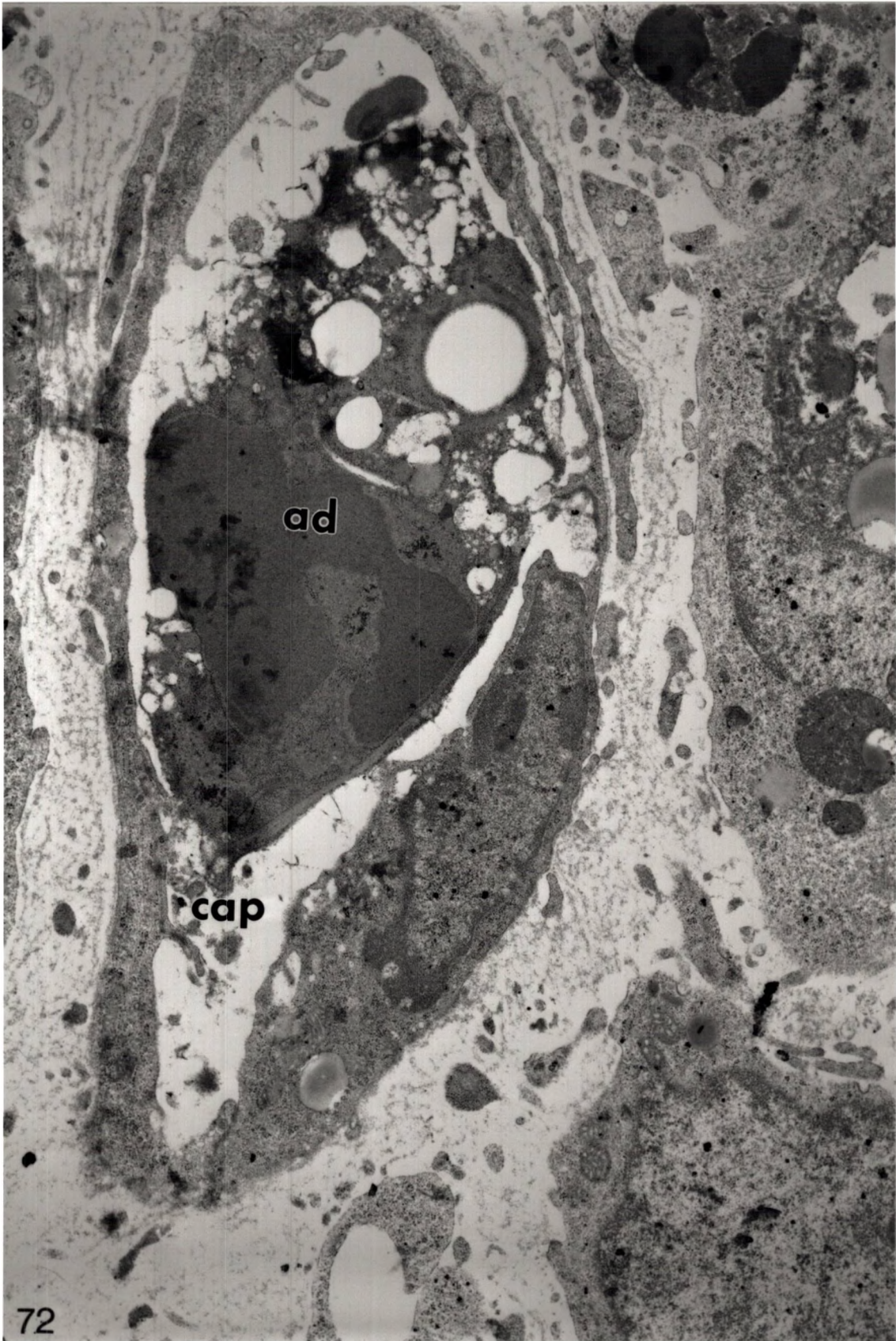


PLATE LI

Figure 73. Photomicrograph of a section of hamster spleen showing esterase positive macrophages (arrows) located at the interface between the red pulp (RP) and white pulp (WP). X 200.

Figure 74. Photomicrograph of sections through the isthmus of a hamster oviduct. The epithelial cells lining the duct lumen are intensely esterase positive. X 100.

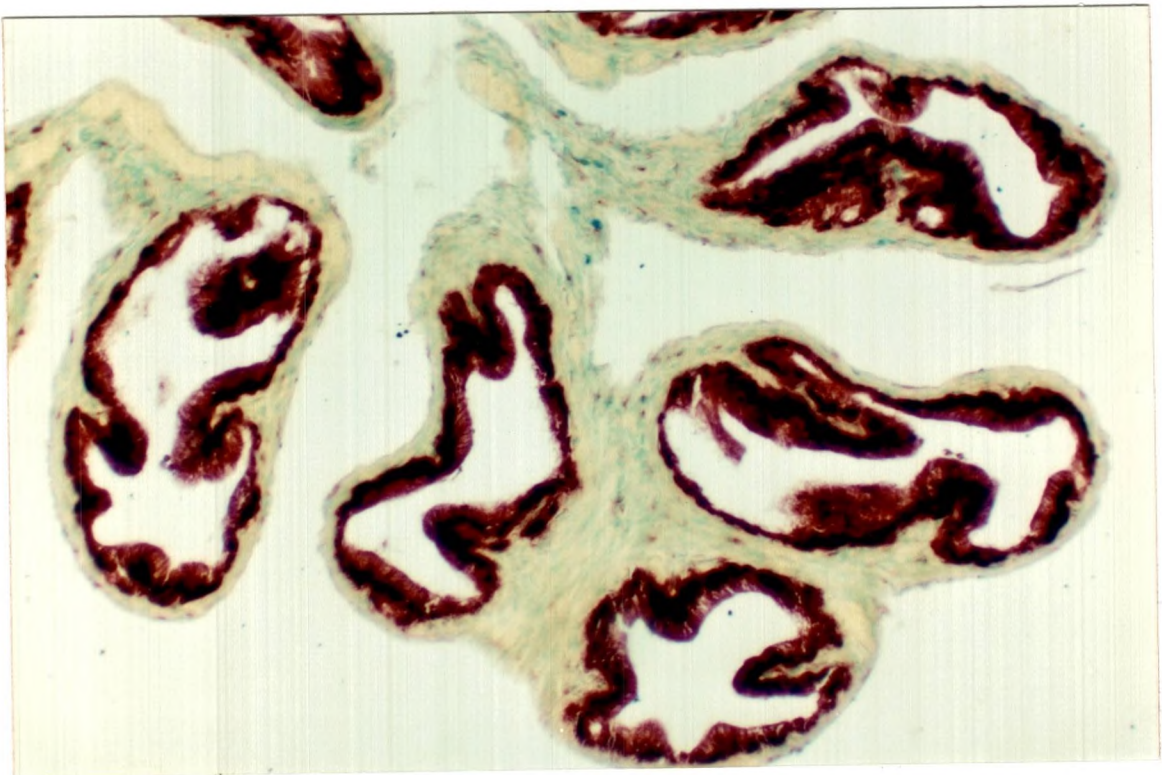
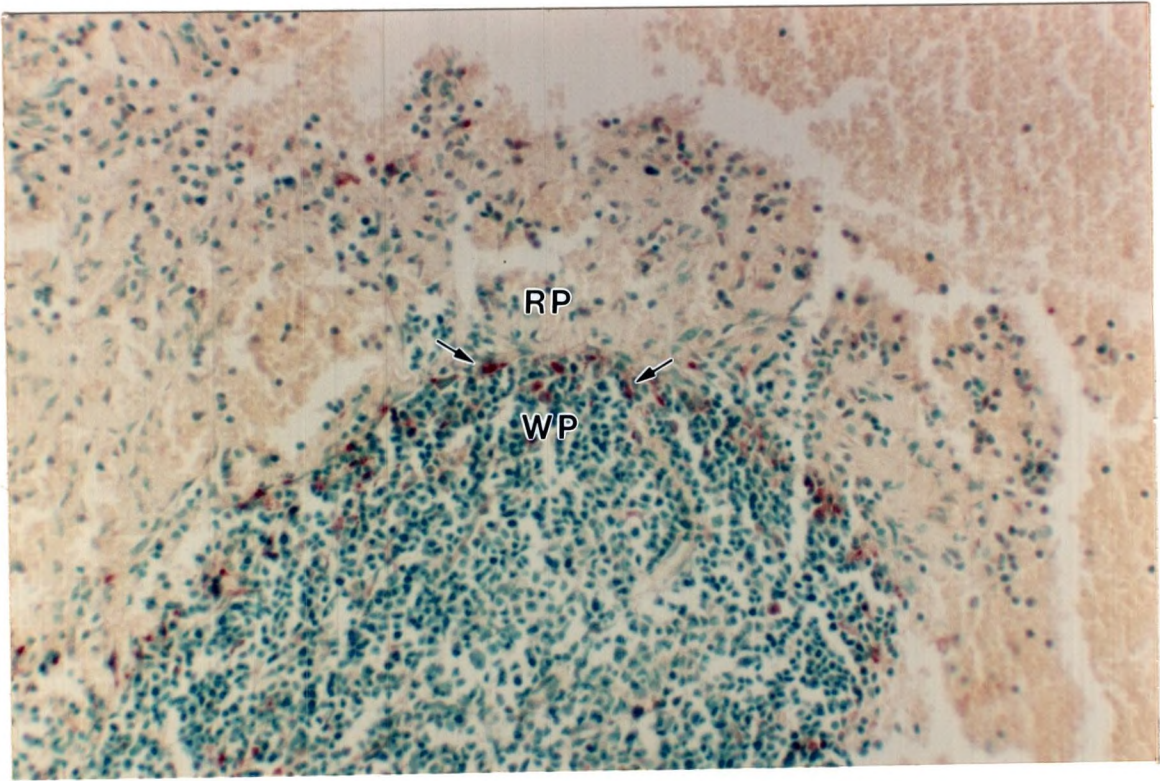


PLATE LII

Figure 75. Photomicrograph of a section through a D4 hamster ovary showing several areas of typical esterase reactivity. A corpus luteum (cl) is present as is an antral follicle (AF) and two atretic follicles (arrows). X 40.

Figure 76. Photomicrograph of a section through a hamster ovary demonstrating two atretic small antral follicles as well as two healthy primary multilaminar follicles. The thecae (te) of both sets of follicles is unreactive while the granulosa of the atretic follicles is highly reactive for esterase. X 200.

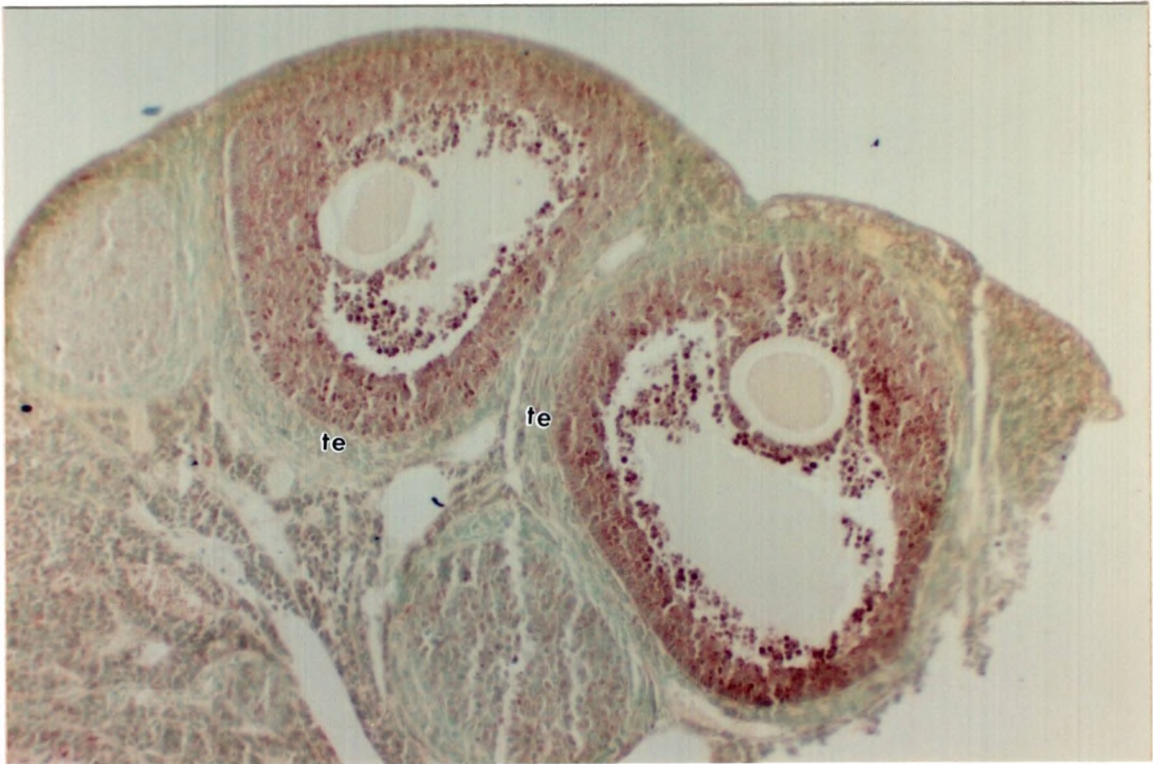
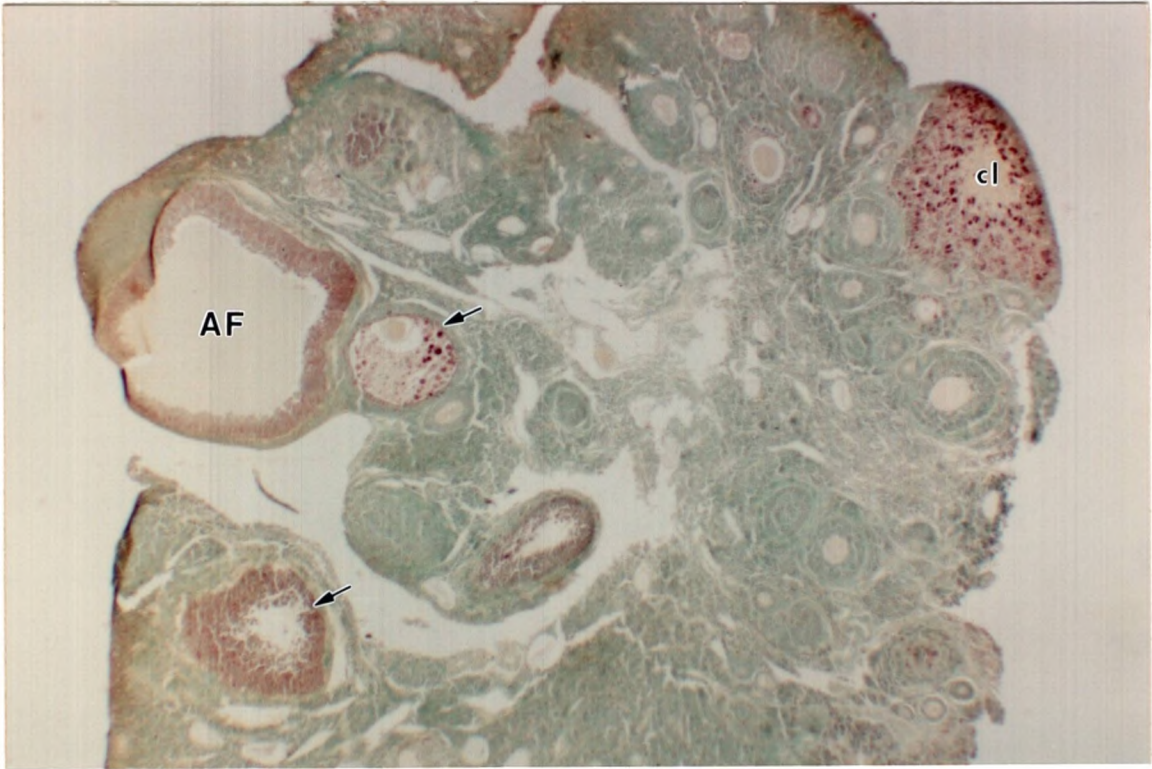


PLATE LIII

Figure 77. Photomicrograph of a section through a hamster ovary displaying the wall of a preovulatory graafian follicle (GF) with diffuse esterase staining of healthy granulosa cells but unreactive theca (te). An advanced atretic follicle opposite the graafian follicle also has unreactive theca while its few remaining granulosa cells are intensely esterase positive. X 200.

Figure 78. Photomicrograph of a section through a hamster ovary showing primary multilaminar follicle in advanced atresia is present. Note the intense esterase reaction visible in the numerous apoptotic bodies which have detached from the granulosa layer. X 200.

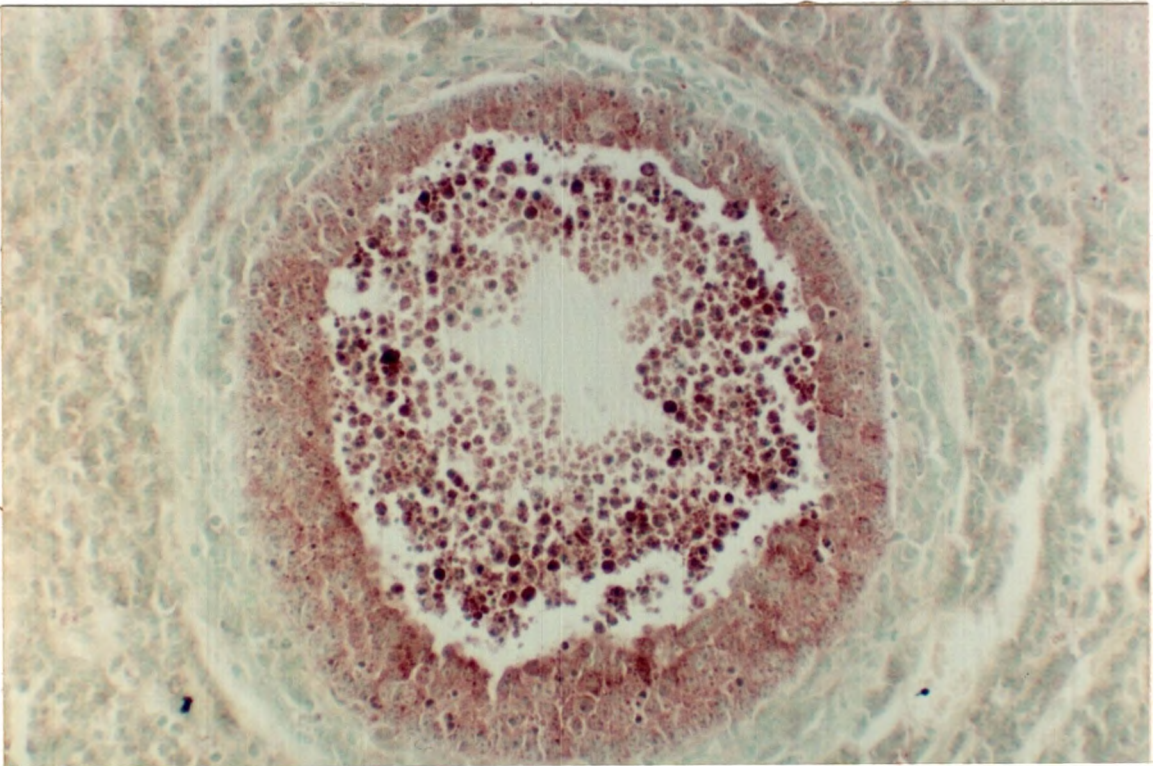
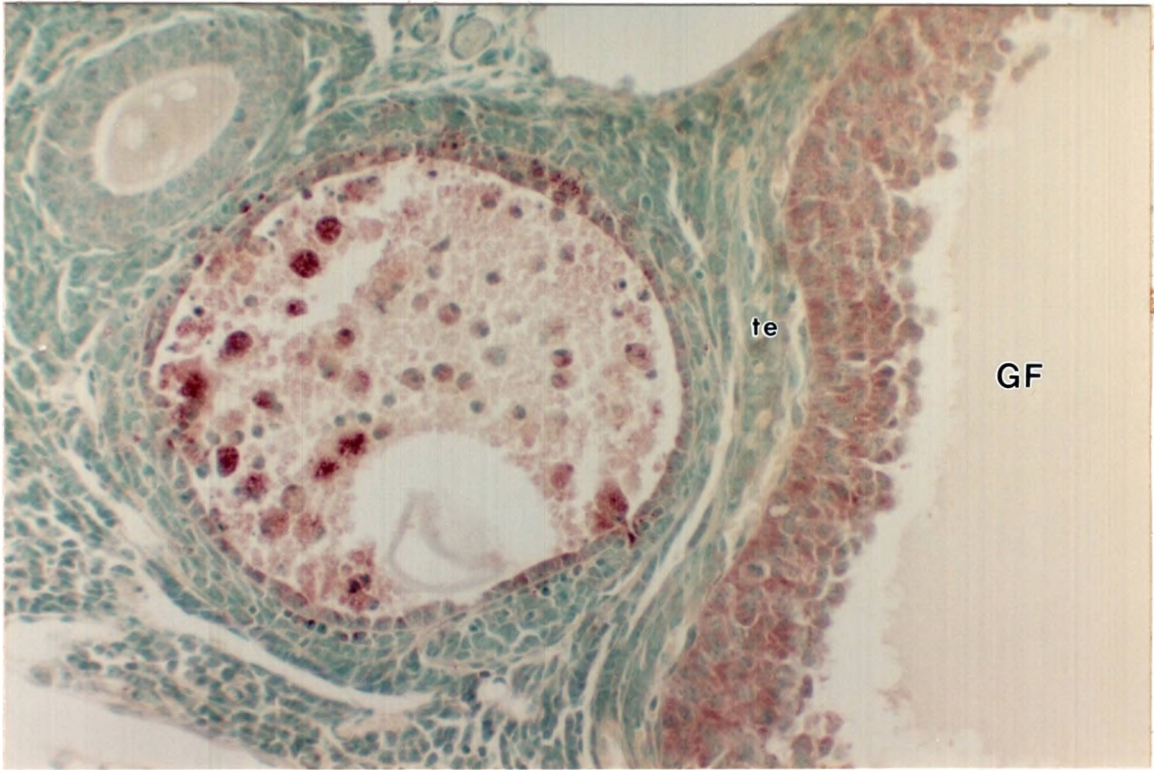


PLATE LIV

Figure 79. Photomicrograph of a section through a hamster ovary showing an atretic follicle with numerous large, nonpyknotic granulosa cells staining intensely esterase positive (arrows). X 400.

Figure 80. Photomicrograph of a section through a hamster ovary displaying an atretic follicle. At the center a large esterase positive transformed granulosa cell is seen (arrow). X 400.

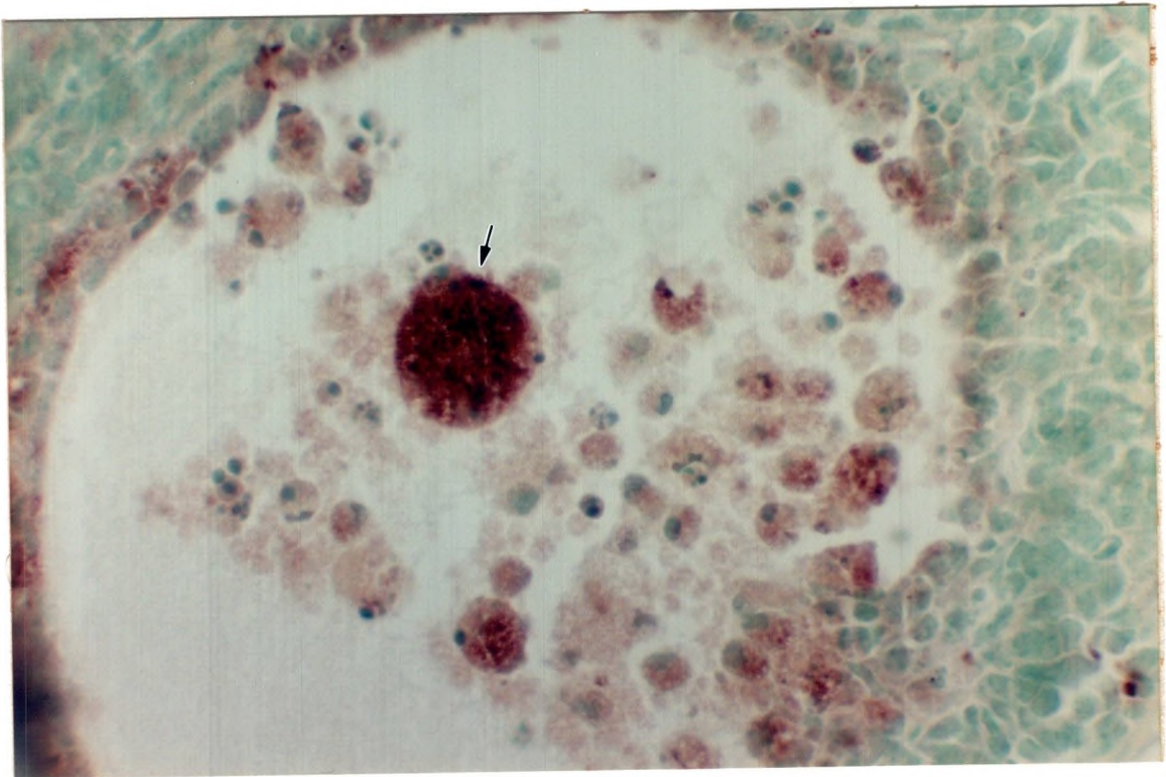
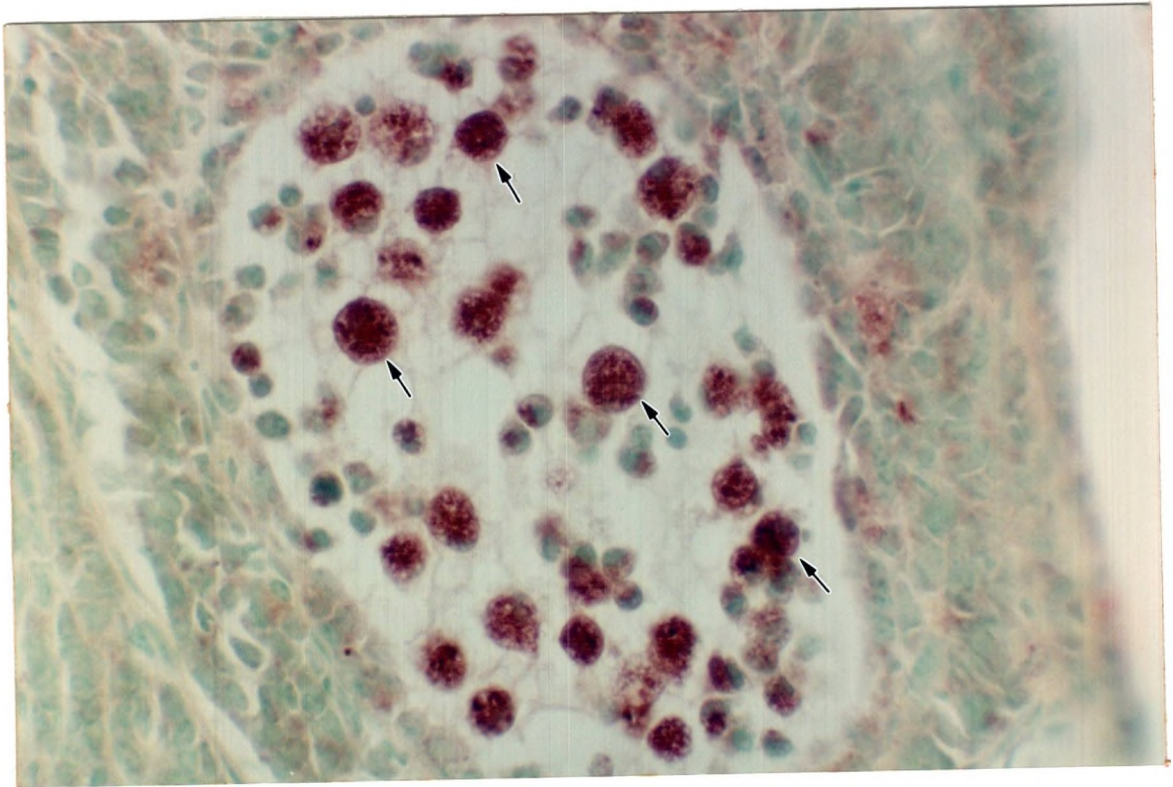


PLATE LV

Figure 81. Photomicrograph of a section through a hamster CL which demonstrates the diffuse esterase staining characteristic on D1. X 100.

Figure 82. Photomicrograph of a section through a hamster CL on D2 which demonstrates diffuse light-staining esterase activity. X 100.

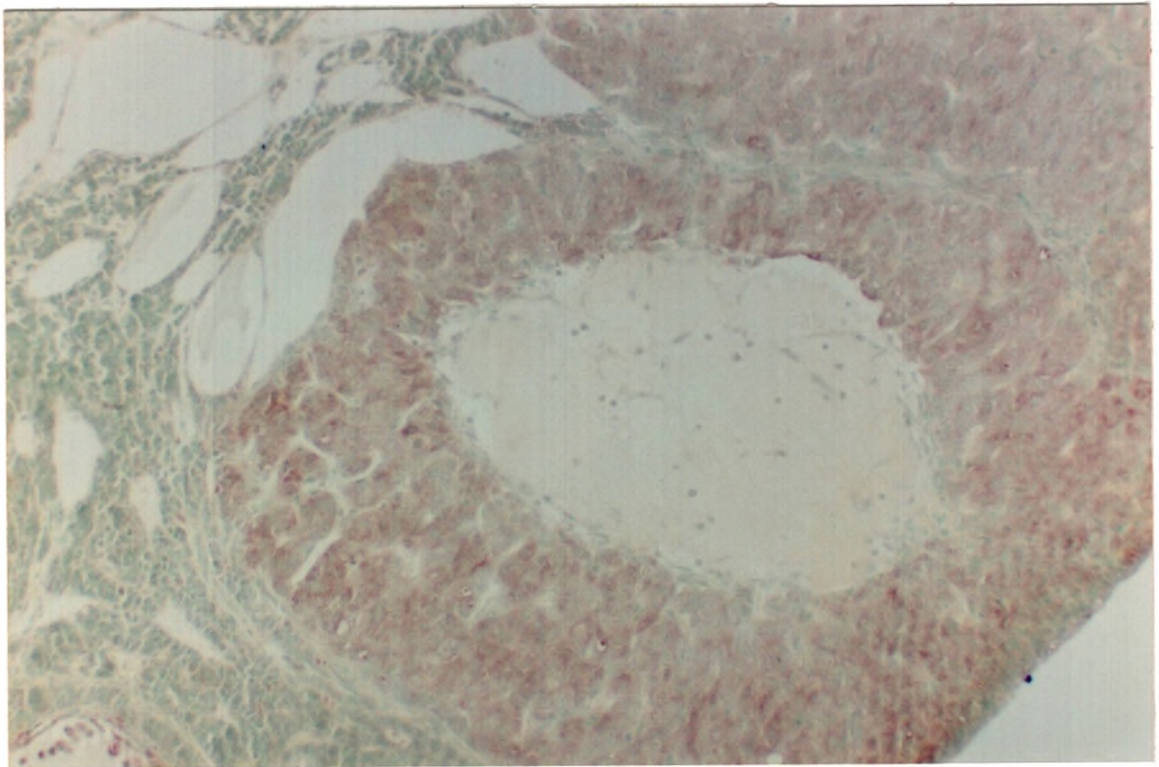
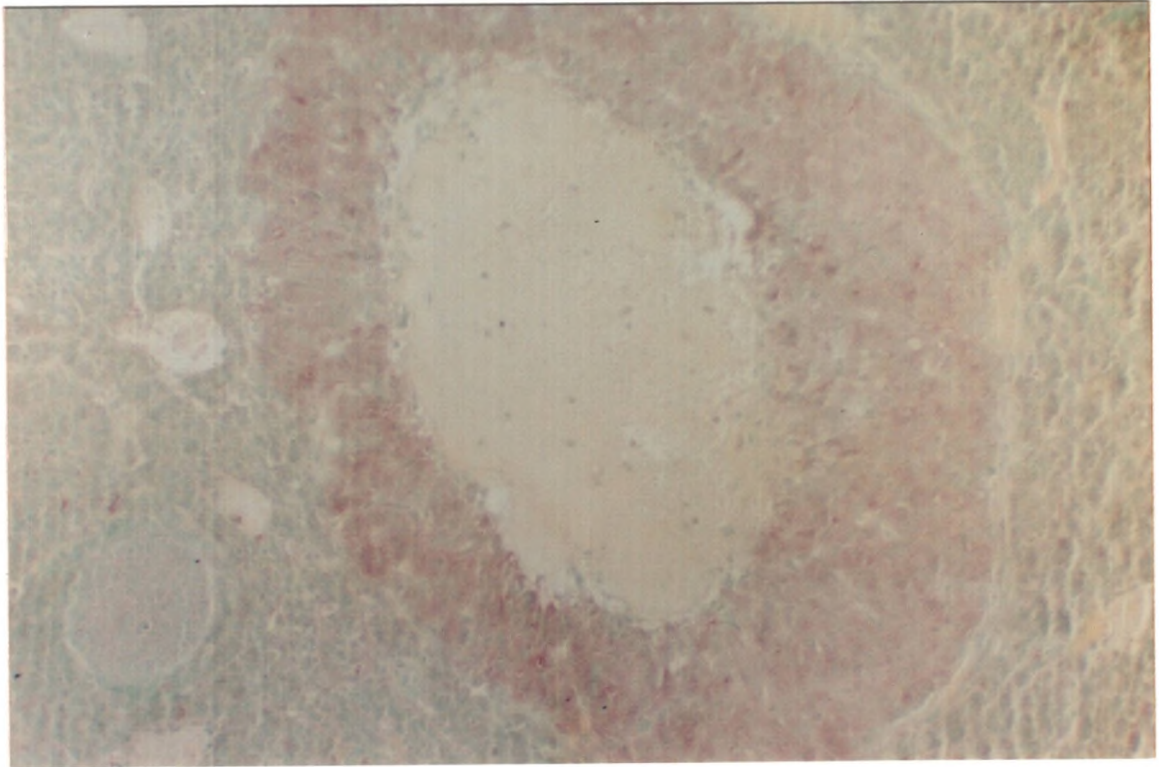


PLATE LVI

Figure 83. Photomicrograph of a section through a hamster CL on D3 with small apoptotic foci of intense esterase activity evident above diffuse background staining. X 100.

Figure 84. Photomicrograph of a section through a hamster CL demonstrating apoptotic foci present within a D3 CL which are stained positively for esterase activity (arrows). X 400.

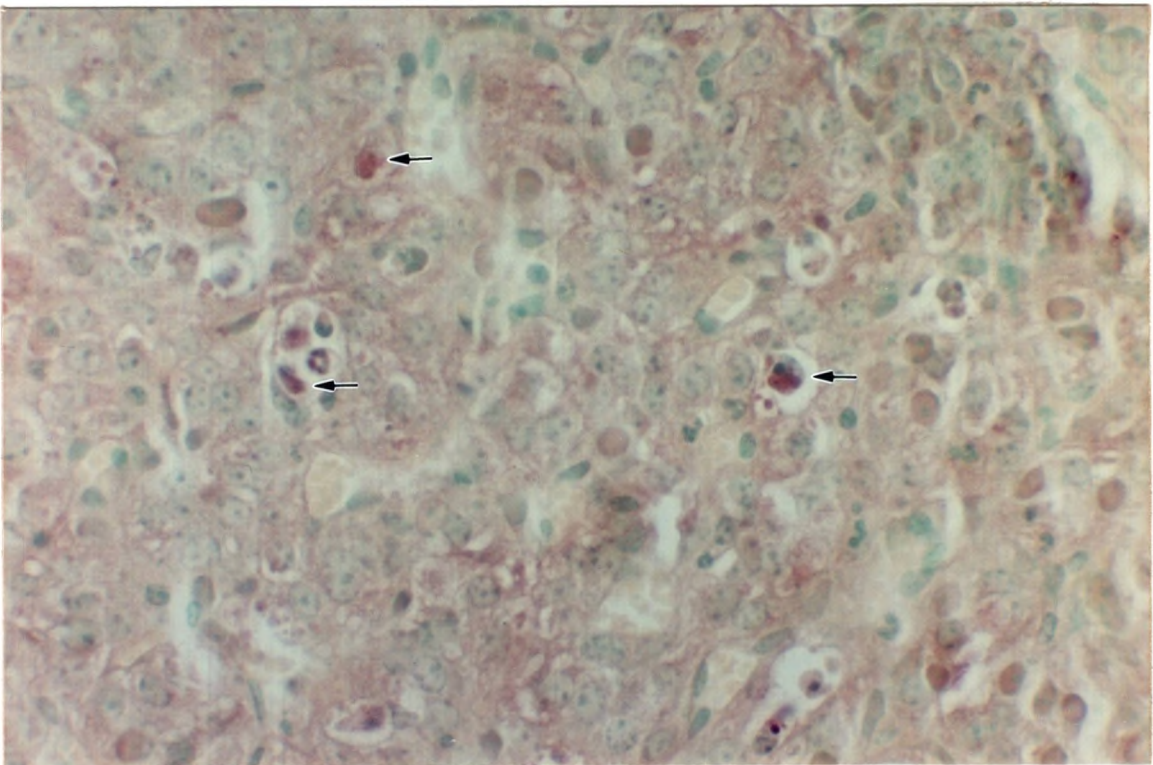
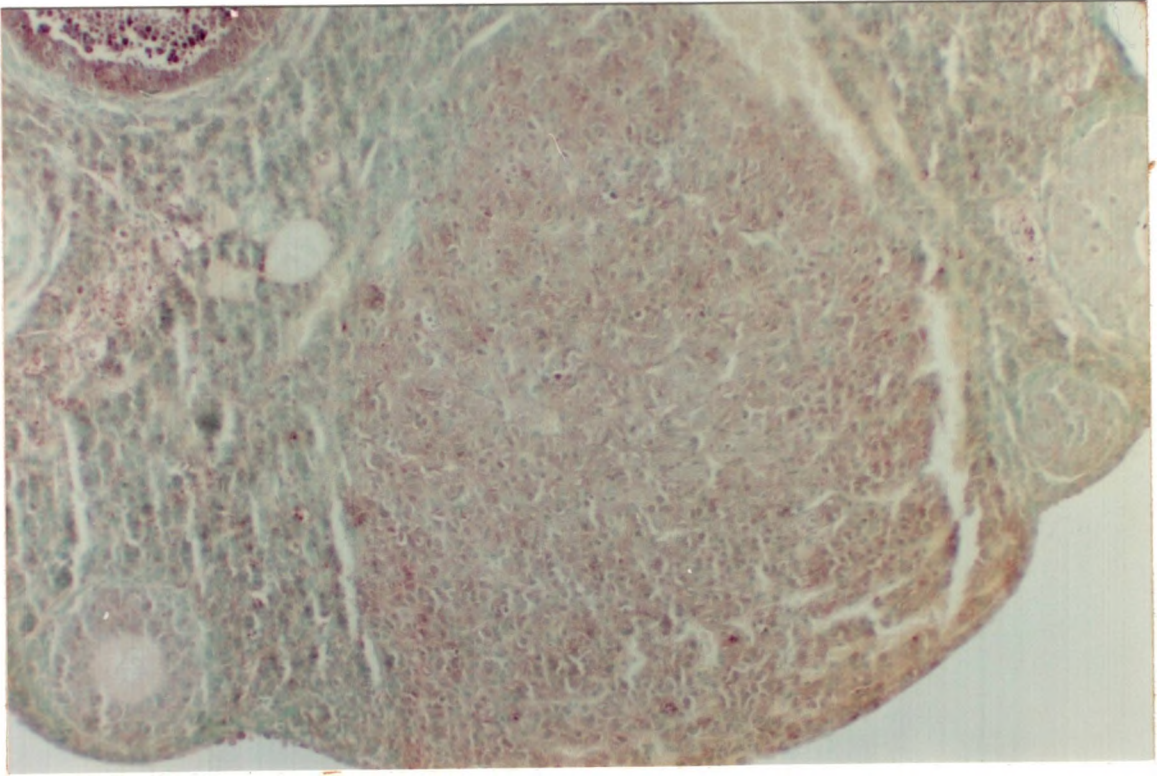


PLATE LVII

Figure 85. Photomicrograph of a section through a hamster D4 CL which is in advanced regression. Numerous foci of intense esterase activity are discernable. X 100.

Figure 86. Highpower photomicrograph of a section through a D4 hamster CL showing several esterase negative PMNL (arrows) amongst remaining healthy and apoptotic cells. X 1000.

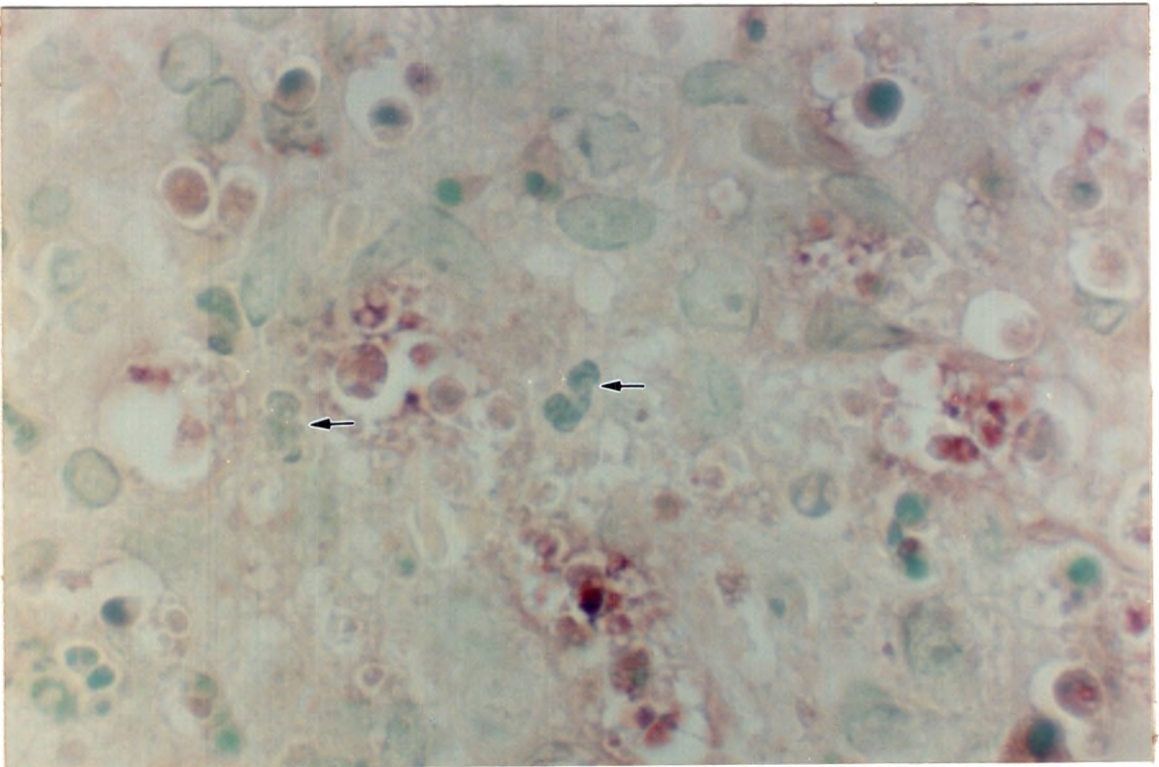
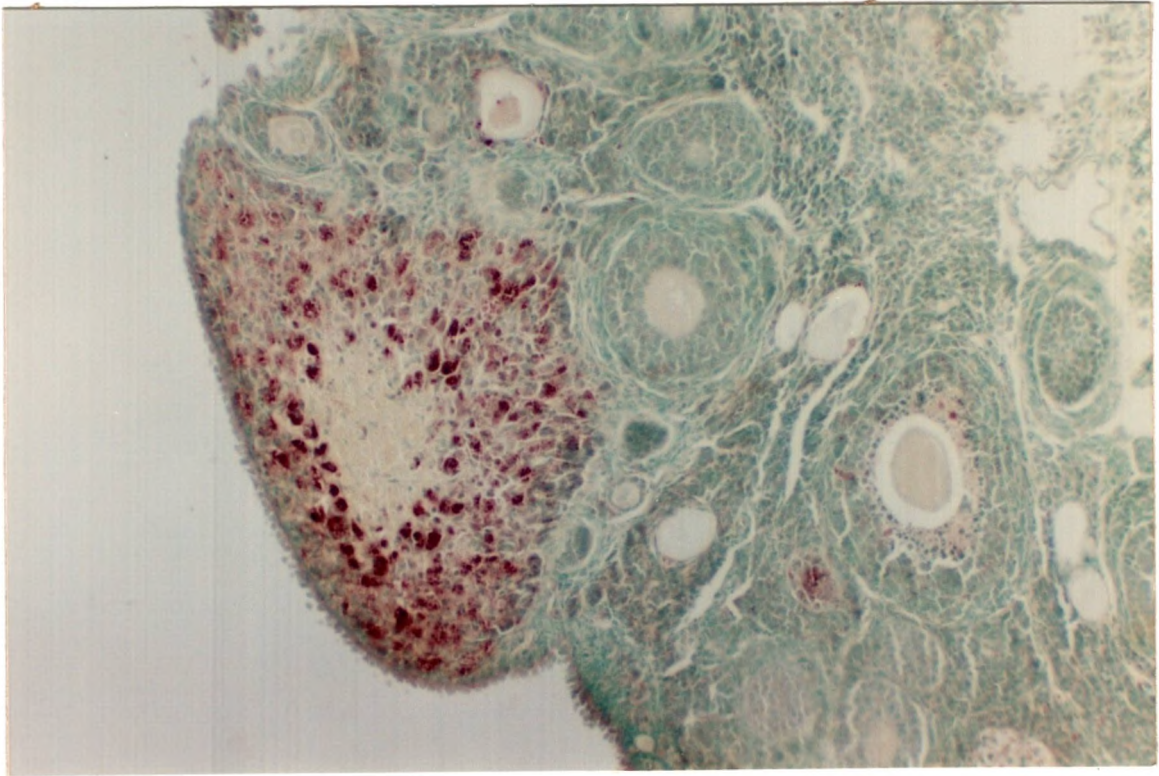


PLATE LVIII

Figure 87. Highpower photomicrograph of a section through a hamster D4 CL showing esterase positive debris accumulating in advanced luteolysis . X 1000.

Figure 88. Photomicrograph of a section through a hamster ovary demonstrating the tiny remnant of a luteolyzed CL still present on D1 of the next cycle. Remnants are seldom seen without a fortunate section. This one is comparable to those seen in figure 44. X 200.

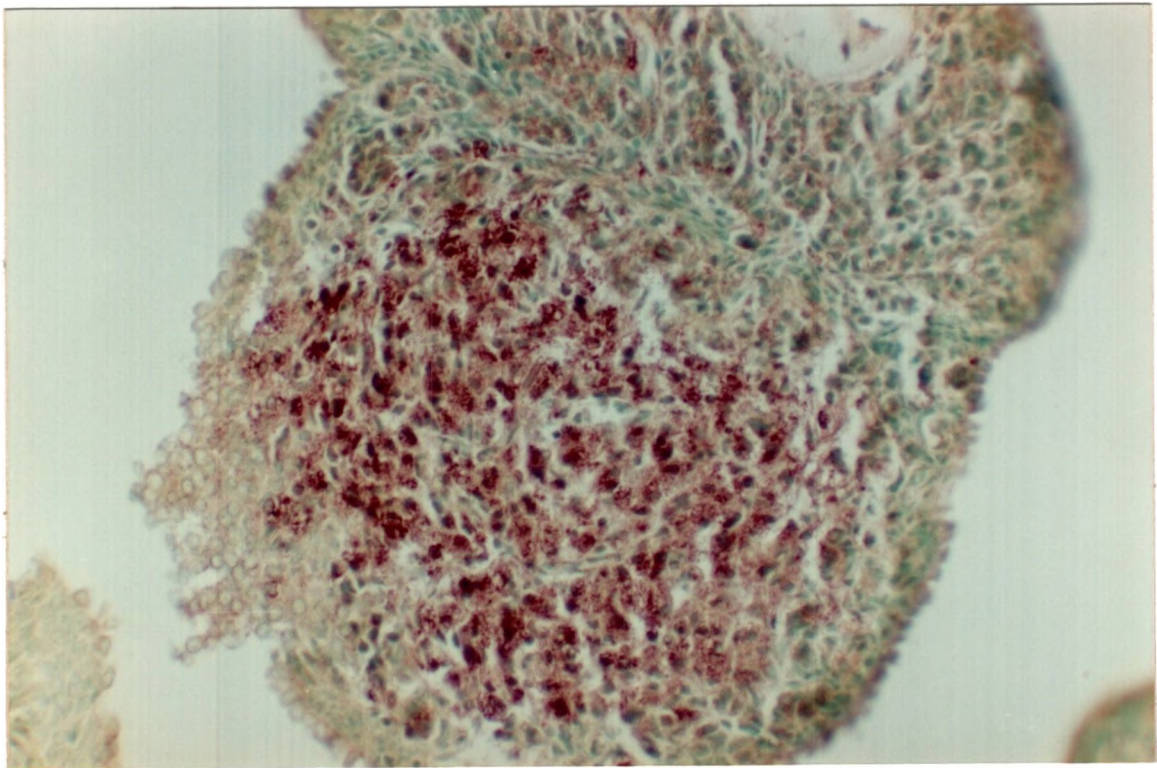
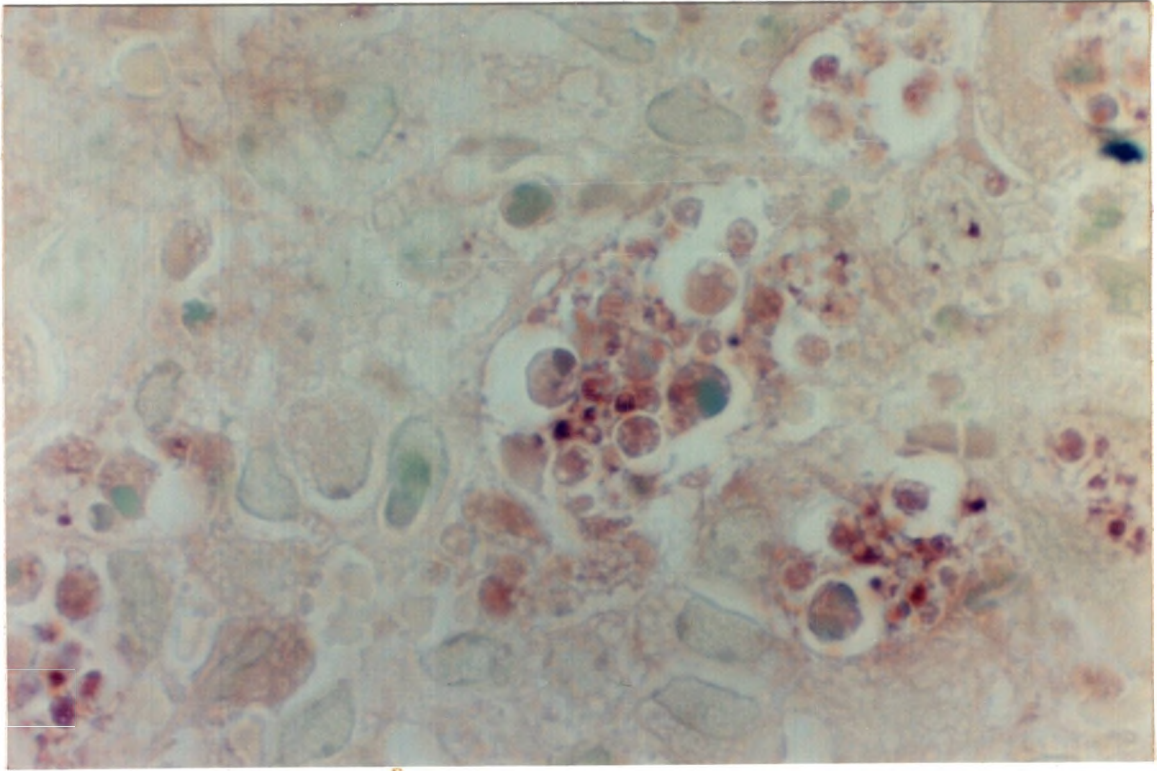
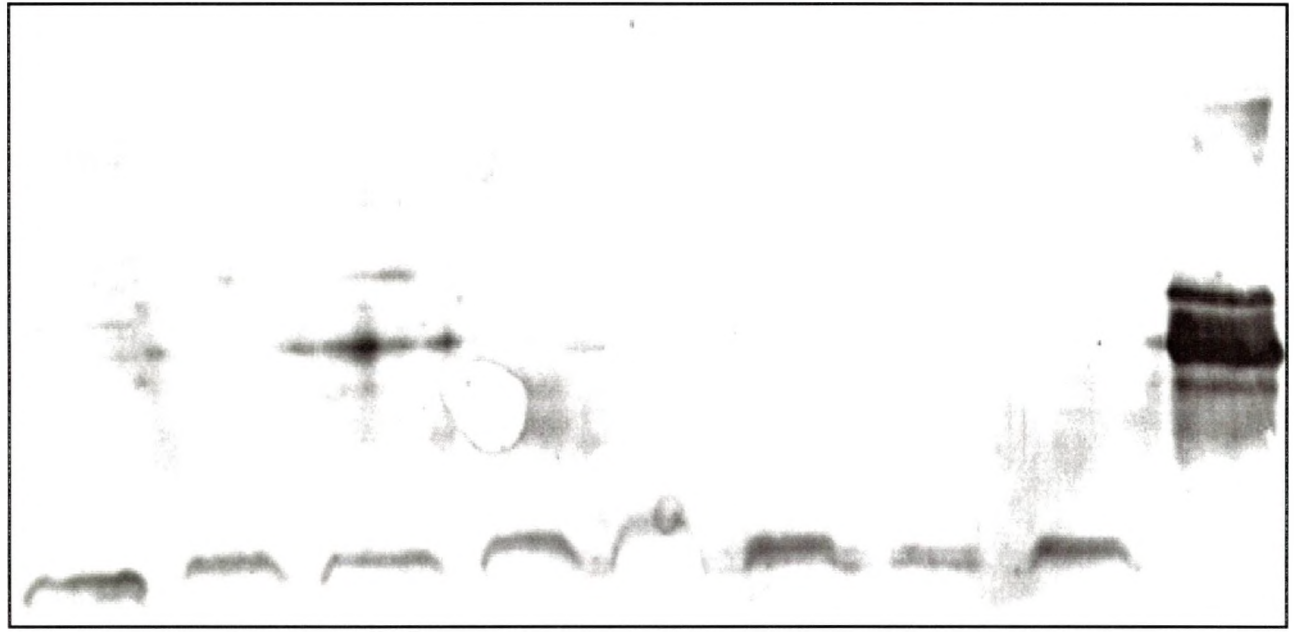


PLATE LIX

Figure 89. Western blot analysis of hamster CL and NLO tissue samples. A reaction of antibody with MPO is indicated by the stained band in the lane for 0600 hours on D3 (arrow). The stained band corresponds with the control band in the far right lane.

MPO →



Day 2 2400 hr Day 3 0300 hr Day 3 0600 hr Day 3 0900 hr Day 2 2400 hr Day 3 0300 hr Day 3 0600 hr Day 3 0900 hr 25 μg MPO

Luteal

Non-Luteal

LITERATURE CITED

- Absolom, D.R. 1986 Basic methods for the study of phagocytosis. In Methods in Enzymology, (G. DiSabato and J. Everse, Eds.) Academic Press Inc., New York, 132:110-111.
- Adashi, E.Y. 1990 The potential relevance of cytokines to ovarian physiology: the emerging role of resident ovarian cells of the white blood series. *Endocr. Rev.*, 11(3):454-464.
- Alison, M.R. and Sarraf, C.E. 1994 Liver cell death: patterns and mechanisms. *Gut*, 35:577-581.
- Andrews, P.C. and Krinsky, N.I. 1986 Human myeloperoxidase and hemi-myeloperoxidase In: Methods in Enzymology, (G. DiSabato and J. Everse, Eds.) Academic Press Inc. New York, 132:110-111.
- Arends, M.J. and Wyllie, A.H. 1991 Apoptosis: mechanisms and roles in pathology. In: International Review of Experimental Pathology (G.W. Richter and K. Soletz, Eds.), Academic Press Inc., San Diego. 32:223-254.
- Aten, R.F., Duarte, K.M. and Behrman 1992 Regulation of ovarian antioxidant vitamins, reduced glutathione and lipid peroxidation by luteinizing hormone and prostaglandin F₂α. *Biol. Reprod.*, 46:401-407.
- Azmi, T.I. and O'Shea, J.D. 1984 Mechanism of deletion of endothelial cells during regression of the corpus luteum. *Lab. Invest.*, 51(2):206-217.
- Bancroft, J.D. 1990 Enzyme histochemistry. In: Theory and Practice of Histological Techniques, (J.D. Bancroft and A. Stevens Eds.) Churchill Livingstone, New York, pp. 389-391.
- Banon, P., Brandes, D. and Frost, J.K. 1964 Lysosomal enzymes in the rat ovary and endometrium during the estrus cycle. *Acta Cytol.*, 8:416-425.
- Baranczuk, R. and Greenwald, G.S. 1973 Peripheral levels of estrogen in the cyclic hamster. *Endocrinology*, 92(3):805-812.
- Barr, P.J. and Tomei, L.D. 1994 Apoptosis and its role in human disease. *Biotechnology*, 12:487-493.
- Benyo, D.F. and Pate, J.L. 1992 Tumor Necrosis Factor α alters bovine luteal cell synthetic capacity and viability. *Endocrinology*, 130(2):854-860.

- Bollag, D.M. and Edelstein, S.J. 1991 Immunoblotting. In: Protein Methods, Wiley-Liss, New York. 8:181-208.
- Bowen, I.D. 1993 Apoptosis or programmed cell death? *Cell Biol. Int.*, 17(4):365-369.
- Bradley, P.P., Priebat, D.A., Christensen, R.D. and Rothstein, G. 1982 Measurement of cutaneous inflammation: estimation of neutrophil content with an enzyme marker. *J. Invest. Dermatol.*, 78:206-209.
- Brännström, M., Giesecke, L., Moore, I.C., Van den Heuvel, C.J. and Robertson, S.A. 1994 Leukocyte subpopulations in the rat corpus luteum during pregnancy and pseudopregnancy. *Biol. Reprod.*, 50:1161-1167.
- Buja, L.M., Eigenbrodt, M.L. and Eigenbrodt, E.H. 1993 Apoptosis and necrosis. *Arch. Pathol. Lab. Med.*, 1208-1214.
- Carp, H. 1982 Mitochondrial N-formylmethionyl proteins as chemoattractants for neutrophils. *J. Exp. Med.*, 155:264-275.
- Chatterjee, S. and Greenwald, G.S. 1976 Biochemical changes in the corpus luteum of the cyclic hamster. *J. Endocrinol.*, 68:251-256.
- Christensen, A.K. and Gillim, S.W. 1969 The correlation of fine structure and function in steroid secreting cells, with emphasis on those of the gonads. In: The Gonads (K. W. McKerns, Ed.), Appelton-Century-Crofts, New York. p. 415.
- Chun, S.Y., Daphna-Iken, D. Calman, D. and Tsafirri, A. 1993 Severe leukocyte depletion does not affect follicular rupture in the rat. *Biol. Reprod.*, 48(4):905-909.
- Cohen, J.J. 1993 Apoptosis: the physiologic pathway of cell death. *Hosp. Pract.*, 30(12):35-43.
- Cotran, R.S., Kumar, V. and Robbins, S.L. 1989 Inflammation and repair. In: Robbins Pathological Basis of Disease, 4th edit., W.B. Saunders Co., Philadelphia. pp. 39, 933, 29, 52.
- Darzynkiewicz, Z., Bruno, S., DelBino, G., Gorczyca, W., Hotz, M.A., Lassota, P. and Traganos, F. 1992 Features of apoptotic cells measured by flow cytometry. *Cytometry*, 13:795-808.

- Dennefors, B., Hamberger, L and Hillensjo, T. 1983 Aspects concerning the role of prostaglandins for ovarian function. *Acta Obstet. Gynecol. Scand.*, Suppl.113:31-41.
- Devlin, T.M 1986 Prostaglandins. In:Textbook of Biochemistry: With Clinical correlations, 2nd edit., John Wiley & Sons, New York. p.424.
- Duby, R.T., McDaniel, J.W., Spilman, C.H. and Black, D.L. 1969 Utero-ovarian relationships in the golden hamster: I. ovarian periodicity following hysterectomy; II. quantitative and local influences of the uterus on ovarian function; III. influence of uterine transplants and extracts on ovarian function following hysterectomy. *Acta Endocrinol.*, 60:595-620.
- Duvall, E., Wyllie, A. H. and Morris, R.G. 1985 Macrophage recognition of cells undergoing programmed cell death (apoptosis). *Immunology*, 56:351-358.
- Eastman, A 1993 Highlights apoptosis: a product of programmed cell death. *Toxicol. and Appl. Pharmacol.*, 121:160-164.
- Edelstam, G.A.B., Lundkvist, O., Venge, P. and Laurent, T.C. 1994 Hyaluronan and myeloperoxidase in human peritoneal fluid during genital inflammation. *Inflammation*, 18(1):13-31.
- Endo, T., Aten, R.F., Leykin, L. and Berhman, H.R. 1993 Hydrogen peroxide evokes anti-steroidogenic and anti-gonadotropic actions in human granulosa luteal cells. *J. Clin. Endocrinol. and Metab.*, 76(2):337-342.
- Espey, L.L. 1980 Ovulation as an inflammatory reaction-A hypothesis. *Biol. Reprod.*, 22:73-106.
- Evans, V.G., 1993 Multiple pathways to apoptosis. *Cell Biol. Int.*, 17(5):461-476.
- Fesus, L., Davies, P.J.A. Piacentini, M. 1991 Apoptosis: molecular mechanisms in programmed cell death. *Eur. J. Cell Biol.*, 56:170-177.
- Fesus, L. 1993 Biochemical events in naturally occurring forms of cell death. *FEBS*, 328(1,2):1-5.
- Forsman, A and McCormack, J.T. 1992 Microcorosion casts of hamster luteal and follicular vasculature during the estrus cycle. *Anat. Rec.*, 233:515-520.

- Gallin, J.I. 1993 Inflammation. In: Fundamental Immunology, 3rd edit. (W.E. Paul Ed.), Raven Press Ltd., New York. 39:1015-1032.
- Grady, K.L. and Greenwald, G.S. 1968 Gonadotropic induction of pseudopregnancy in the cyclic hamster. *Endocrinology*, 83:1173-1180.
- Greenwald, G.S. 1967 Luteotropic complex of the hamster. *Endocrinology*, 80:118-130.
- Greenwald, G.S. 1973 Further evidence for a luteotropic complex in the hamster: progesterone determinations of plasma and corpora lutea. *Endocrinology*, 92:235-242.
- Greenwald, G.S. and Rothchild, I. 1968 Formation and maintenance of corpora lutea in laboratory animals. *J. Anim. Sci., Suppl. I*:139-163.
- Guyara, S.S. and Greenwald, G.S. 1965 A histochemical study of the hamster ovary. *Am. J. Anat.*, 116:257-268.
- Haslett, C. 1992 Resolution of acute inflammation and the role of apoptosis in the tissue fate of granulocytes. *Clin. Sci.*, 83:639-648.
- Hesla, J.S., Miyazaki, T., Dasko, L.M., Wallach, E.E. and Dharmarajan, A.M. 1992 Superoxide dismutase activity, hydrogen peroxide production and corpus luteum steroidogenesis during natural luteolysis and regression induced by oestradiol deprivation of the ovary in pseudopregnant rabbits. *J. R.F.*, 95:915-924.
- Juengel, J.L., Gaverik, H.A., Johnson, A.L., Youngquist, R.S. and Smith, M.F. 1993 Apoptosis during luteal regression in cattle. *Endocrinology*, 132:249-254.
- Karnovsky, M.J. 1965 A formaldehyde-glutaraldehyde fixative of high osmolality for use in electron microscopy. *J. Cell Biol.*, 27:137a-138a.
- Kent, G.C., Jr. 1968 Physiology of reproduction. In: The Golden Hamster: Its Biology and Use in Medical Research (R.A. Hoffman, P.F. Robinson and H. Magahalaes Eds.), The University of Iowa Press, Ames. 8:119-138.
- Kerr, J.F.R., Wyllie, A.H. and Currie, A.R. 1972 Apoptosis: a basic biological phenomenon with wide ranging implications in tissue kinetics. *Br. J. Cancer*, 26:239-257.
- Kiernan, J.A. 1990 Histological & Histochemical Methods: Theory and Practice, Pergamon Press, New York. pp. 112-113.

- Kimball, F.A. and Porteus, S.E. 1978 Effect of in vivo prostaglandin treatment on ^3H - $\text{PGF}_{2\alpha}$ uptake in hamster corpora lutea. *Prostaglandins*, 16(3):427-432.
- Kosco, M., 1991 Antigen presentation to B cells. *Curr. Opin. Immunol.*, 3:336- 339.
- Krause, K.H., Demaurex, N., Jaconi, M. and Lew, D.P. 1993 Ion channels and receptor-mediated Ca^{++} influx in neutrophil granulocytes. *Blood Cells*, 19:165-175.
- Krawisz, J.E., Sharon, P. and Stenson, W.F. 1984 Quantitative assay for acute intestinal inflammation based on myeloperoxidase activity. *Gastroenterology*, 87:1344-1350.
- Kumar, V., Cotran, R.S. and Robbins, S.L. 1992 Cell injury and adaptation. In: Basic Pathology, 5th edit., W.B. Saunders Co., Philadelphia. pp. 4-5.
- Lasky, L.A. 1993 Combinatorial mediators of inflammation? *Curr. Biol.*, 3(6):366-368.
- Laemmli, U.K. 1970 Cleavage of structural proteins during the assembly of the head of bacteriophage T4. *Nature*, 227:680-685.
- Lau, I.F., Sakasena, S.K. and Chang, M.C. 1975 Effect of indomethacin an inhibitor of prostaglandin biosynthesis on the length of pseudopregnancy in rats and hamsters. *Acta Endocrinol.*, 78:343-348.
- Leavitt, W.W., Basom, C.R., Bagwell, J.N. and Blaha, G.C. 1973 Structure and function of hamster corpus luteum during the estrus cycle. *Am. J. Anat.*, 136:235-250.
- Lobel, B.L., Rosenbaum, R.M. and Wendler Deane, H. 1961 Enzymatic correlates of physiological regression of follicles and corpora lutea in ovaries of normal rats. *Endocrinology*, 68:232-247.
- McClellan, J.H., Abel, Jr. and Niswender, G.D. 1977 Function of lysosomes during luteal regression in normally cycling and $\text{PGF}_{2\alpha}$ - treated ewes. *Biol. Reprod.*, 16:499-512.
- McCracken, J.A., Glew, M.E. and Scaramauzzi, R.J. 1970 Corpus luteum regression induced by prostaglandin $\text{F}_{2\alpha}$. *J. Clin. Endocrinol. Metab.*, 30:544-546.
- Michael, A.E., Abayasekara, D.R.E. and Webley, G.E. 1994 Cellular mechanisms of luteolysis. *Mol. Cell. Endocrinol.*, 99:R1-R9.

- Milvae, R.A., Alila, H.W. and Hansel, W. 1986 Involvement of lipoxygenase products of arachadonic acid metabolism in bovine luteal function. *Biol. Reprod.*, 35:1210-1215.
- Moore, N.C., Anderson, G., Williams, G.T., Owen, J.J.T. and Jenkinson, E.J. 1994 Developmental regulation of bcl-2 expression in the thymus. *Immunology*, 81:115-119.
- Mulder, K. and Colditz, I.G. 1993 Migratory responses of ovine neutrophils to inflammatory mediators in vitro and in vivo. *J. Leukoc. Biol.*, 53:273-278.
- Nathan, C.F. 1987 Neutrophil activation on biological surfaces: massive secretion of hydrogen peroxide in response to products of macrophages and lymphocytes. *J. Clin. Invest.*, 80:1550-1560.
- Nawroth, P.P. and Stern, D.M. 1986 Modulation of endothelial cell hemostatic properties by tumor necrosis factor. *J. Exp. Med.*, 163:740-745.
- Niswender, G.D. and Nett, T.M. 1988 The corpus luteum and its control. In: The Physiology of Reproduction (E. Knobil and J. Neill, Eds.), Raven Press Ltd., New York. 13:489-525.
- Niswender, G.D., Juengel, J.L., McGuire, W.J., Belfiore, C.J. and Wiltbank, M.C. 1994 Luteal function: the estrus cycle and early pregnancy. *Biol. Reprod.*, 50:239-247.
- Norman, R.J. and Brannstrom, M. 1994 White cells and the ovary - incidental invaders or essential effectors? *J. Endocrinol.*, 140:333-336.
- Orlicky, D.J., Fisher, L., Dunscomb, N. and Miller, G.J. 1992 Immunohistochemical localization of PGF₂α receptor in the rat ovary. *Prostaglandins, Leukot. Essent. Fatty Acids*, 46:223-229.
- O'Shea, J.D., Nightingale, M.G. and Chamley, W.A. 1977 Changes in small blood vessels during cyclical luteal regression in sheep. *Biol. Reprod.*, 17:162-177.
- Oxberry, B.A. and Greenwald, G.S. 1982 An autoradiographic study of the binding of ¹²⁵I-labeled follicle stimulating hormone, human chorionic gonadotropin and prolactin to the hamster ovary throughout the estrous cycle. *Biol. Reprod.*, 27:505-516.

- Paavola, L.G. 1977 The corpus luteum of the guinea pig. Fine structure at the time of maximum progesterone and during regression. *Am. J. Anat.*, 150:565-604.
- Pearse, A.G.E. 1972 *Histochemistry: Theoretical and Applied*, Williams and Wilkins Co., Baltimore. pp. 795-797.
- Pepperell, J.R., Wolcott, K. and Behrman, H. 1992 Effects of neutrophils in rat luteal cells. *Endocrinology*, 130(2):1001-1008.
- Pettipher, E.R., Salter, E.D., Breskow, R., Raycroft, L. and Showell, H.J. 1993 Specific inhibition of leukotriene B₄ (LTB₄)-induced neutrophil emigration by 20-hydroxy LTB₄: implications for the regulation of inflammatory responses. *Br. J. Pharmacol.*, 110:423-427.
- Piacentini, M., Autuori, F., Dini, L., Forrace, M.G., Ghibelli, L., Piredda, L. and Fesus, L. 1991 "Tissue" transglutaminase is specifically expressed in neonatal rat liver cells undergoing apoptosis upon epidermal growth factor-stimulation. *Cell Tissue Res.*, 263:227-235.
- Ranki, A. and Häyry, P. 1979 Histochemical distinction between lymphocytic and monocytic acid A-naphthyl acetate (ANAE) esterases. *J. Clin. Lab. Immunol.*, 1:333-338.
- Ranki, A., Reitamo, S., Konttinen, Y.T. and Häyry, P. 1980 Histochemical identification of human T lymphocytes from paraffin sections. *J. Histochem. Cytochem.*, 28(7):704-707.
- Ridley, K and Greenwald, G.S. 1975 Progesterone levels measured every two hours in the cyclic hamster. *Proc. Soc. Exp. Biol. Med.*, 149:10-12.
- Robaye, B., Mosselmans, R., Fiers, W., Durmont, J.E. and Garland, P. 1991 Tumor necrosis factor induces apoptosis (programmed cell death) in normal endothelial cells in vitro. *Am. J. Pathol.*, 138(2):447-453.
- Rochon, Y.P. and Frojmovic, M.M. 1992 A model for the recruitment of neutrophils at sites of inflammation. physiological relevance of in vivo neutrophil aggregation. *Med. Hypotheses*, 38:132-138.
- Rothchild, I. 1981 The regulation of the mammalian corpus luteum. *Recent Prog. Horm. Res.*, 37:183-298.

- Saidapur, S.K. and Greenwald, G.S. 1978 Sites of steroid synthesis in the ovary of the cyclic hamster: a histochemical study. *Am. J. Anat.*, 158:71-86.
- Sarraf, C.E. and Bowen, I.D. 1986 Kinetic studies on a murine sarcoma and an analysis of apoptosis. *Br. J. Cancer*, 54:989-998.
- Savill, J. 1992 Macrophage recognition of senescent neutrophils. *Clin. Sci.*, 83:649-655.
- Sawada, M. and Carlson, J.C. 1988 Superoxide radical production in plasma membrane samples from regressing rat corpora lutea. *Can. J. Physiol. Pharmacol.*, 67:465-471.
- Sawada, M. and Carlson, J.C. 1991 Rapid plasmamembrane changes in superoxide radical formation, fluidity and phospholipase A₂ activity in induction of luteolysis. *Endocrinology*, 128(6):2992-2998.
- Schulte-Hermann, R., Bursch, W., Kraupp-Grasl, B., Oberhammer, F., and Wagner, A. 1992 Programmed cell death and its protective role with particular reference to apoptosis. *Toxicol. Lett.*, 64:569-574.
- Schulte-Hermann, R., Bursch, W., Kaupp-Grasl, B., Oberhammer, F., Wagner, A. and Jirtle, R. 1993 Cell proliferation and apoptosis in normal liver and preneoplastic foci. *Environ. Health Perspect.*, 101(suppl.5):87-90.
- Stern, J. and Coulam, C.B. 1992 New concepts in ovarian regulation: an immune insight. *Am. J. Reprod. Endocrinol.*, 27:136-144.
- Tamura, H. and Greenwald, G.S. 1987 Role of luteinizing hormone in luteotropic complex of pregnant hamster. *Am J. Physiol. Endocrinol. Metab.*, 252:E500-504.
- Terranova, P.F. and Greenwald, G.S. 1978 Steroid and gonadotropin levels during the luteal-follicular shift of the cyclic hamster. *Biol. Reprod.*, 18:170-175.
- Tilly, J., Kowalski, K.I., Johnson, A.L. and Hseuh, A.J.W. 1991 Involvement of apoptosis in ovarian follicular atresia and postovulatory regression. *Endocrinology*, 129(5):2799-2801.
- Trush, M.A., Egnner, P.A. and Kensler, T.W. 1994 Myeloperoxidase as a biomarker of skin irritation and inflammation. *Fd. Chem. Toxic.*, 32(2):143-147.

- Vasalli, P. 1992 The pathophysiology of tumor necrosis factors. *Annu. Rev. Immunol.*, 10:411-452.
- Wang, L.J., Pascoe, V., Petrucco, O.M., and Norman, R.J. 1992 Distribution of leukocyte subpopulations in the human corpus luteum. *Hum. Reprod.*, 7(2):197-202.
- Ward, M.C. 1946 A study of the estrus cycle and the breeding of the golden hamster, *Cricetus auratus*. *Anat. Rec.*, 94:139-162.
- Waring, P., Kos, F.J. and Mullbacher, A. 1991 Apoptosis or programmed cell death. *Med. Res. Rev.*, 11(2):219-236.
- Wedmore, C.V. and Williams, T.J. 1981 Control of vascular permeability by polymorphonuclear leukocytes in inflammation. *Nature*, 289:646-650.
- Weiss, S.J. 1989 Tissue destruction by neutrophils. *N. Engl. J. Med.*, 320(6):365-376.
- Wu, X.M., Sawada, M. and Carlson, J.C. 1992 Stimulation of phospholipase A₂ by xanthine oxidase in the rat CL. *Biol. of Reprod.*, 47:1053-1058 Stimulation of phospholipase A₂ by xanthine oxidase in the rat CL. *Biol. Reprod.*, 47:1053-1058.
- Wu, X.M., Yao, K. and Carlson, J.C. 1993 Plasma membrane changes in rat corpus luteum induced by oxygen radical generation. *Endocrinology*, 133(2):491-495.
- Wyllie, A.H. 1993 Apoptosis (the 1992 Frank Rose memorial lecture). *Br. J. Cancer*, 67:205-208.
- Zeleznik, A.J., Ihrig, L.L. and Bassett, S.G. 1989 Developmental expression of Ca⁺⁺/Mg⁺⁺ dependent endonuclease activity in rat granulosa and luteal cells. *Endocrinology*, 125(4):2218-2220.